Master's thesis

NTNU
Norwegian University of Science and Technology
Faculty of Engineering
Department of Civil and Environmental Engineering

Nitish Sapkota

Numerical modelling of hydraulics and sediment at the inlet location of Sediment Bypass Tunnel (SBT) - Test Case: Upper Arun Hydroelectric Project, Nepal

Master's thesis in Hydropower Development

Supervisor: Nils Rüther

Co-Supervisor: Diwash Lal Maskey

June 2020

NTNU
Norwegian University of
Science and Technology

Nitish Sapkota

Numerical modelling of hydraulics and sediment at the inlet location of Sediment Bypass Tunnel (SBT) - Test Case: Upper Arun Hydroelectric Project, Nepal

Master's thesis in Hydropower Development
Supervisor: Nils Rüther
Co-Supervisor: Diwash Lal Maskey
June 2020

Norwegian University of Science and Technology
Faculty of Engineering
Department of Civil and Environmental Engineering

NTNU
Norwegian University of
Science and Technology

Abstract

The study aims to analyse the effects of sediment bypass tunnel inlet location on intake hydraulics and suspended sediment removal for a reservoir of Upper Arun Hydroelectric Project (UAHEP) using numerical modelling program, SSIIM 2. The primary idea is to assess the suitability of numerical model for optimization study in collaboration with physical hydraulic model, thereby supporting the hybrid modelling concept.

The physical hydraulic models have limitations on scaling suspended sediments and hence, these models might not fully capture the behaviour of sediments questioning the reliability of result. Similarly, the time, energy and cost involved for various modifications in physical hydraulic model would be greater leading to exclusion of various probable possibilities. Therefore, it might be better to calibrate the numerical model using the physical hydraulic model data and study the effects of different modifications and parameters to optimize the result. For the test case, relevance of shifting sediment bypass tunnel inlet location upstream of the initial location has been studied based on various sensitive numerical parameters.

The hydraulic and sediment (suspended) simulations have been carried out for a fixed water level of 1,625masl and 877m^3/s discharge converted to a model scale of 1:50, for two different sediment bypass tunnel inlet locations (i.e. initial and shifted locations). Hydraulic simulation is used to finalize the bed deposition geometry and necessary algorithms along with parameters for sediment simulation. The simulation is calibrated by comparing the surface velocities at various cross sections with physical model test results for the initial location. Similarly, suspended sediment

concentration at sediment bypass tunnel (SBT) outlet has been compared with physical model test results to validate the sediment simulation. In case of shifted location, suspended sediment simulation has been carried out using previously calibrated hydraulic model, by shifting the sediment bypass tunnel inlet location further upstream. Among two inlet locations, higher suspended sediment concentration at sediment bypass tunnel outlet and higher reservoir trapping have been observed for shifted inlet location. Similarly, smoother flows with increased erosion, upstream of the sediment bypass tunnel have been observed in shifted location. Thus, better results for shifted inlet location signifies it being more relevant for suspended sediment handling than the initial one. Further, the effect of various parameter like roughness height (k_s), sediment transport formula etc have also been analysed which would rather be difficult in physical hydraulic model. The conformance of the numerical model's surface velocities and sediment concentration at SBT outlet with physical model signifies, the ability of numerical model to replicate the physical model, thereby providing fore grounds for further analysis and hybrid modelling.

Good quality and large number of measurement data are required for properly replicating physical model into numerical model. The unavailability of required number of bed deposition data in this study, might have affected the accuracy of results. Also, simulation have been carried out for only one operating condition. So, different operating conditions have to be checked before finalising the sediment bypass tunnel inlet location. Similarly, limitations of the program, SSIIM 2, like inability to use different density materials, roughness values etc leads to uncertainty in results. Therefore, further work to minimize above discrepancies and result verification with the final physical model tests are recommended.

Preface

This report is a master's thesis at the Department of Civil and Environmental Engineering, Norwegian University of Science and Technology. The objective of this project is to analyse the effects of sediment bypass tunnel inlet locations on intake hydraulics and suspended sediment removal in a reservoir using a numerical model, SSIIM 2. As well as to present numerical model as a potential optimization tool for selecting best SBT inlet alternatives to conduct further physical model tests, thereby supporting a fundamental idea of hybrid modelling between physical and numerical models.

The work on thesis started on January and was concluded by June 2020. However, as a part of data collection, visit to Nepal was carried during summer break of 2019 i.e. July and August 2019. Upper Arun Hydro Electric Limited, sister organization of Nepal Electricity Authority (NEA), provided the relevant data and further assured to provide other, after receiving from its Chinese consultant. The physical modelling of the project's headworks is being carried out at River house of Yangtze River Science Academy in Wuhan. However, due to the Covid-19 situation, the relevant data couldn't be received, restraining the study on limited data. As a hindrance, the SSIIM 2 numerical model couldn't be completely validated which led the further research based on relative comparison between change in hydraulics and sediment at two sediment bypass tunnel inlet locations.

Acknowledgements

This section belongs to all those wonderful people without whom this study would not have been possible. It is my genuine pleasure to express my gratitude to all the people who inspired, encouraged, believed and guided me all along this incredible journey.

First, I am highly indebted for all the timely advices and valuable support provided by supervisor Professor Nils Rüther and express my heartfelt respect for all that guidance.

I would like to extend my gratitude to co-supervisor Diwash Lal Maskey, Ph.D. candidate at Department of Civil and Environmental Engineering, for his effortless dedication, commitment and support that pushed me on moving forward.

Mr. Ram Chandra Paudel, Manager and Mr. Surya Narayan Shrestha, Assistant Manager, Upper Arun Hydro Electric Limited, have been an important part of this work and I am very thankful for their valuable time on providing necessary suggestions and documents, despite of their busy schedule.

At the end I would like to thank my parents and rest of my family and friends who have supported me, tolerated me and encouraged me throughout this work.

Table of Contents

List of Figures

List of Tables

List of Abbreviations

1-D One dimensional

2-D Two dimensional

3-D Three dimensional

CAP Reservoir capacity

CFD Computational Fluid Dynamics

CIR Capacity inflow ratio

D/S Downstream

ERCOFTAC European Research Community on Flow, Turbulence and Combustion

FSL Full Supply Level

HEP Hydroelectric Plant

HPP Hydropower Plant

HRWL Highest Regulated Water Level

ICOLD International Commission on Large Dams

IPCC Intergovernmental Panel on Climate Change

LLO Low Level Outlet/Bottom Outlet

LRWL Lowest Regulated Water Level

MAR Mean annual runoff

MAS Mean annual sediment inflow

MOL Minimum Operating Level

MW Mega Watt

NEA	Nepal Electricity Authority
PMSV	Physical Model Surface Velocity
POW	Power- Law Scheme
PPM	Parts Per Million
PROR	Peaking Run of River
R-O-R	Run- of- River
SBT	Sediment Bypass Tunnel
SIMPLE	Semi-Implicit Method for Pressure-Linked Equations
SIMPLEC	Semi-Implicit Method for Pressure-Linked Equations-Consistent
SOU	Second Order Upwind Scheme
SSC	Suspended Sediment Concentration
SSIIM	Sediment Simulation In Intakes with Multiblock option
SSL	Suspended Sediment Load
U/S	Upstream
UAHEP	Upper Arun Hydroelectric Project

List Symbols

a	Acceleration
cm	Centimetre
m^3	Cubic meter
cumecs	Cubic meter per second
m^3/s	Cubic meter per second
ε	Dissipation of turbulent kinetic energy
F	Force
Gt	Gigaton
kg	Kilogram
km	Kilometer
M	Mass
d_{50}	Median diameter
d_{90}	90% particles are finer than this sediment size
m	Meter
m/s	Meter per second
masl	Meter above sea level
mm	Millimetre
MCM	Million cubic meter
Mt	Million ton
k_s	Roughness height
Q_{95}	Flow is available for 95% of the time

s	Second
m^2	Squared meter
k_{st}	Strickler's roughness coefficient
t	Ton
k	Turbulent kinetic energy
ν_T	Turbulent eddy viscosity
x or i	X direction
y or j	Y direction
z or k	Z direction

1 Introduction

1.1 Background

In the world there are 57,985 large dams, among which 48.7% and 17.6% are classified as single purpose and multipurpose dams respectively. Among the single purpose dams, 47% are used for irrigation, 22% for hydropower, 12% for water supply, 9% for flood control and remaining for other purposes(ICOLD, 2020). These dams ensure that the water is readily available to the growing population. With increasing population, demand for water is steadily increasing and would reach 2-3% per year over the coming decades (ICOLD, 2020). Similarly, spatial and temporal variability in availability of water has changed significantly due to the climate change (IPCC, 2007). This signifies the growing importance of dams as a means of storing water.

Moreover, its importance had already been realised and large reservoirs were constructed around 1950s-1990s. These large reservoirs provided water benefits on one hand whereas on other, changed the river flow pattern and thereby depositing large amount of sediments upstream of dams. Since, research on sedimentation were very little at that time, effect of sediments was undermined. As these dams are more than 50 years old now, sediment deposition has led to a reduction in storage capacity, in addition to its effects on the operational efficiency of different hydraulic structures attached to the project, such as bottom outlet gates, hydropower plants, and different water intakes with different purposes (Mohammad *et al.*, 2020). In case of some recent reservoirs like, Ronghua (1983-2014) and Nanhua (1993-in operation) reservoirs in Taiwan, probable remaining operational life has been decreased to zero and 35 years respectively due to

sedimentation (Wang *et al.*, 2018). In a whole scenario, mean annual sedimentation rates vary from 0.2% to some 2 to 3% of the reservoir volume with a global annual average rate of about 1%. Worldwide, increase in sedimentation volume exceeds increase in reservoir capacity revealing a gross storage loss (Auel *et al.*, 2017). Similarly, as few high-quality sites for new reservoirs remain (Annandale, Morris and Karki, 2016), the existing storage capacity is more valuable to maintain (Wang *et al.*, 2018). Therefore, sediment management and handling are very essential to sustain the life of reservoirs and reap full benefits in a sustainable way.

Sustainable sediment management to maintain reservoir capacity can be accomplished by a suite of strategies, as described in detail by Morris and Fan (Morris and Fan, 1998), and Annandale (Annandale, Morris and Karki, 2016). The most promising and long-term solutions include sediment bypass tunnels, as demonstrated in Japan and Switzerland (Sumi and Kantoush, 2011; Auel and Boes, 2011), and sediment flushing (Kondolf, 2013). However, the efficiency and feasibility of strategies vary according to their compatibility with operations at individual reservoirs, particularly those with carryover storage, synchrony with natural sediment supply, water demand for each unit of sediment managed, effectiveness in maintaining reservoir capacity, and ability to meet necessary infrastructure and hydraulic conditions, among other factors (Wang *et al.*, 2018).

Among all, sediment bypass tunnels (SBT) have become effective strategy for handling both bed and sediment loads recently, as it can be constructed even at existing dams, prevents loss of stored water caused by lowering of reservoir water level (Sumi and Kantoush, 2011), shifts the risk of bottom outlet being clogged to new structure i.e. SBT (Auel *et al.*, 2011) and also improves the ecological function in rivers by connecting the up and

downstream reaches in terms of sediment continuity (Auel *et al.*, 2017). Similarly, studies on sediment handling by SBT showed high sediment routing efficiency of 80% (Sumi and Kantoush, 2011) and 77% (Auel *et al.*, 2017) in Miwa and Asahi dam respectively. Although having such advantages, the number of SBTs are limited to about 30 worldwide; especially to small and medium sized reservoirs ($<10^7$ m^3 (Auel *et al.*, 2017) and CIR 0.003 to 0.3 (Boes, Müller-Hagmann and Albayrak, 2019)). This limitation is by the fact that the optimal efficiency of SBTs depends on proper location of SBT inlet and reservoir operation strategy. Considering the location, it attributes to the hydraulic patterns for movement of sediments towards the SBT inlet as well as the length of tunnel whose cost due to invert abrasion are much higher in adopting SBT for sediment handling.

Generally, for considering the proper location and designing of SBT inlet, physical model tests are preferred. It has been found out that the physical model tests are best suited for bed load sediment study where scale effect phenomena have least effect. However, in case of suspended sediments, involving higher degree of scale effects, physical models might not depict the true picture. Therefore, with technological advancement, numerical models have become able to solve various sediment related problems effectively and aid physical hydraulic models. Further, numerical models assist to optimize best suitable location for conducting more detailed physical model study thereby supporting hybrid modelling concept. In overall, the main advantages of using such models are their reduction in costs and time in comparison of the physical models alone (Mohammad *et al.*, 2020). Therefore, to investigate the effects of inlet location on intake hydraulics and sediment removal via a suspended sediment SBT, a test case

of Upper Arun Hydroelectric Project (UAHEP) in Nepal has been considered in this study.

As SBT is first of its kind in Nepal, the Upper Arun Hydro Electric Limited has been conducting thorough physical model study on sedimentation for peaking reservoir project (UAHEP) at River house of Yangtze River Science Academy in Wuhan. This project is characterized by high head, small storage capacity and heavy load of abrasive quartz sediment where 70% of the suspended sediments (82.4% of the total sediments are suspended sediments) are finer than 0.1mm with median diameter of 0.057mm (Changjiang Survey and Sinotech Engineering Consultants, 2019a). Similarly, sediment discharge and runoff from May to October accounts for 99.6% and 85.5% of the whole year with abrasive quartz sediment. Therefore, the project aims to divert the maximum flow with suspended sediments using the SBT and flush the bed load via the bottom outlet at the dam (Changjiang Survey and Sinotech Engineering Consultants, 2019b). In this study, it has been aimed to investigate the reliability of SBT efficiency based on two alternative inlet locations and sediment strategies proposed by physical hydraulic modelling using numerical model in SSIIM 2.

1.2 Master's Thesis Work

The purpose of this thesis is to study the effect of SBT inlet location on the intake hydraulics and suspended sediment removal in the UAHEP reservoir using a three-dimensional numerical model, SSIIM 2. The main objectives of this study are:

- Literature review of the sediment handling techniques at headworks and 3D CFD numerical modelling for suspended and bed load sediments.
- Numerical modelling of hydraulics and suspended sediments at the proposed inlet location of SBT in model scale.
- Optimization study based on the SBT inlet locations (initial and shifted locations), supporting hybrid modelling concept
- Sensitivity Analysis of different numerical parameters.
- Conclusion and recommendations for future work.

2 Literature Review

2.1 Sediment Deposition in Reservoirs

Sediments are generally the naturally occurring fragments of rocks and minerals formed by physical or chemical weathering processes or erosion, and are subsequently transported by action of wind, water, ice or the action of gravity acting on particles. In rivers, these sediments may be classified by relative grain size and abundance in the movable streambed and by mode of transport as bed load, suspended load and wash load (Einstein, 1964); cited from (Morris and Fan, 1998). The bedload includes particles rolling or sliding along the bed plus the saltation load which accounts for less than 15% of the total sediment load in rivers. Suspended load are the particles moving in suspension and sustained in the water column by turbulence or in colloidal suspension. Wash load is composed of suspended sediments which do not touch the river bed. They come from upstream of the considered reach and are "washed through" the reach of interest (no exchange with bed material) (Morris and Fan, 1998).

The sediment transport is a complex process depending on various factors like catchment properties, river discharge, river morphology, sediment yield, delivery ratio, density, concentration, turbulence etc. However, with higher velocities and less concentration in river, more sediments can be transported out of the considered reach. Similarly, with higher concentration and lower flow velocities, more sediments can settle. Thus, a delicate hydraulic sedimentological equilibrium is maintained in the natural river system.

When a river/tributary enters an impounded reach, flow velocity decreases, and sediment load begins to deposit. The bed load and coarse fraction of

the suspended load are deposited in upstream part of reservoir to form delta deposits. Whereas, finer sediments with lower settling velocities are transported further into the reservoir by either stratified or non-stratified flow as shown in Figure 2.1. Most sediments are transported within reservoirs to points of deposition by three processes: (1) transport of coarse material as bed load along the topset delta deposits, (2) transport of fines in turbid density currents, and (3) transport of fines as non-stratified flow. The longitudinal deposition pattern varies drastically from one reservoir to another, influenced by pool geometry, discharge and grain size characteristics of the inflowing load, and reservoir operation. In deep reservoirs which have been operated at different levels, distinct deltas may be formed at different water levels. Conversely, in long, narrow reservoirs, the bathymetric profile commonly associated with delta deposits may be absent, but an area characterized by a rapid shift in grain size marking the downstream limit of coarse material deposition may still be present (Morris and Fan, 1998).

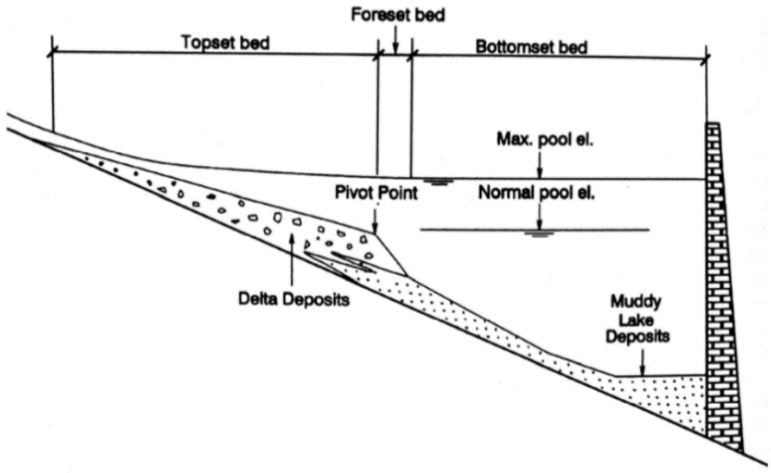

Figure 2.1 Sediment deposition zones in the reservoir (Morris and Fan, 1998)

2.1.1 Sediment problems in reservoirs

The construction of different hydraulic structures, such as barrages, weirs, and dams; for different purposes (e.g., storage, flood control, power generation, and multipurpose dams) changes sediment transportation balance. In dam reservoirs, gradual expansion of flow section when the flow approaches reservoir inlet leads to sediment load deposition that is coarser and then finer toward the flow direction (Mohammad *et al.*, 2020). After years of dam operation, sediment deposition leads to a reduction in storage capacity. Due to very high costs and scarcity of resources, it is very difficult to replenish the lost reservoir storage capacity. Morris and Fan quantified the world's total sediment deposit between 15 to 40 Gt per year (Morris and Fan, 1998). The costs for restoring these losses and rebuilding the dams can be estimated at US$ 13 billion per year (Annandale *et al.*, 2003). Further, Annandale estimated that global net reservoir storage has been declining from its peak of 4200 km^3 in 1995 because rates of

sedimentation exceed rates of new storage construction. With increasing demands for water storage, and fewer feasible and economically justifiable sites available for new reservoirs, loss of capacity in our existing reservoirs threatens the sustainability of water supply (Annandale, 2013); cited from (Kondolf, 2013).

Besides storage loss, reservoir sedimentation causes various severe problems such as (1) a decrease of the active volume leading to both loss of energy production and water available for water supply and irrigation; (2) a decrease of the retention volume in case of flood events; (3) endangerment of operating safety due to blockage of the outlet structures; and (4) increased turbine abrasion due to increasing specific suspended load concentrations (5) deprivation of essential sediments to maintain the downstream channel form and to support the riparian ecosystem. These problems will intensify in the very next future, as reservoir sedimentation will progress if no countermeasures are taken (Auel and Boes, 2011). Therefore, it is very essential to foresee sedimentation problems at the earliest and incorporate essential measures for sustainability of reservoir.

2.2 Sediment Management in Reservoirs

There are a wide range of sediment management techniques to preserve reservoir capacity and pass sediment downstream, many of which represent ways to achieve the goals expressed by the Chinese expression, “Store the clear water and release the muddy.” Many of them have been successfully employed in reservoirs in a range of settings, as described by Morris and Fan, Annandale, Sumi et al., and Wang and Hu (Kondolf, 2013). Although terminology differs somewhat, the reservoir sediment management classifications of Morris and Fan distinguishes among four broad categories. Three categories focus on improving the sediment balance

across reservoirs by: (1) reducing sediment yield from the watershed, (2) routing sediment laden flows around or through the storage pool, and (3) removing sediment following deposition. The fourth category consists of adaptive strategies which respond to capacity loss, without addressing the sediment balance (Figure 2.2) (Morris, 2020).

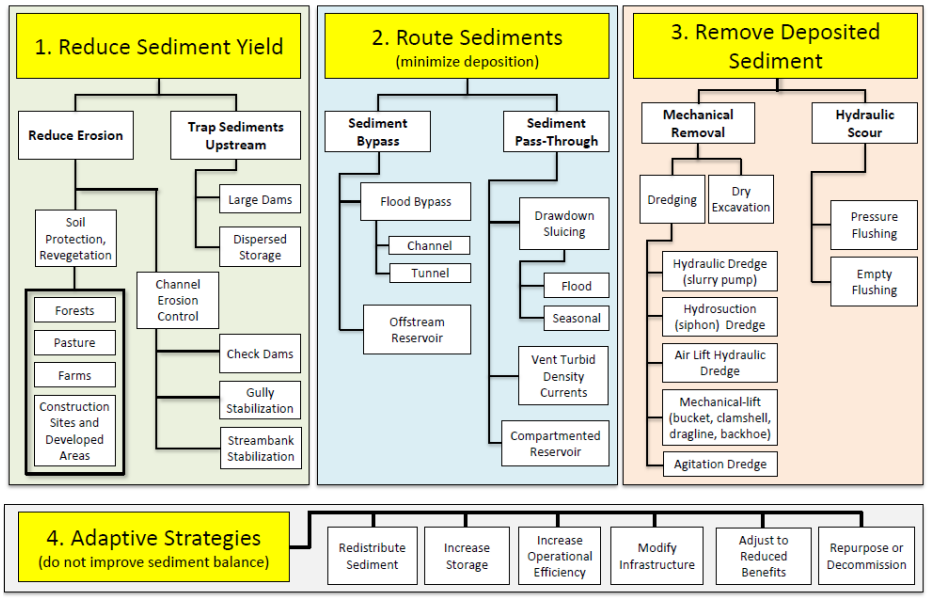

Figure 2.2 Classification of strategies for reservoirs (Morris, 2020)

As each reservoir and its catchment properties are unique to itself, several management strategies have to be combined for achieving a proper balance. For example, Miwa dam in Japan uses check dam, excavating, dredging and bypass tunnel to manage the incoming sediments (Sumi and Kantoush, 2011). Based on various sediment management strategies used around the world, Annandale (2013), complied a chart depending on the turnover rate of water (CAP/MAR = Reservoir capacity/Mean annual runoff) and sediment (CAP/MAS = Reservoir capacity/Mean annual inflow sediment)

as shown in Figure 2.3 . It can be preliminarily used to select appropriate strategies.

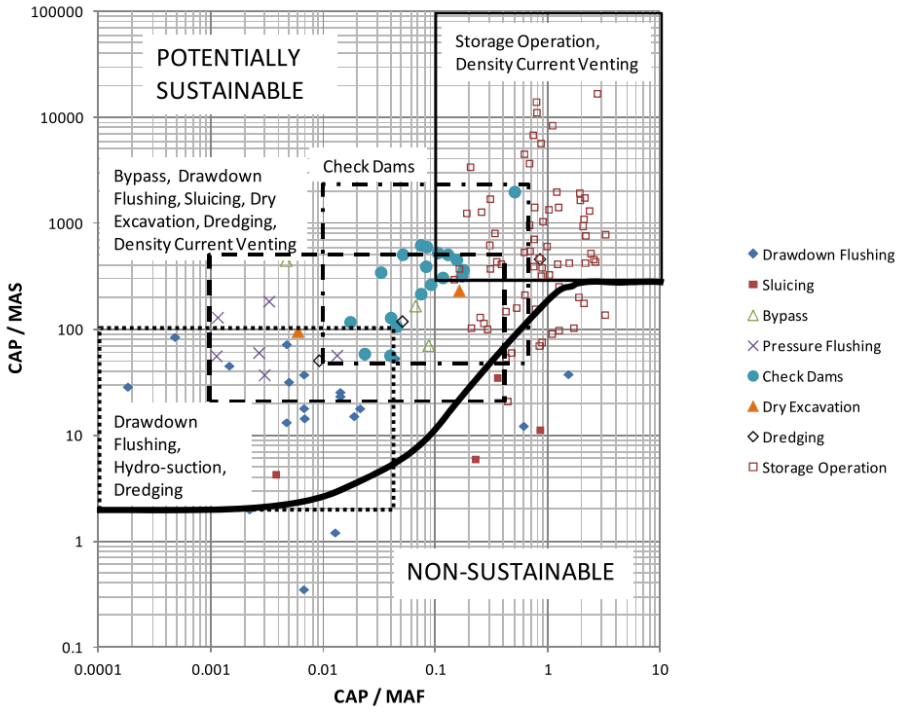

Figure 2.3 Graph comparing previous experience with implementing sedimentation management approaches (Annandale, 2013)

Among all, sediment routing is ecologically favorable compared to other measures as the sediments are conducted downstream during high flows when sediment load is itself high in the rivers. Similarly, only the sediments delivered upstream of the bypass are diverted and hence the sediment concentration downstream of the dam is not affected as well as the river keeps its natural character (ICOLD, 2009). In general, knowledge of both the rate and pattern of sediment deposition in a reservoir is required to predict the types of service impairments which will occur, the time frame

in which they will occur, and the types of remedial strategies which may be practicable (Morris and Fan, 1998).

2.2.1 Sediment routing

Sediment routing is a technique to minimize or balance reservoir deposition by influencing hydraulics in order to pass sediment laden water through or around the reservoir. Typically, sediment-laden waters are diverted at a weir upstream of the reservoir into a high-capacity tunnel or diversion channel, which conveys the sediment-laden waters downstream of the dam, where they rejoin the river (Figure 2.4). Normally, weir diverts during high flows when sediment loads are high, but once sediment concentrations fall, water is allowed into the reservoir (Kondolf, 2013).

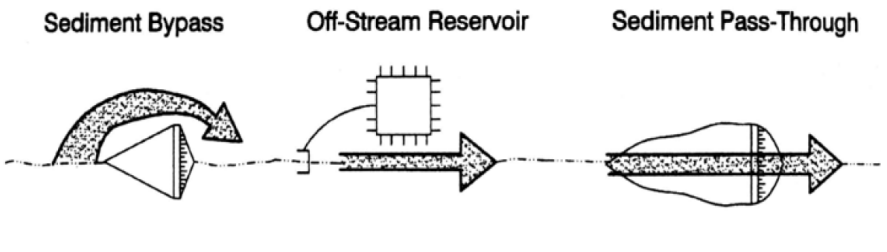

Figure 2.4 Sediment Routing Strategies (Morris and Fan, 1998)

Among the routing techniques, Sediment Bypass Tunnel is considered the best option with due consideration to topography, hydrology and tunnel abrasion. Research on Japanese SBT Asahi and Nunobiki showed that on average, 77% and 94% of the incoming sediments were diverted to the downstream river reach, and the estimated reservoir life was prolonged to 450 and 1200 years, respectively (Auel, Kantoush and Sumi, 2016). Generally, an SBT consists of a guiding structure in the reservoir, intake structure with a gate, short steeply sloped acceleration section, a long and smooth sloped bypass tunnel section, and an outlet structure. Based on

topographical and economic factors, SBT inlet is placed either at the reservoir head or inside the reservoir affecting entire bypass tunnel design and reservoir operation during sediment routing. Two different intake options (**Option a**: SBT intake at reservoir head; **Option b**: SBT intake inside the reservoir) with its associated structures are shown in Figure 2.5.

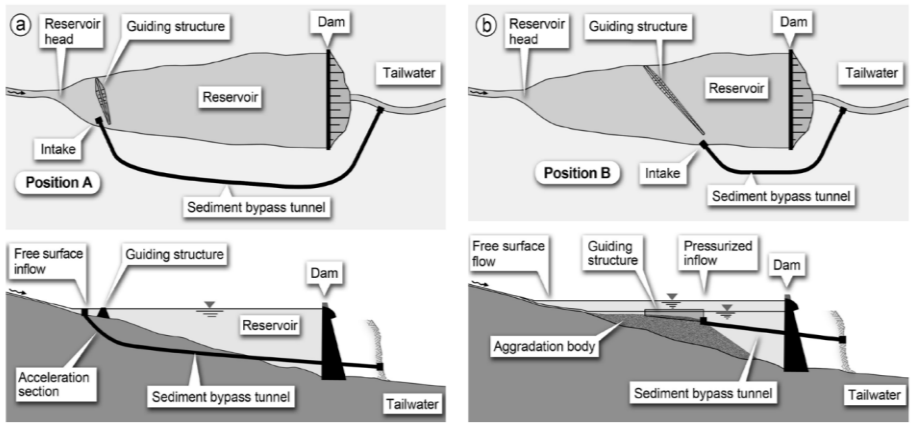

Figure 2.5 Different option for SBT intake (Auel and Boes, 2011)

As 70% of the incoming suspended loads are smaller than 0.1mm (d_{50} = 0.057mm), a circular SBT has been proposed in the UAHEP to bypass the flood discharge till 816m^3/s. Therefore, the present study focuses on the inlet position of SBT and its effectiveness.

2.3 Numerical Modelling

The flow and sediment deposition exhibit a complex pattern owing to the topography and geometry of reservoir. As flow pattern changes, deposition and erosion in the reservoir changes, thereby making it very difficult to quantify the sedimentation process in reservoir. Suitable solutions in such cases are usually determined either by physical laboratory models or numerical models. Physical models are well suited for analyzing problems involving complex geometry, river morphology, or flow curvature which

result in sediment concentration profiles and deposit pattern varying in both the transverse and longitudinal directions (Morris and Fan, 1998). However, physical modelling of sediment transport is more difficult because of different scaling laws for suspended sediments and erosion / bed load transport (Kobus and Abraham, 1984). It is also difficult to scale the finer particles down because of the influence of cohesive forces occurring when the sand particles are very small. The magnitude of bed forms is almost impossible to properly scale in a physical model (Haun and Olsen, 2012).

With increased development of sediment modules in computational fluid dynamics (CFD) and the high capacity and speed of modern computers, it has been possible to use numerical models for natural river reaches and reservoirs (Haun *et al.*, 2013). Various numerical models have been successfully applied for the numerous reservoir problems with high degree of reliability. Numerical models have several important advantages over physical models: lower cost, ease of re-running to simulate a variety of different conditions, ability to simulate some types of problems numerically that are unsuitable for physical modelling because of the scaling laws involved (e.g., sediment cohesion), portability, and reproducibility. A numerical model study for flushing in Shihmen reservoir, Taiwan, shows that the physical model may under predict the sediment rate sluiced through the outlets by about 10% (Lai and Wu, 2018). However, the disadvantage of using numerical models is that the solution is complicated and it takes years to create the computer program (Olsen, 2010).

2.3.1 CFD models

The physical aspects of any fluid flow are governed by the following three fundamental principles: (1) mass is conserved; (2) F = M*a (Newton's second law); and (3) energy is conserved. These fundamental principles can be expressed in terms of mathematical equations, which in their most general form are usually partial differential equations. Computational fluid dynamics is, in part, the art of replacing the governing partial differential equations of fluid flow with numbers and advancing these numbers in space and/or time to obtain a final numerical description of the complete flow field of interest (Wendt, 2009).

The numerical models of sediment transport can simulate flow in one, two or three dimensions. Generally, 1-D models are used for a long-term simulation and simulation of sediment transport along a reach. Whereas, 2-D and 3-D models are used to study sediment transportation and deposition when the purpose is to determine how sediment is distributed across the flow section, or at certain locations in reservoirs like gates, intakes, and power plant inlets. However, these models require more data and greater computing time (Mohammad *et al.*, 2020).

For rivers and reservoirs usually a fully three-dimensional model is necessary because of the hydraulic boundaries and the complex flow situation (e.g. an influence of secondary currents in river bends) (Haun *et al.*, 2013). Considering this, the numerical model SSIIM 2 (Sediment Simulation In Intakes with Multiblock option) is used in the current study to study the effects of SBT inlet location on intake hydraulics and sediment removal for a reservoir of Upper Arun Hydroelectric Project in Nepal. The surface velocity at different cross section of physical hydraulic model is

considered for model calibration and the suspended load concentration from the SBT outlet is used for verification.

2.3.2 Errors and uncertainties

As there are number of uncertainties in CFD modelling, and approximations in the algorithms, results may have numerous errors. The European Research Community on Flow, Turbulence and Combustion (ERCOFTAC) have published Best Practice Guidelines for CFD, where the errors are classified according to the following list (Olsen, 2017):

1. Modelling errors
2. Errors in numerical approximations
3. Errors due to not complete convergence
4. Round- off errors
5. Errors of boundary conditions and input data
6. Human errors
7. Bugs in the software

3 SSIIM

3.1 Introduction

SSIIM is an abbreviation for Sediment Simulation In Intakes with Multiblock option. The program was initially developed to simulate the sediment movements in general rivers/channel geometries, which has later been extended to other hydraulic engineering topics like spillway modelling, head loss in tunnels etc. However, main focus of the program is to model sediment transport in rivers, reservoirs and around the hydraulic structures (Olsen, 2018). The program solves the Navier-Stokes equations in a three dimensional almost non orthogonal grid, using the k-ε turbulence model and SIMPLE method to compute the pressure. SSIIM solves convection diffusion equations for water quality constituents like sediment, temperature, algae, pollutants etc. Time dependent changes in bed and surface levels are also computed (Olsen, 2017).

The main strength of SSIIM compared to general purpose CFD programs is the capability of modelling sediment transport with moveable bed in a complex geometry. This includes a number of algorithms for different sediment process, including sorting, bed load and suspended load; bed forms and effects of sloping beds. The latest modules for wetting and drying in the unstructured grid further enables complex geomorphological modelling (Olsen, 2018).

Similar to other CFD models, SSIIM is divided into three components namely: a preprocessor, a solver and a post processor. The preprocessor includes tools to generate computational grids and input data. Various modules are present for calculation of water velocity, sediment flow, bed level changes, water level changes and/or water quality. The post processor

is used for viewing results. An interactive user interface shows the velocity vectors and scalar variables in a two-dimensional view of the three-dimensional grid, in plan view, a cross section or a longitudinal profile. Similarly, results can be exported to programs like Tecplot or ParaView for post processing. One of the distinct feature of SSIIM is that, its computational module is directly connected with graphics such that the graphics updates with each internal processes computation (Olsen, 2018).

There are two versions of SSIIM: SSIIM 1 and SSIIM 2. SSIIM 1 uses structured grid and SSIIM 2 uses unstructured grid. The main advantage of unstructured version is its ability to model complex geometries, wetting/ drying and lateral movements of a river. Similarly, SSIIM 2 has some water quality and sediment transport algorithms that are not in SSIIM 1. However, SSIIM 1 has a fast solver and uses less memory per cell (Olsen, 2018). As UAHEP, has complex geometries along the computational reach with SBT protruding out from middle of the reservoir, SSIIM 2 has been preferred for simulation. Besides these, it has been found out that SSIIM 2 has been successfully used in various reservoirs with hydraulic structures. For example, it was applied to the Angostura hydropower reservoir in Costa Rica to review the suspended load distribution and pattern of sediment deposition (Haun *et al.*, 2013). Similarly, it has been used for modelling sediment deposition and flushing process in different reservoirs (Haun and Olsen, 2012; Nepal, 2019; Hoven, 2010; Agrawal, 2005). Brief theoretical basis, input and output files and grid generation process are described in this section. For a detailed explanation, about the model, it is recommended to refer SSIIM user's manual.

3.2 Theoretical Basis

3.2.1 Water flow calculation

The Reynolds Averaged Navier-Stokes (RANS) equations are solved in three dimensional, together with the continuity equation, to compute the water motion for turbulent flow, as follows:

$$\frac{\partial U_i}{\partial x_i} = 0 \tag{1}$$

with i = 1, 2, 3.

$$\frac{\partial U_i}{\partial t} + U_j \frac{\partial U_i}{\partial x_j} = \frac{1}{\rho}\frac{\partial}{\partial x_j}\left(-P\delta_{ij} - \rho\overline{u_i u_j}\right) \tag{2}$$

where U is averaged velocity, x is the spatial geometrical scale, ρ is the density of water, P is the dynamic pressure, δ_{ij} is the Kronecker delta and $-\rho\overline{u_i u_j}$ are the turbulent Reynolds stresses modelled by Boussinesq approximation:

$$-\rho\overline{u_i u_j} = \rho\nu_T\left(\frac{\partial U_i}{\partial x_j} + \frac{\partial U_j}{\partial x_i}\right) - \frac{2}{3}\rho k\delta_{ij} \tag{3}$$

where ν_T is turbulent eddy viscosity, k is the turbulent kinetic energy.

Combining and arranging the terms in equations (2) and (3) gives the following expression:

$$\frac{\partial U_i}{\partial t} + U_j \frac{\partial U_i}{\partial x_j} = \frac{1}{\rho}\frac{\partial}{\partial x_j}\left[-\left(P + \frac{2}{3}k\right)\delta_{ij} + \rho\nu_T\frac{\partial U_i}{\partial x_j} + \rho\nu_T\frac{\partial U_j}{\partial x_i}\right] \tag{4}$$

The transient and convective terms are denoted by the first and second terms on the left-hand side and on the right-hand side, the three terms

represent pressure and kinetic energy, diffusion, and stress terms respectively (Olsen, 2017).

The finite volume method is applied as discretization scheme to transform the partial differential equations into algebraic equations. Different options are available in the SSIIM module for discretization of velocity and turbulence equations using K 6 data set. Some of the mostly used scheme are first order power law (POW) scheme and second order upwind (SOU) scheme. Similarly, pressure correction equation uses different approach for the discretization. Further, the standard k-ε model has been applied to model the turbulent Reynold stresses. The unknown pressure field is computed in accordance to the SIMPLE method. The free water surface algorithm is implicit and calculates changes in the water surface in accordance to the pressure gradient between the cell and the neighboring cell (Haun *et al.*, 2013; Olsen, 2018).

3.2.2 Sediment transport calculation

The sediment transport is calculated as suspended and bed load transport. The suspended load is calculated with the convection-diffusion equation for the sediment concentration, C (volume fraction in SSIIM):

$$\frac{\partial \mathrm{C}}{\partial \mathrm{t}} + U_j \frac{\partial \mathrm{C}}{\partial \mathrm{x_j}} + w \frac{\partial \mathrm{c}}{\partial \mathrm{z}} = \frac{\partial}{\partial \mathrm{x_j}} \left(\Gamma \frac{\partial \mathrm{C}}{\partial \mathrm{x_j}} \right) + S \qquad (5)$$

Where, C is sediment concentration, U is flow velocity, w is settling velocity, Γ is diffusion coefficient and S is pick up rate of sediments due to erosion.

The sediment resuspension criteria can be specified as a concentration on bed cell or using a pickup rate as the source term. The diffusion coefficient, Γ, is computed from the eddy viscosity, ν_T, in the k-ε model:

$$\Gamma = \frac{\nu_T}{S_c} \tag{6}$$

S_c is the Schmidt number equal to 1.0 in default.

For suspended sediment load calculation, the formula by Van Rijn is used.

$$C_{bed,\,susp,i} = 0.015\frac{d_i}{a}\frac{\left(\frac{\tau-\tau_{c,i}}{\tau_{c,i}}\right)^{1.5}}{\left[d_i\left(\frac{\rho_S}{\frac{(\rho_W-1)g}{\nu^2}}\right)^{\frac{1}{3}}\right]^{0.3}} \tag{7}$$

where, $C_{bed,\,susp,I}$ is concentration of sediment load at bed for i^{th} fraction, d_i is diameter of the i^{th} fraction, a is height of the bed cell set equal to the roughness height, $\boldsymbol{\tau}$ is bed shear stress for d_i , $\boldsymbol{\tau_{c,i}}$ is critical shear stress for d_i calculated from shield's diagram, ρ_s is density of sediment, ρ_w is density of water and ν is kinematic viscosity.

Bed load can be calculated by different formulae like Meyer- Peter and Müller formula, Van Rijn formula, Einstein formula, etc. The Van Rijn empirical formula to calculate bed load is shown below:

$$\frac{q_{bi}}{d_i^{1.5}\sqrt{((\rho_s-\rho_w)g)/\rho_w}} = 0.053\frac{\left(\frac{\boldsymbol{\tau}-\boldsymbol{\tau_{c,i}}}{\boldsymbol{\tau_{c,i}}}\right)^{2.1}}{d_i^{0.3}\left(\frac{(\rho_s-\rho_w)g}{\rho_w\nu^2}\right)^{0.1}} \tag{8}$$

Where, q_{bi} is transport rate of i^{th} fraction of bed load per unit width (Olsen, 2017).

3.2.3 Boundary conditions

The boundary condition can be specified mainly to inflow, outflow, water surface and bed/wall. Dirichlet boundary conditions are given at the inflow boundary. Zero gradient boundary conditions can be used at outflow

boundaries for all variables. Similarly, for water surface, zero gradient boundary conditions are often used for ε and k is set to zero. For bed/wall, as the flux through bed/wall is zero, no boundary conditions are used. However, as flow gradient towards, the wall is very steep, and it would require a significant number of grid cells to dissolve the gradient sufficiently, a wall law is used, transformed by integrating it over the cell closest to the bed. Wall law for rough boundaries is used:

$$\frac{\mathrm{U}}{u_*} = \frac{1}{k}\ln\left(\frac{30y}{k_s}\right) \tag{9}$$

Where, U is the velocity, $u_*$is shear velocity, k is Von Kármán coefficient, k_s is roughness height and y is the distance from the wall to the center of the cell (Olsen, 2017; 2018).

3.3 Input and Output Files

There are various input and output files used in SSIIM. The most relevant files used in present study are discussed below:

Geodata file

The geodata file is used for bed interpolation to generate the bed level of the reservoir/river grid. This file contains the geometry of the specific project in x, y and z or i, j and k coordinates.

Control file

It is the main file to run the simulation. All the commands for simulation can be provided here, thereby reducing work to use the graphical user interface control. In the control file, various parameters for grid properties, discharges, water levels, roughness coefficient, sediment properties, etc. are given. To invoke these parameters different data sets beginning with capital letters like F, G, W, K, S, etc. are used as per the SSIIM user's

manual. However, one should be careful, not to use capital letters anywhere than intended. Else, the program reads the capital letter and error may result in simulation.

Boogie file

It is an important file for debugging and storing the intermediate processes and results. If any error is seen in the program, then, it is written in this file, helping user to identify error and location. Similarly, intermediate results and any comments on the results can be archived from this file.

Koordina file

This file contains the grid geometry or three-dimensional coordinates of the grid intersection points. The program generates this file itself after the grid is made.

Unstruc file

In SSIIM 2, this file stores the information about the grid coordinates and discharges. It is the main file which is read first before any other operations.

Timei file

The information about variation in input parameters like discharge, water elevation, sediment concentration etc. are addressed by using *timei* file.

Result file

This is the output file containing result of hydraulic computation with velocities, pressure and turbulence. The result file can be written either after completion of prescribed iterations or from the graphical menu.

Bedres file

The bedres file is used to see the changes in bed elevation and water level after computation.

ParaView file

This is the output file and can be read by software named ParaView. Through the ParaView software the results can be easily viewed and interpreted. Like ParaView file, there is another file called Tecplot which is an input for Tecplot software.

3.4 Convergence

In SSIIM a solution is said to be converged if the residuals for velocity in x, y, z directions, turbulent kinetic energy (k), dissipation of k (ε) and continuity are below 1.0E-4. The convergence criteria depend on several factors which are described as follows:

- Good grid: The degree of non-orthogonality of the grid affects the convergence. A higher degree of non-orthogonality and strong gradients give slower convergence.
- Proper relaxation coefficients: Starting from a guessed value, the equations involved in calculations are solved and these guessed values are refined to obtain the converged final solution. The relaxation coefficients are used to improve the guessed value. For the most cases, lower relaxation coefficients will give less instabilities during the convergence, but a slower convergence. Whereas, higher relaxation coefficient will give rapid convergence, if there are no instabilities. For most of the instability cases, lowering values on the K 3 data set (in the *control* file) is advised. The relaxation coefficient to guess a value is used as such:

$$U = r * U_i + (1 - r) * U_{i-1} \quad (10)$$

where, i and i-1 represents the finished iterations, U is the new guessed velocity for i+1 iteration and r is the relaxation coefficient (Olsen, 2017; 2018).

- Boundary condition: Boundary condition should be checked in case of the slow convergence and undesirable results. The convergence is improved by using correct boundary conditions.
- Fast solver: The speed of convergence is highly influenced by the choice of solver. For SSIIM 1, block correction will lead to faster convergence whereas in SSIIM 2 multigrid algorithm implemented for use in shallow flows gives faster convergence. The multigrid algorithm can be set up using F 168 and K 5 data sets in SSIIM 2.
- Stable numerical algorithm: Stable numerical algorithms should be invoked by different data sets in case of instabilities.

3.5 Grid

Grid preparation is the most important and time-consuming process in devising of input data for SSIIM. General idea for grid generation is to divide the water body into cells. The shape of cell is generally triangular, tetrahedral or hexahedral. The accuracy of the calculation, convergence and computational time highly depends on the grid orientation, size and density (Almeland *et al.*, 2019; Olsen, 2018). The grid in SSIIM 2 is unstructured and makes it easy to adapt the grid to complex geometries without loss of accuracy or slow convergence. Similarly, in SSIIM 2 adaptive grid can be used, that can move as per the solution of equation. For e.g. change in water can induce vertical movements whereas meandering of river can cause lateral movements. For a good quality of grid, following points should be considered:

- The grid lines should be made perpendicular to each other as possible. It is not advisable to have intersections with an angle of less than 45 degrees. The non-orthogonality of the grid affects the convergence and makes it slower.
- The grid lines should be aligned in the streamwise direction parallel to velocity vectors. This will reduce the false diffusion.
- The distortion or aspect ratio (ratio of two perpendicular sides of the cell) and the expansion ratio (ratio of the two neighboring grid cell size) should be kept as low as possible.

3.6 Limitation of the Program

Some of the limitations of the SSIIM program are (Olsen, 2018):

- The program neglects non-orthogonal diffusive terms.
- The grid lines in the vertical direction have to be exact vertical.
- Kinematic viscosity of the fluid is equivalent to water at 20 degrees Centigrade. This has been hardcoded and cannot be changed.
- The program is not made for the marine environment, so all effects of the density gradients due to salinity gradients are not taken into account.

4 Project Description

Most of the information in this chapter are based on the following documents provided by the Client, Upper Arun Hydro Electric Limited:

- Volume III- Annex B: Hydrology and Sediment Investigation Report (Draft), Document No: 478(UA)-P1-POR-Vol 3-Rev 0, dated March 2019
- Volume IV- ANNEX H-1 Sediment Numerical Simulation, Document No: 478(UA)-P1-UFSR-Vol 4-Rev 1, dated November 2019
- Volume IV- ANNEX H-2 Research Outline of the Sediment Physical Model, Document No: 478(UA)-P1-UFSR-Vol 4-Rev 1, dated November 2019
- Volume IV- ANNEX H-3 Preliminary Results of the Sediment Physical Model, Document No: 478(UA)-P1-UFSR-Vol 4-Rev 1, dated November 2019

4.1 Background

Upper Arun Hydroelectric Project (UAHEP) is a 1,040MW, daily peaking run of river hydropower project located on the upper reaches of the Arun river, a tributary of Koshi river basin in eastern Nepal. The UAHEP is planned to be developed by utilizing the water discharge from Arun river and a steep gradient loop between Chepu khola and Lesuwa Khola, covering river length of about 15km.

Figure 4.1 Location of UAHEP (Adapted from report ANNEX H-3)

The project utilizes a gross head of 545m (measured from the FSL 1,640masl to turbine centre level at 1,095masl) and design discharge of 235.44m^3/s to produce 1040MW from six Pelton turbines. The firm capacity of the project is 697MW under Q_{95} inflow conditions, daily peaking for 6 hours during the dry season from December to May. The UAHEP diverts the water utilizing 91m high concrete gravity dam located in Chepuwa village via 8,362m long tunnel followed by 467m pressure drop shaft which further branches to supply design discharge to six Pelton turbines of 176.87MW each capacity, housed in an underground powerhouse at Hatiya village. The water after producing the energy is discharged back into the river by two tailrace tunnels of about 602m length each. It has been planned to remove the deposited sediments in the reservoir utilizing the three bottom outlets at dam and the suspended sediments via a SBT located on the left bank in the middle of reservoir.

Salient features of the project are shown in Table 4-1. A general layout of project, conceptual configuration, general layout of headworks, upstream view of dam and section of SBT are shown in the figures below. Recently, the power intake and SBT location shown in Figure 4.4 and Figure 4.6 have been revised. The power intake is integrated in dam as frontal intake (Figure 4.5) and the SBT has been moved further upstream by 100m with incorporating changes in design.

Table 4-1 Salient features of UAHEP

Description	Value	Unit
Mean inflow	217	m^3/s
2- year return period flood	1,050	m^3/s
Sediment inflow: Suspended/Bed	13.81/2.43	Mt/year
Gradient of river	2.8	%
Pondage factor	0.035	%
Sediment load ratio	0.43	
Full supply level (FSL)	1,640	masl
MOL during peak	1,625	masl
Drawdown depth	15	m
Storage under FSL	5.07	MCM
Peaking pondage (live storage)	2.41	MCM
Storage under MOL under peak	2.66	MCM
Design discharge	235.44	m^3/s
Installed/Firm capacity	1,040/697	MW
Turbine/Units	Pelton/Six	
Dam height	91	m
Spillway crest level	1,640	masl
Bottom outlet sill level	1,590	masl

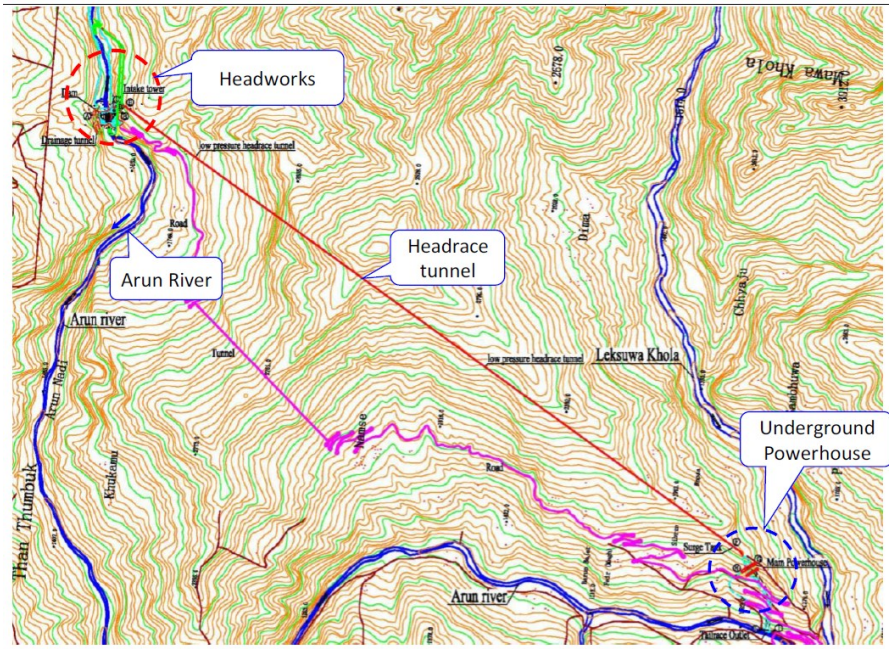

Figure 4.2 General layout of the project (Adapted from report ANNEX H-1)

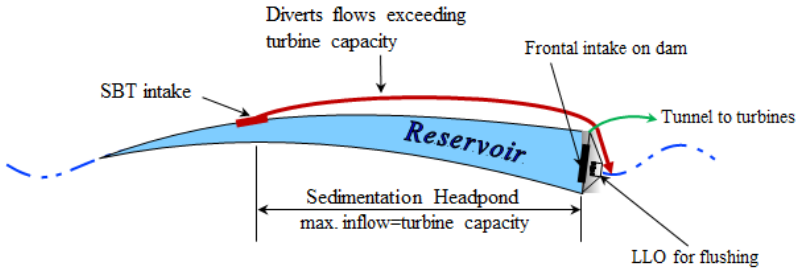

Figure 4.3 Conceptual configuration (Adapted from report ANNEX H-3)

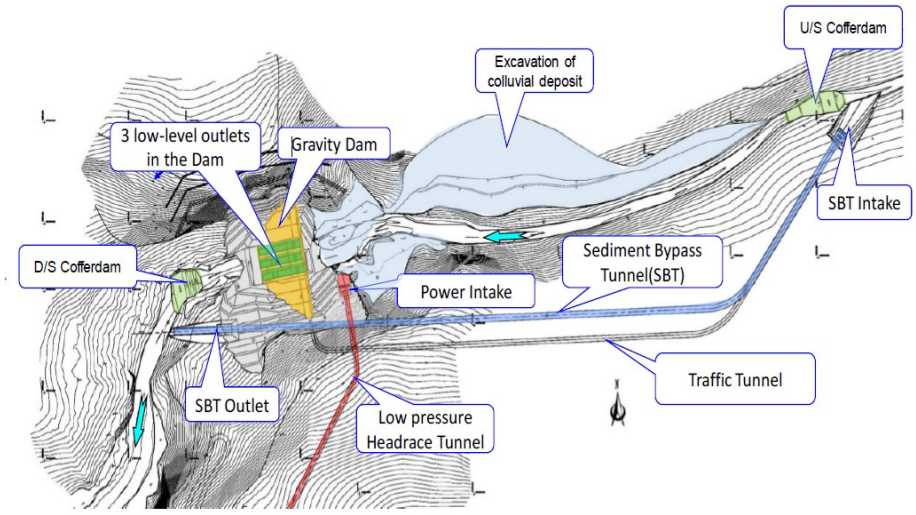

Figure 4.4 General layout of headworks (Adapted from report ANNEX H-3)

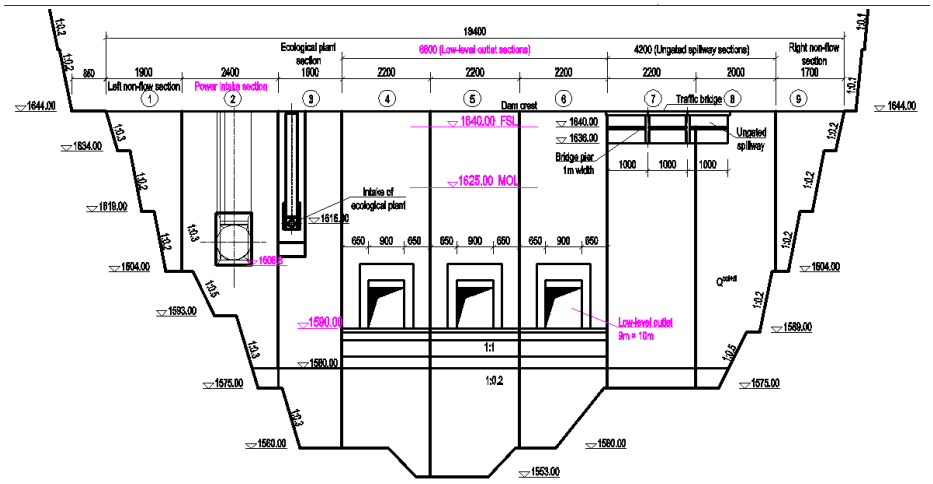

Figure 4.5 Upstream view of dam (Adapted from report ANNEX H-3)

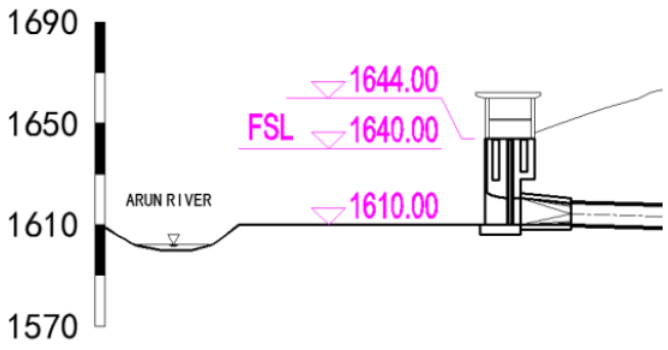

Figure 4.6 Longitudinal profile of SBT intake (Adapted from report ANNEX H-3)

4.2 Hydrology

Arun river originates from a glacier on the north slope of Mt. Xixabangma Feng, a part of the Himalayan range in the south part of Tibetan highland, and is locally called as Pum Qu within Tibet, China. The catchment area of the proposed UAHEP dam is 25,700km^2 of which about 98% lies in Tibetan part and only 2% lies in Nepal. The Tibetan portion belongs to cold, arid zone with less precipitation whereas the Nepalese portion belongs to mild climatic zone with higher precipitation. The annual mean river discharge of Arun river is 217m^3/s and the average annual runoff is 6.69 x 109m^3. The seasonal distribution of the precipitation in the project area within Nepal is dominated by rainy season i.e. June to October, when the monsoons bring about 90% of the annual precipitation. Due to the high elevation and low temperatures in most parts of the Arun River basin, a certain portion of the precipitation is in the form of snow. The probable maximum flood (PMF) and glacial lakes outburst flood (GLOF) at dam site are 4,400m^3/s and is 7,822m^3/s respectively. Annual average temperature on Tibetan side (Dingri County region) is 3ºC and maximum and minimum temperatures of 14ºC and -26.4ºC respectively. Annual temperature

difference is 18ºC, with the average temperatures in July and January of 12ºC and -7.5ºC respectively.

4.3 Sediments

The riverbed of UAHEP is mainly composed of block stones, pebbles and silt. The annual mean sediment inflow from the Arun river basin above the dam site is 16.15 x 10^6t, of which the suspended load is 13.81 x 10^6t, the bed load is 2.43 x 10^6t. The annual average suspended sediment concentration (SSC) is 2.013kg/m^3. About 98.84% of the annual suspended sediment load occurs in the monsoon, June to October. As per the report "ANNEX H-3 Preliminary Results of the Sediment Physical Model", of the total suspended load 70% are finer than 1mm and the median diameter is 0.057mm. Similarly, the median diameter of the bed load is 208.7mm. The ratio of reservoir storage capacity over the annual mean sediment load is about 0.4, which is characterized by high head, small storage capacity, and heavy load of abrasive quartz sediment.

4.3.1 Grain size distribution

The grain size distribution of the suspended and the bed load as per the report "ANNEX H-3 Preliminary Results of the Sediment Physical Model" are shown below:

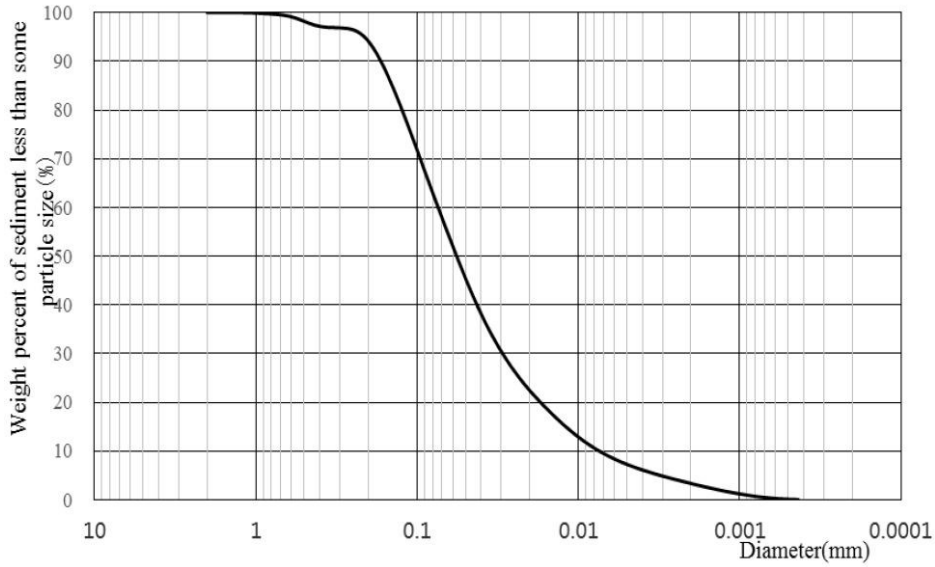

Figure 4.7 Measured grading curve of SSL (Adapted from report ANNEX H-3)

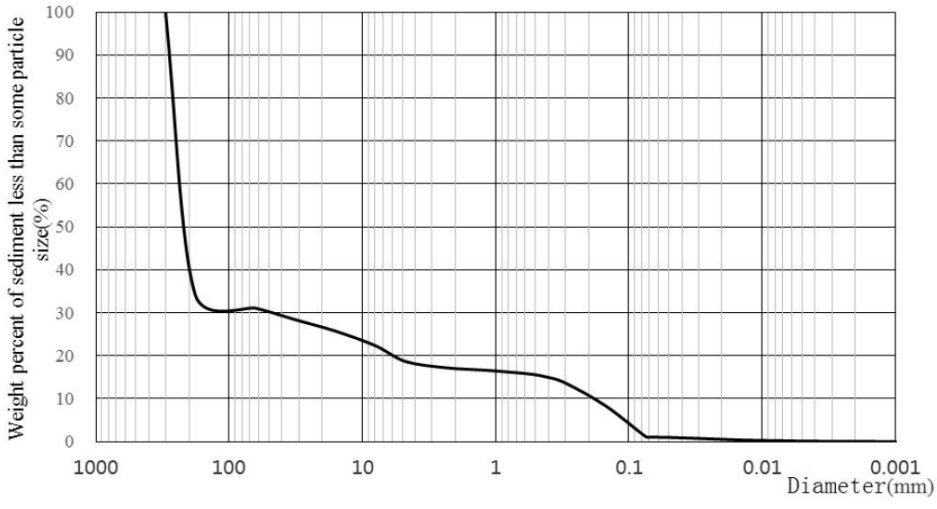

Figure 4.8 Measured Grading curve of bed load (Adapted from report ANNEX H-3)

4.4 Operational Mode of Reservoir

For the sustainable operation of the UAHEP peaking reservoir, following operational mode have been proposed and are being rectified using the physical hydraulic model. The proposed operation mode aims to pass the flood discharge and the suspended load via SBT; and the deposited bed load via the bottom outlets. As per the physical model study, it seems that the operational mode is capable of bringing the reservoir to its initial state at the end of monsoon. The mode consists of six flushing with each flushing extended for two continuous days.

4.4.1 Daily peaking operation mode

When the inflow (excluding the ecological flow) is less than the full discharge of the available units (excluding the maintenance units), a daily peaking operation mode will be adopted. Details are as follows:

1) From 24 p.m. to 6 p.m., when the reservoir water level is lower than 1,640masl (Full Supply Level), the water level will be allowed to gradually rise at a rate of no more than 2.5m/h; after the reservoir water level reaches Full Supply Level, all the inflow will be used as discharge for power generation.

2) From 6 p.m. to 24 p.m., the power plant will operate in peaking mode, with a firm capacity of not less than 697MW, and controlling the drawdown rate of the reservoir water level at not more than 2.5m/h.

4.4.2 Flushing operation mode

From June to October, when the inflow is larger than or equal to 575m^3/s, an enforced outage operation mode will be applied, and the SBT will be shut down. The following operations will be adopted:

1) The LLOs will be opened to lower the reservoir water level for 2-days of continuous sediment flushing, under the following conditions:

- The drawdown rate of the reservoir water level is not more than 2.5m/h;
- After emptying the reservoir, the discharge for power generation will be equal to the inflow.

2) After sediment flushing:

- When the inflow is less than 1,050m^3/s (50% frequency peaking flood means 2-year return period flood), the LLOs will gradually be closed; the reservoir water level should be allowed to rise at a rate of no more than 2.5m/h. After the reservoir water level rises to 1,635masl, the SBT will be opened and all available units will operate for power generation for at least 7 days until the next sediment flushing cycle starts.
- When the inflow is equal to or larger than 1,050m^3/s (50% frequency peaking flood), an enforced outage mode will be adopted, and the SBT will be shut down; the LLOs will be fully open for sediment flushing (the drawdown rate of the reservoir water level shall not exceed 2.5m/h), until the inflow is less than 1,050m^3/s; then this operation mode is suspended.

4.4.3 Annual operation mode

1) From November to May of the next year

- When the inflow is less than the full discharge of the available units, a daily peaking operation mode is adopted.
- When the inflow is equal to or larger than the full discharge of the available units, these units will run at the designed discharge, the

reservoir water level will be maintained at 1,640masl and the excess water will be discharged through the LLOs.

2) From June to October

- When the inflow is less than or equal to 235.44m^3/s, the operation mode will be the same as that described above for November to May.
- When the inflow is larger than 235.44 m^3/s, but less than 575m^3/s, the SBT will be open, and the available units will run at their designed discharge. The excess water will be diverted through the SBT.
- When the inflow is larger than or equal to 575m^3/s, sediment flushing operation mode will be applied.

4.5 Physical Hydraulic Model

The dam reach of UAHEP is characterized by large quantity of sediments during monsoons with high abrasive mineral, quartz. When the project is put into operation, the water level will be raised to FSL 1,640masl (70m high than the initial bed level i.e. 1,570masl), the flow velocity will be reduced, thus resulting in sediment deposition in the reservoir area. A high rate of sedimentation in the reservoir will exert severe effect on the regulation capacity of reservoir and abrasion of the turbines. Therefore, a physical model study was planned to verify and optimize the layout scheme of the headworks and dispatching operation mode of the reservoir.

As per the requirements, the physical model has been set up with a 1: 50 scale using Froude law at the River house of Yangtze River Science Academy in Wuhan. The model area is about 2.2 km in the upstream of the dam site and about 0.6 km in the downstream. As both suspended and bed

load are used simultaneously in the model, the suspended sediments are modelled by light weight Zhuzhou clean coal with specific gravity 1.33 and dry bulk density 0.75-0.9 t/m^3. Whereas, for the bed load, pebbles with density 2,650kg/m^3 has been used. The suspended and bed load are scaled using the grain size scale 1.2 and 50 respectively as shown in Table 4-2 and Table 4-3. These tables have been taken from the report "ANNEX H-3 Preliminary Results of the Sediment Physical Model".

Table 4-2 PSD of prototype and model suspended sediment

Weight percent of sediment less than a certain particle size (%)	6.17	11.26	19.33	31.59	50.00	83.64	96.95	98.63	99.60	99.96	100.00
Prototype sediment (mm)	0.004	0.009	0.016	0.032	0.057	0.150	0.30	0.60	0.96	1.20	2.00
Model Sediment (mm)	0.003	0.007	0.015	0.025	0.048	0.125	0.25	0.50	0.80	1.00	1.67

Table 4-3 PSD of prototype and model bed sediment

Weight percent of sediment less than a certain particle size (%)	17.2	20.2	24.26	27.25	29.08	29.95	32.08	45.23	50	100
Prototype sediment (mm)	2.36	6.25	12.5	25	40	50	100	200	210	300
Model Sediment (mm)	0.048	0.125	0.25	0.5	0.8	1	2	4	4.2	6

As per the report "ANNEX H-3 Preliminary Results of the Sediment Physical Model", initially, the physical model tests were conducted for various discharges with the water levels at 1,625masl and 1,635masl. For 1,625masl, delta head of the bed load was at 1,200m away from the dam causing SBT to lie in a variable backwater area. Whereas, for 1,635masl, delta head was at 1,500m from the dam and had no effect to water level at SBT. For the numerical modelling, 1,625masl has been considered with discharge 877m^3/s. As discharge considered for numerical modelling i.e.

877m^3/s, is after flushing of the reservoir for three times, it has been considered that the delta will have very less effect on the water level near SBT. However, various attempts have been made to check if there are any effects of delta. The Table 4-4 below shows the flushing and SBT operation modes used in physical model. The highlighted discharge is taken for the numerical model simulation and the ones in Italics are for flushing. An extended version of this table can be referred in *Appendix B - Project Description Table B. 1.* Further, the physical hydraulic model setup with initial SBT and modified SBT are also shown in Figure 4.10 and Figure 4.11. Also, materials for roughening the river banks to achieve appropriate roughness as that of prototype is shown in Figure 4.12.

Table 4-4 Model test elements

Time	Days	Inflow	SCC	Bed load	Reservoir level	SBT	Intake	LLOs	Ecological
		m^3/s	kg/m^3	kg/s	masl	m^3/s	m^3/s	m^3/s	m^3/s
1986.6.26 - 6.27	*2*	*623*	*2.885*	*305.55*	*1595.28*	*0*	*0*	*617.59*	*5.41*
1986.6.28 - 6.30	3	760	3.99	515.51	1625	516.75	237.84	0	*5.41*
1986.7.1 -7.14	14	467	1.822	144.66	1625	223.75	237.84	0	*5.41*
1986.7.15 - 7.16	*2*	*726*	*3.7*	*456.65*	*1595.85*	*0*	*0*	*720.59*	*5.41*
1986.7.17 - 7.18	2	653	3.105	344.69	1625	409.75	237.84	0	*5.41*
1986.7.19 -7.23	5	742	3.814	481.1	1625	498.75	237.84	0	*5.41*
1986.7.24 - 7.25	*2*	*794*	*4.26*	*575.01*	*1596.21*	*0*	*0*	*788.59*	*5.41*
1986.7.26 - 7.27	**2**	**877**	**5.005**	**746.2**	**1625**	**633.75**	**237.84**	**0**	***5.41***
1986.7.28 - 8.1	5	754	3.928	503.49	1625	510.75	237.84	0	*5.41*
1986.8.2 - 8.3	*2*	*770*	*4.065*	*532.11*	*1596.08*	*0*	*0*	*764.59*	*5.41*
1986.8.4 - 8.17	14	488	1.96	162.6	1625	244.75	237.84	0	*5.41*
1986.8.18 - 8.19	2	552	2.37	222.4	1625	308.75	237.84	0	*5.41*
1986.8.20 - 8.21	*2*	*605*	*2.755*	*283.35*	*1595.18*	*0*	*0*	*599.59*	*5.41*
1986.8.22 - 8.25	4	558	2.413	228.9	1625	314.75	237.84	0	*5.41*
1986.8.26 - 8.27	2	607	2.76	284.8	1625	363.75	237.84	0	*5.41*
1986.8.28 - 9.11	15	454	1.732	133.68	1625	210.75	237.84	0	*5.41*
1986.9.12 - 9.13	*2*	*610*	*2.785*	*288.8*	*1595.21*	*0*	*0*	*604.59*	*5.41*

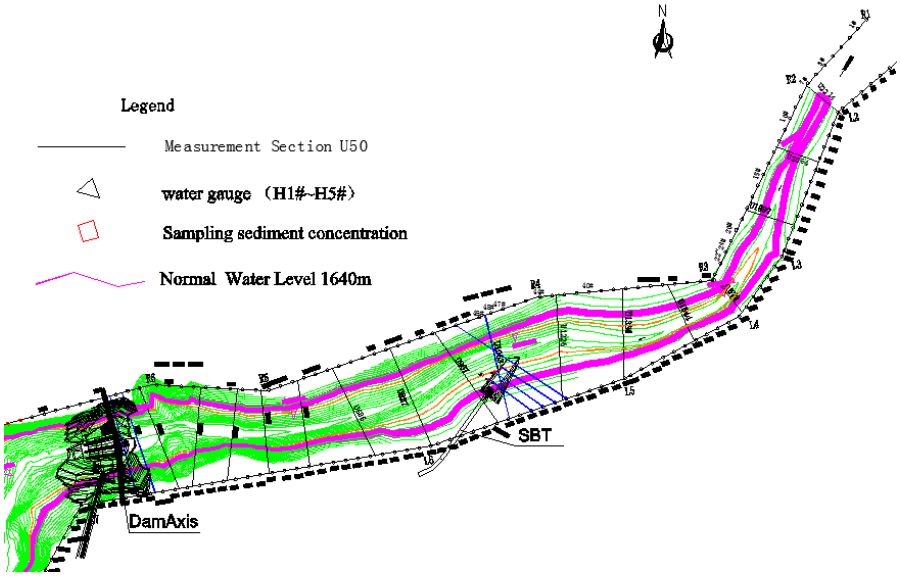

Figure 4.9 Location of dam, initial SBT and 1,640masl water level (Adapted from report ANNEX H-3)

Figure 4.10 Initial SBT (left) from report ANNEX H-3 and modified SBT intake (right) (Adapted from report ANNEX H-2)

Figure 4.11 Initial SBT and modified SBT location (#2) (Adapted from report ANNEX H-3)

Figure 4.12 River banks roughened with blocks and plastic straw mat (Adapted from report ANNEX H-3)

5 Grid Generation for Numerical Model

As per objective of the study, headworks, mainly the SBT part has been numerically modelled. For generating grid, initial information of the headworks topography has been obtained from the drawings provided by Upper Arun Hydro Electric Limited. This drawing has been scaled down to the model scale of 1:50 using *AutoCAD* software and the boundary for numerical modelling has been set from 748.62m to 1,593.45m measured from the dam. Although some extra portion (from 550.119m to 1,692.2m) were considered for generating the geodata file. A geodata file consists of x, y, z coordinates preceded by a letter E; and a letter Z is used at the end to indicate the last line of the file (Olsen, 2018). A typical example of geodata file is presented in Figure 5.1

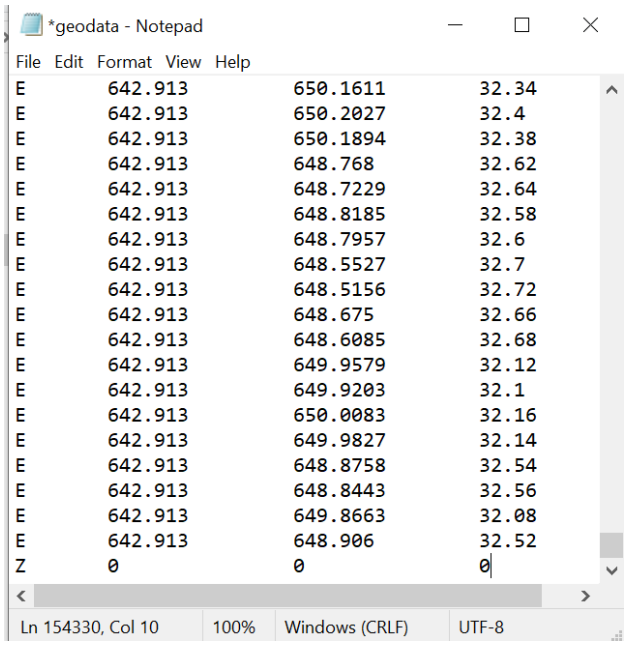

Figure 5.1 Geodata file

The points of the geodata file can be viewed in the graphical interface of SSIIM called the grid editor. The points with different water depth are specified with different colors. Whereas, all points with same color in the grid editor specifies error in the geodata points. A 2-D grid is created in xy-plane as per the topographical requirements and the vertical number of cells are specified in G 1 and G 3 data set of the control file. This will form a 3-D grid easily from a 2-D grid plane, which is a specialty of finite volume method. These grids can be either multiblock or single block (Olsen, 2018).

5.1 Grid Options

UAHEP has a protruding SBT section on the left bank, therefore, it is difficult to make a proper grid as per the rules specified in Section 3.5. However, three different ways have been tried upon to make appropriate grid for UAHEP. Among the three methods, one method includes making a single bigger grid than required and extruding the required part using F 112 data set. As this option requires higher elevation than water surface (numerical modelling water level is 1,625masl), geodata file is made to incorporate features till 1,640masl. These water levels when converted to model scale will be 32.5masl (1,625masl in prototype scale) and 32.8masl (1,640masl in prototype scale) respectively. The second option is similar to the first option, with a difference in making grid lines at SBT. Finally, the third option uses multiblock to create grid.

In first option, a single rectangular block bigger than water body, including the SBT has been created. The grid number in xy-plane are specified such that the grid cells along streamwise direction are made somewhat longer than the transverse direction. The water level specified in W 1 data set defines the water surface for the grid generation. The grid is generated at this water level with only wet cells and *unstruc* file have been written.

Inflow and outflow are specified in this file. At this moment, the water level is higher than the required level, therefore, F 112 1 data set has been invoked in control file to lower down the grid to the required level. Before, invoking the F 112 data set, a *koordina* file with initial water level has to be made by modifying the *koordina.t* file. The F 112 1 data set reads the original *unstruc* file and water level from *koordina* file and hence the grid is generated at the required water level as a single block (Olsen, 2018; Nepal, 2019).

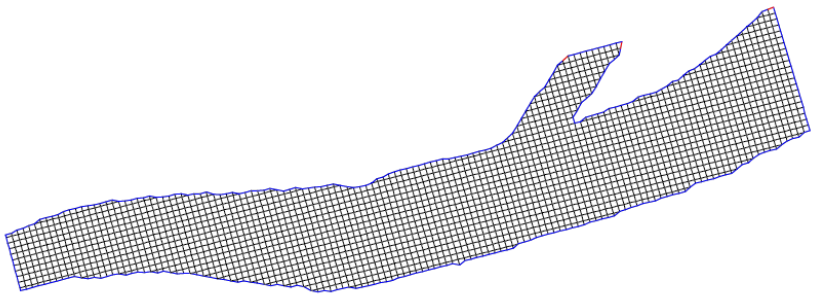

Figure 5.2 One block grid (Option 1)

This approach is easy and quick to make a complex geometry with orthogonal and uniform sized grid cell. Further, it is advantageous when one has to make finer grid. However, the longer parts of the cells in SBT may not be aligned along the streamwise direction as well as the bed level interpolation for outer lining of SBT may vary, forming a zigzag boundary.

The second option is similar to the first, except that the grid nodes of the block are dragged on to the boundary of desired location in grid editor. This make it possible to align the whole grid along stream wise direction. However, exact orientation may not be achieved. Further, all the grid lines in this option are used, in comparison to first option, where some grid above

required water level are excluded. Initially, in this option, grid near SBT are aligned along SBT followed by adjusting the grids of main river, which are dragged along boundaries to adjust the whole grid.

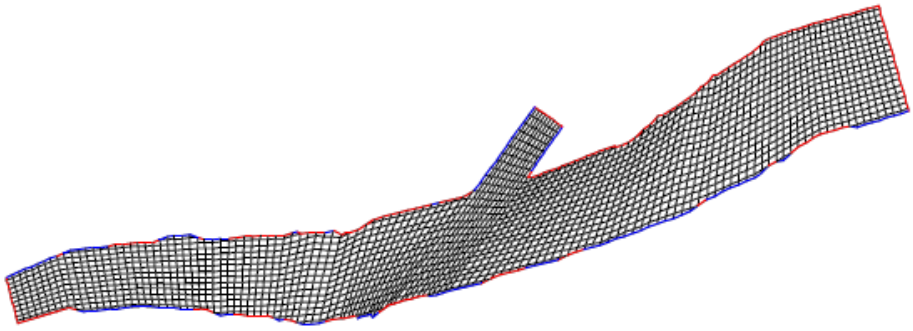

Figure 5.3 One block grid (Option 2)

This method provides an option to align grid along river direction as well as minimizes deformations on the outer lining or boundary of SBT. However, it is a time-consuming method and the grid cells can't maintain its uniformity.

Finally, the third option is a multiblock option, where more than one block can be created and glued together to represent the whole water surface. This option utilizes the dragging characteristics of second option; however, separate blocks are made for main river and SBT. Therefore, grids can be aligned along the streamwise direction properly. However, number of gridlines of main river in the vicinity of SBT, determines the number of grid lines in x direction of SBT, thereby, making a coarser grid in SBT.

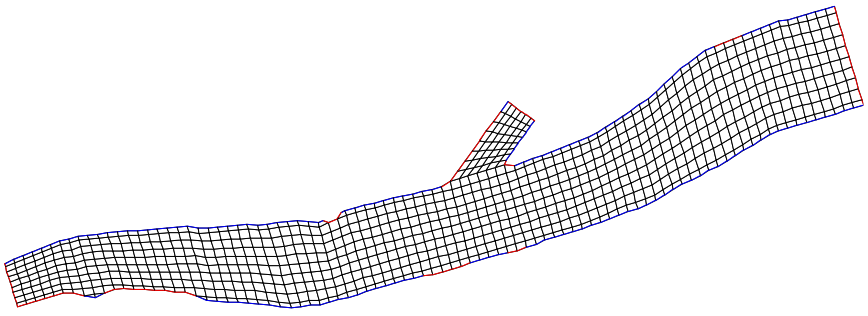

Figure 5.4 Multiblock grid (Option 3)

This grid is easy to make and provides desired regular outline in SBT. Similarly, grids along main river and SBT can be aligned along respective streamwise direction.

All these three options have been modelled for same parameters and results for velocity are similar (*Refer Appendix C - Grid Generation for Models Figure C. 1)*. Among these, higher divergence problem was seen in Option 1 due to the boundary cells being triangular when F 112 1 data set is used. Similarly, the divergence problem co-exists in the Option 2 also, due to the higher accumulation of cells near SBT region. Whereas, due to the smooth boundary in case of Option 3, divergence problems are minimized providing a stable solution. As a stable solution is achieved as well as the time required to construct the grid is less in multiblock option (Option 3), it has been considered for further analysis.

5.2 Discharge Input

Since the SSIIM 2 grid is unstructured, it is not possible to provide inflow and outflow discharges as well as flow of other constituents directly in control file. Therefore, discharges are set out in the graphical interface called discharge editor. In this interface, inflow and outflow locations along with discharge values can be specified. There can be more than one inflow

and outflow discharge groups, however, the continuity of flow must be maintained. That means, sum of the inflow discharge must be equal to the outflow discharge. After specifying the discharge, it should be saved by writing the *unstruc* file.

5.3 Grid Generation and Conformity

For the calibration of the numerical model, only the surface velocities at different cross sections of the physical model are available. These velocities were measured for different discharges and bed deposition. Availability of few cross sections for the bed deposition at each discharge and lack of measurement time for the surface velocities in the physical model test report, made it very difficult to finalize the grid. In an attempt to replicate the physical model surface velocity (PMSV) in numerical model, various bed deposition options have been carried out and finally one set up is chosen. For all the options, the grids are made with multiblock grid option. Previously, while selecting the multiblock option, some preliminary grid sensitivities had been carried out. The results suggested that the main river grid with block size of 260 * 21 had little difference in flow pattern and magnitude as compared to finer grid of 500 * 40. As it is evident that, with the finer grid, the convergence is slower and the simulation time is higher, the coarser grid with a block size of 271 * 41 had been selected for the main river. Whereas, for the SBT, the x direction grid number is controlled by the number of main river grid in the vicinity of SBT intake. While the y direction grid number, is considered based on maintaining the cell size, longer along the flow direction. Therefore, in general, the block size of SBT is 12 to14 * 18 to 20.

Typically, the model cell size varies as we move from upstream to downstream. The cell sizes in x * y directions are 7cm * 1 cm, 5 cm * 3 cm

and 5cm * 4cm for the main river. This variability in the cell size is due to the river geometry which is represented by a narrow upstream part and wider downstream part. Therefore, on increasing the number of the grid lines in x direction, would have made the cells at downstream part smaller in streamwise direction. This would eventually cause the grid cells to be square or longer in transverse direction increasing the false diffusion. The total number of cells for a typical grid of 877m^3/s discharge without any bed rise is 62,794. Initially, the grid had 10 cells in vertical direction which has been further reduced to 5 cells based on the k_s value.

5.3.1 Bed deposition and associated grid types

Among different bed deposition contours prepared, some of them are discussed here. At first, only the initial contour of the river topography with cross sections were available in the form of *AutoCAD* drawing. For the bed deposition, excel plot of few cross sections namely U500, U967, U1226, U1544, U1672 and a longitudinal profile of deposition along the initial thalweg were available (Figure 5.6, Figure 5.7, Figure 5.8 and Figure 5.9). The representation U500 means, the cross section is at 500m upstream from the dam. Similarly, among various discharges, the highest 877m^3/s has been considered for the development of bed deposition contour. At this discharge, the SBT might lie in the variable backwater flow area i.e. between 1200m to 900m from the dam, due to the delta head (Figure 5.5). Since, the model has been made for bed deposition after flushing, it is assumed that the delta has very minimal effect on backwater level at SBT.

However, to be sure of the effects of delta head, the model has been initially prepared such that inflow in model would be provided at 1,593.5m and 1,226m from the dam (Refer *Appendix C - Grid Generation for Models Figure C. 2*). The 1,593.5m would include the delta head deposition as well

as incorporate the bend effects above the SBT. Whereas, 1,226m would avoid the delta head as well as the bend effect. This would ensure that the delta head had least effect on the model as well as provide the significance of including the bend effect, which is ignored in 1,226m model. Some representative bed deposition cross sections and longitudinal profile of thalweg are plotted below. The orange line at the middle of the river, in Figure 5.6, represents the initial thalweg. Similarly, five red lines are the available bed deposition cross sections in which line near the dam represents U500 cross section. The Figure 5.7 and Figure 5.8 represents the deposition at thalweg before and after flushing respectively. For the bed deposition contour preparation, date 1986.7.25 representing 877m^3/s (as per Table 4-4) after flushing has been considered. The data from these plots were extracted using *AutoCAD* software and analysed in *Microsoft excel.* Available deposition cross sections are shown, starting from *Appendix C - Grid Generation for Models Figure C. 3 till Figure C. 7.*

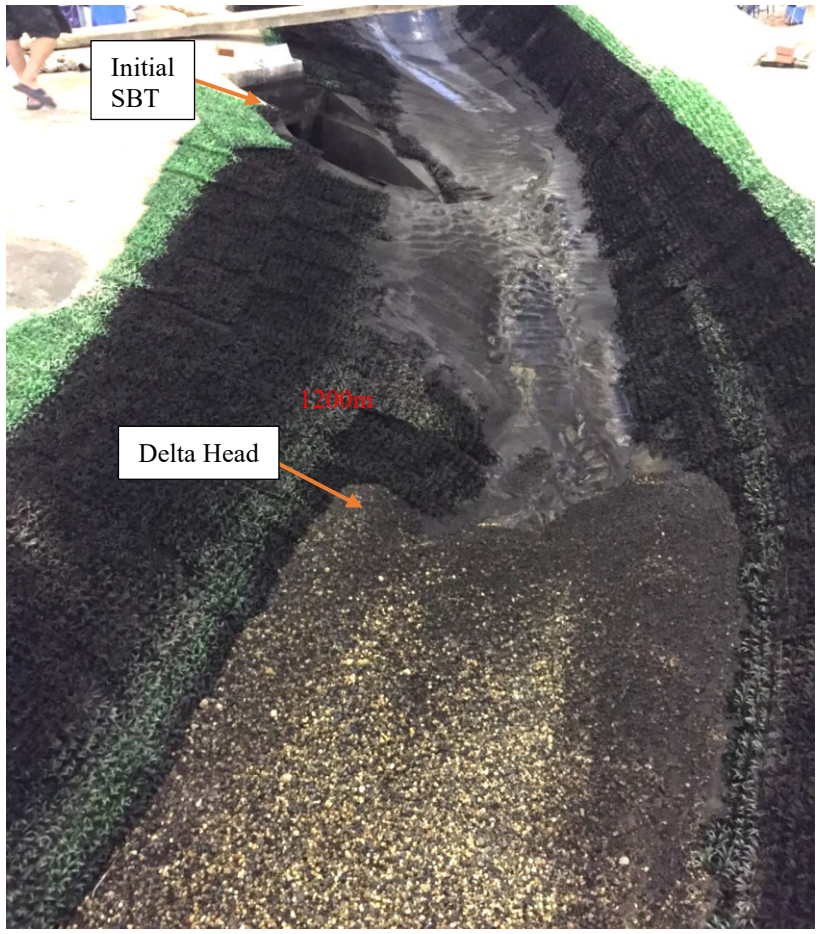

Figure 5.5 Delta head upstream of initial SBT before flushing (Adapted from report ANNEX H-3)

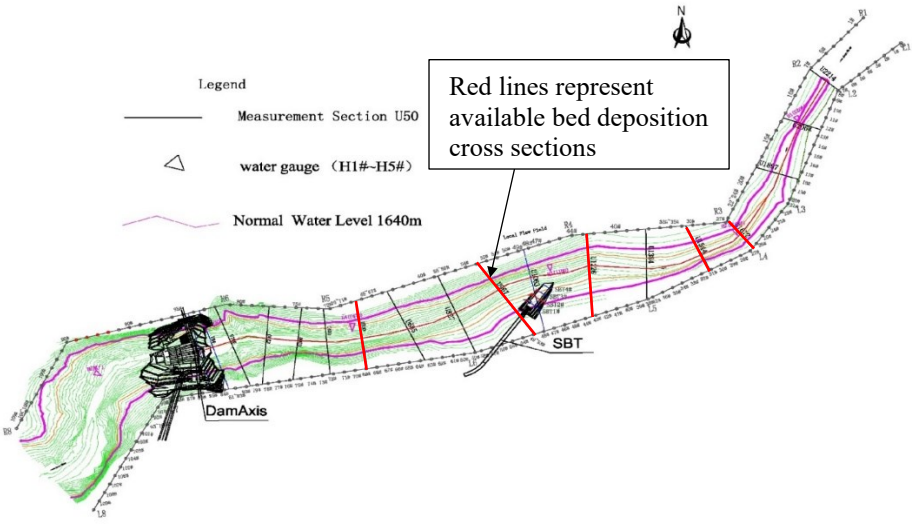

Figure 5.6 Plan view of measurement cross sections for bed deposition (Adapted from report ANNEX H-3)

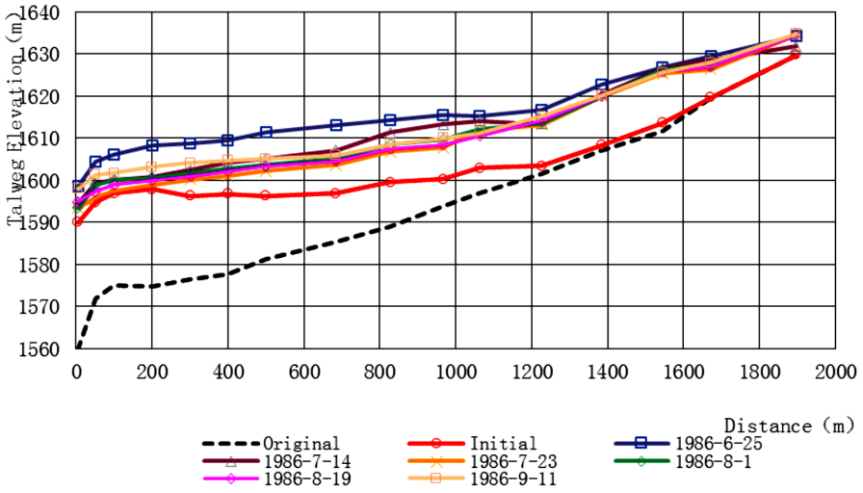

Figure 5.7 Thalweg at start of every flushing (Adapted from report ANNEX H-3)

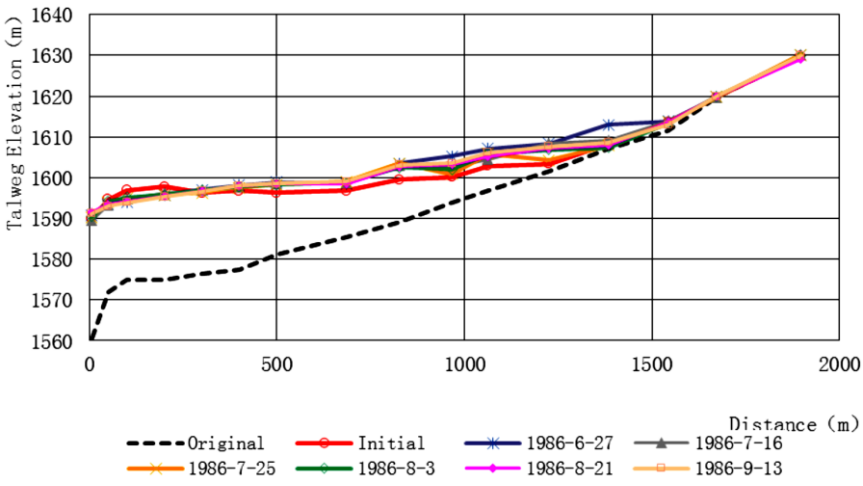

Figure 5.8 Thalweg at the end of every flushing (Adapted from report ANNEX H-3)

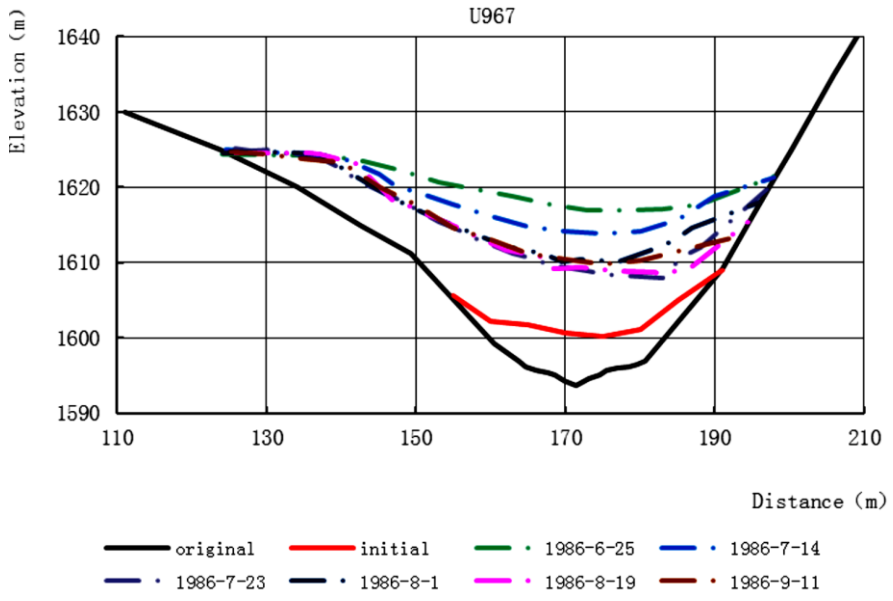

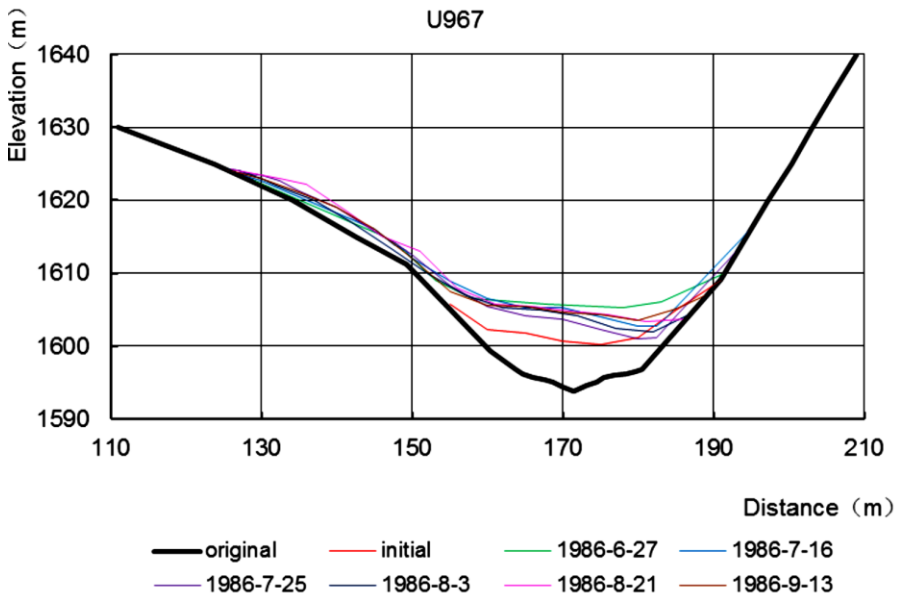

Figure 5.9 Before (upper) and after (lower) flushing cross sections at 967m (Adapted from report ANNEX H-3)

The extracted data from the plots and the initial topographical data of the river have been merged to obtain the bed deposition contour using the *Golden Software: Surfer*. The *Surfer* uses kriging method to interpolate elevation between points and develop the bed contour. However, the contours consisted of plateau areas which have to be manually rectified before running them again in *Surfer* to obtain the finalized contour. An example of rectification can be seen from Figure 5.10 to Figure 5.12.

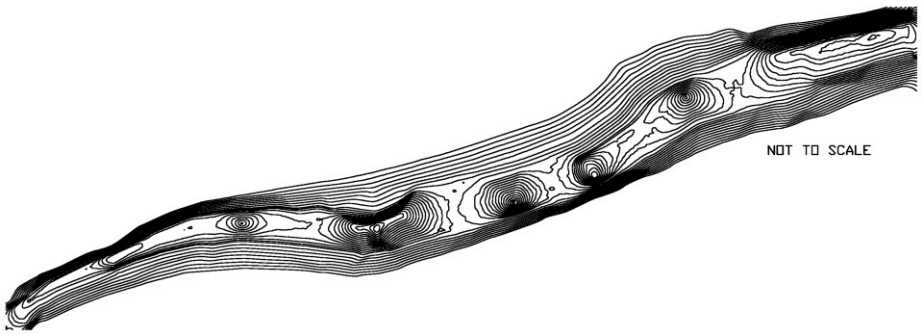

Figure 5.10 Initial contour from Surfer

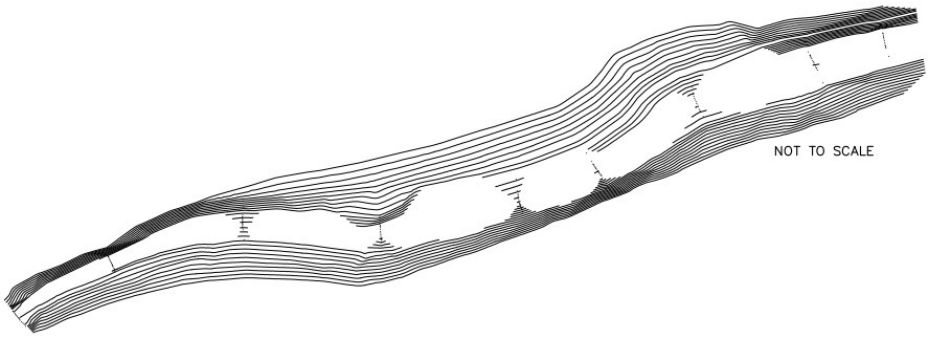

Figure 5.11 Modified for recontouring

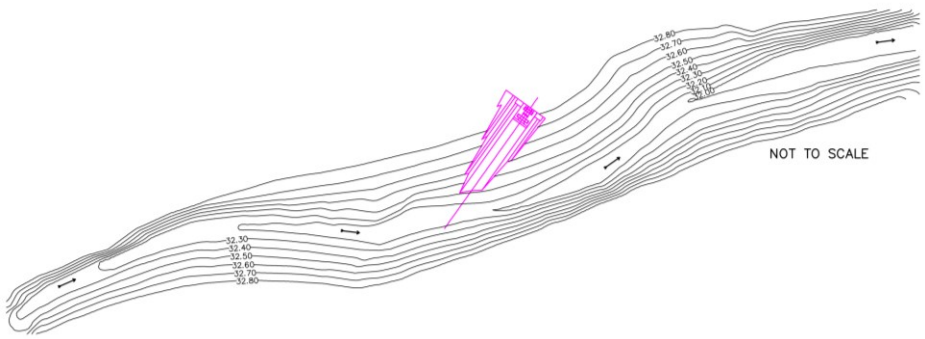

Figure 5.12 Final contour for SSIIM model

A hydraulic simulation using roughness value (k_s) 16.9mm, model inflow discharge 0.04961m^3/s and outflow discharges 0.03587m^3/s from SBT and 0.01374m^3/s from main river has been carried out for both 1,593.5m and

1,226m. The results showed that the flow couldn't develop properly in 1,226m model in the upstream section above SBT. However, in both the cases the magnitude of the surface velocity is lower as compared to the physical model surface velocity. This might be due to the relocation of the delta head owing to the flushing, which might have increased the bed elevation in the physical model, thereby reducing the depth and increasing the velocity at these sections. These have been further discussed in the hydraulic simulation part. However, considering the length required to develop the inflow discharge and incorporating the bend effect 1,593.5m, model has been considered for further analysis.

As the velocity magnitude and the pattern at some section didn't match, due to inconsistent bed geometry, various bed rise options have been considered. These are:

- Option 1: Without bed rise: This option is the same one described above for 1,593.5m. The bed deposition contour generated from *Surfer* is used for the hydraulic simulation.
- Option 2: With 4cm bed rise: The whole option 1 bed deposition has been risen by 4cm except the SBT part.
- Option 3: With 8cm bed rise: The whole option 1 bed deposition has been risen by 8cm except the SBT part.
- Option 4: Combination of no bed rise and 8cm bed rise: In this option, certain portion upstream of section 3 is kept at its initial state as of Option 1. While the bed for the remaining section has been risen by 8cm.

All these options are hydraulically simulated for different roughness value (k_s) and the best option representing the physical model surface velocity magnitude and pattern is selected.

5.3.2 Problems faced

Due to the unavailability of bed deposition data, bed deposition contours had to be generated from the graphical plots as shown in Figure 5.9. As the scale of the cross-section map (Figure 5.6) and graphical plot differed, it was difficult to extract data. Similarly, the scale of the cross section map (Figure 5.6) differs between each cross section, making it further difficult to insert the data at exact location of *AutoCAD* drawing for contour generation.

6 Hydraulic Simulation

It was difficult to adopt final bed deposition contour and the grid, so, the hydraulic simulation and grid finalization have been carried out simultaneously. The hydraulic simulation is very important and should be stable before any sediment simulation. Generally, discretization scheme, boundary roughness, grid size, discharge etc. are finalized by the hydraulic simulation for use in sediment simulation.

6.1 Data for Model Validation

Before starting the hydraulic simulation, the data for calibrating the model had to be predefined. These are the surface velocities at different cross section of the physical model test carried for 877m^3/s discharge at 1,625masl water level. The different cross sections have been defined from upstream to downstream as shown in Figure 6.1. Similarly, the Figure 6.2 shows surface velocities along the cross sections, in the physical model, which were extracted using *AutoCAD* software and *Microsoft Excel*. The detailed tabulated surface velocities for each cross section can be referred in *Appendix D - Hydraulic Simulation - Details of Surface Velocities*

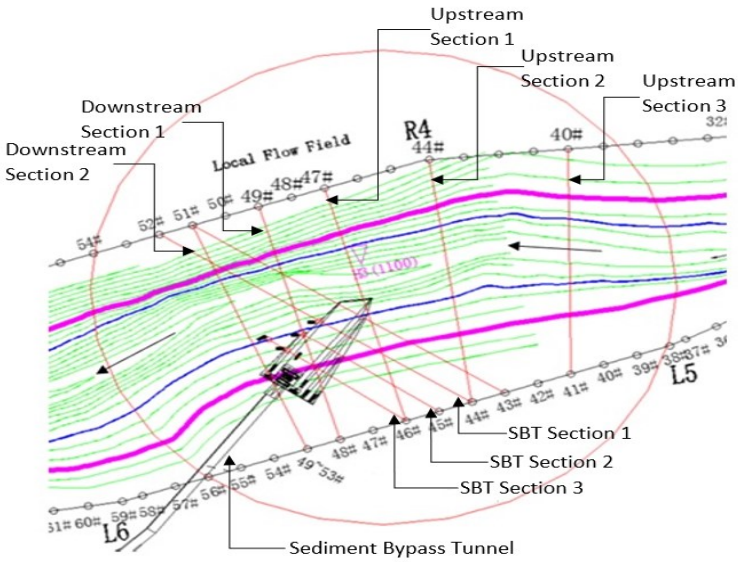

Figure 6.1 Plan showing different flow velocity measurement sections

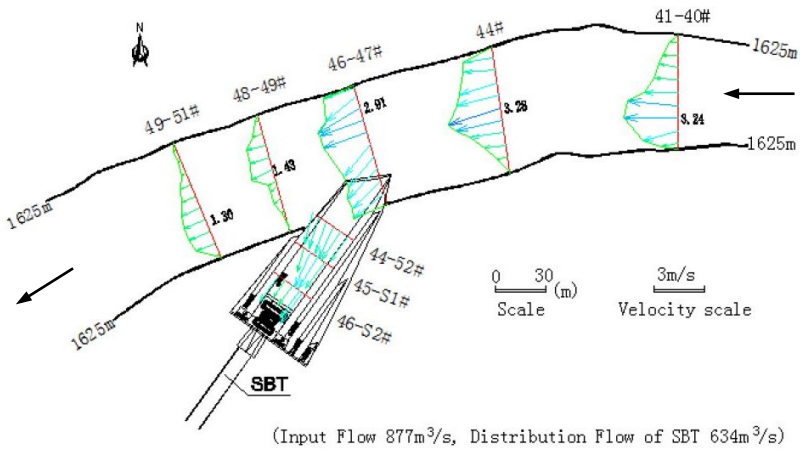

Figure 6.2 Physical model surface velocities for 877m^3/s

6.2 Roughness for the Model

As per the report "ANNEX H-3 Preliminary Results of the Sediment Physical Model", the Manning's roughness for prototype channel in the experimental reach is 0.06-0.12, which is converted to the physical model value of 0.031-0.063 using a scale factor of 1.92. Further, the bank slopes are roughened to a range of 0.0274-0.08 using the dense plastic straw mat to achieve similar resistance to prototype (Changjiang Survey and Sinotech Engineering Consultants, 2019a). Figure 4.12 can be referred for observing the placement of blocks and plastic straw mat in river banks. When these values are converted to Strickler's coefficient (k_{st}), the k_{st} ranges from 12.5 to 32.25 which when used in W 1 data set will yield a very high value for roughness (k_s) in numerical model. The k_s in model is calculated using the Van Rijn's formula

$$k_{st} = \frac{26}{d_{90}^{1/6}};\ k_s = 3d_{90} \tag{11}$$

As such a high value of k_s is not physically true, the roughness (k_s) has been calculated using d_{90} value for bed load. The prototype d_{90} is equal to 283.02mm which converted to model scale becomes 5.66mm. The resulting k_s is equal to 16.9mm. This value is initially used in F 16 data set, which is further reduced to see the effects of lower roughness. The F 16 data set specifies roughness coefficient on side walls and bed of the model.

6.3 Simulation Criteria and Input Data

A steady state computation with fixed water surface and fixed bed has been considered for hydraulic simulation. The water surface level is kept constant at 32.5masl (1,625masl in prototype) using W 1 data set and

koordina file. The inflow discharge 0.04961m^3/s (877m^3/s in prototype) is provided at the upstream end. Whereas, 0.03587m^3/s (634m^3/s in prototype) and 0.01374m^3/s (243m^3/s in prototype) outflow discharges are set up at SBT and main river outlets using the discharge editor. Initial roughness is considered to be 16.9mm which has been further reduced to 3.39mm. First order power-law (POW) scheme for discretization is considered as it provides stable simulation (Olsen, 2018; Hoven, 2010). The river banks are made smoother by changing the shape of the cells near the boundary using F 102 1 data set. As the initial water level for creating the *unstruc* file is higher than the required level, F 112 1 data set is used to lower the water level. The topography for each bed deposition contours has been provided as geodata file. Finally, multiblock option is used to make the grid sizing 271 * 41 and 13 * 19 for main river and SBT blocks respectively. The main input files are *geodata, koordina, control* and *unstruc* file. To obtain surface velocities as output, an interpol file consisting the coordinates for location where velocity profiles are required, has been provided. This is achieved by F 48 5 data set in the *control* file. A detailed description of the data sets and their functions used in input file are provided in *Appendix D - Hydraulic Simulation - Detail Description of Data Set and Their Functions (Input files).*

6.4 Simulation and Results

As per the section 5.3.1, the grid with inflow at 1,593.5m from dam is considered for further analysis. The reasons for considering 1,593.5m grid are the under developed flow in upstream cross sections and exclusion of bend effects in 1,226m. The Figure 6.3 represents the physical model, 1,226m and 1,593.5m surface velocities by green, blue and red lines

respectively. The legend NDCM refers to New bed deposition contour model with inflow boundary either at 1,593.5 or 1,226m distance from the dam in numerical model and k_s represents the roughness height. All models have been termed NDCM since previous simulations were ran with the initial river topography i.e. without bed deposition.

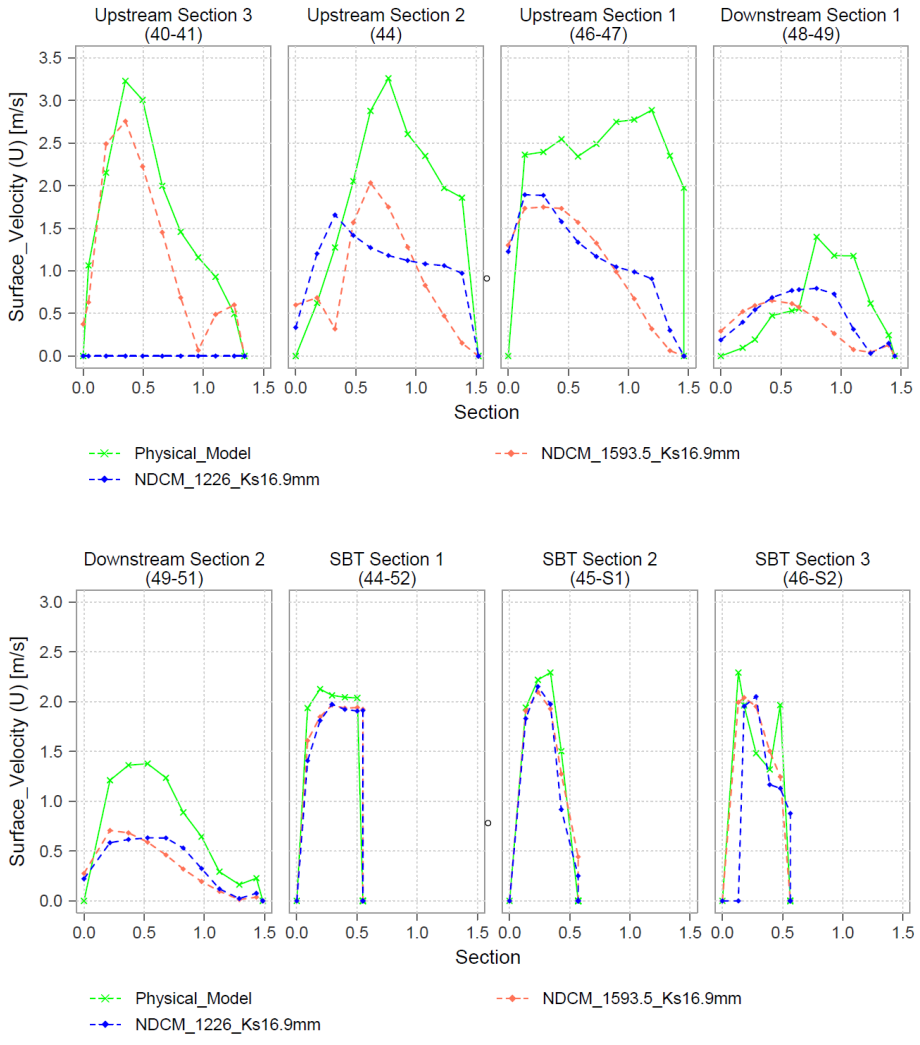

Figure 6.3 Comparison of surface velocity for 1,593.5m and 1,226m

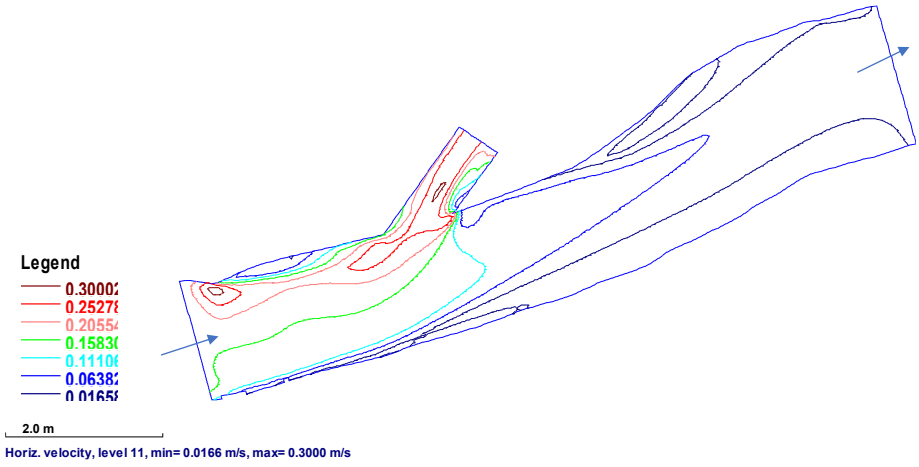

Figure 6.4 Horizontal velocity for inflow from 1,226m

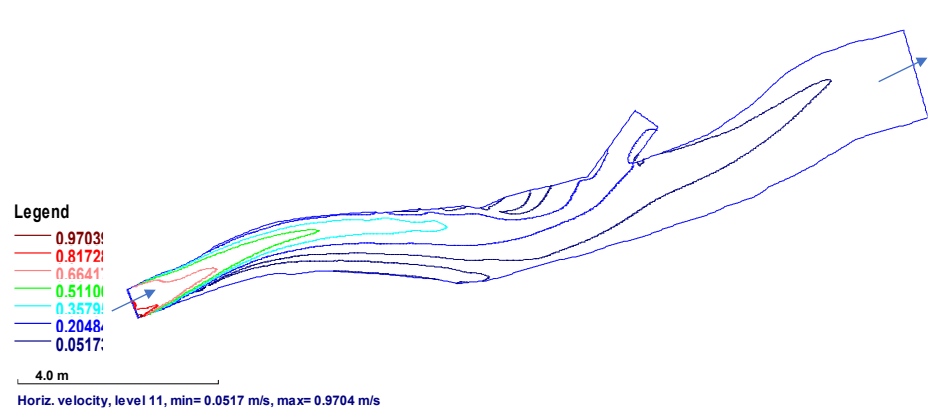

Figure 6.5 Horizontal velocity for inflow from 1,593.5m

As 1,226m model doesn't incorporate upstream section 3, surface velocities for this cross section couldn't be retrieved as seen in Figure 6.3. Similarly, the flow velocity at upstream section 2, shows that the flow has not fully developed. Further, the effect of upstream bend on the flow pattern can be recognised easily from Figure 6.4 and Figure 6.5. In 1,226m, highest velocity is along the left bank whereas, in 1,593.5m, highest velocity has shifted from left bank to middle of river before entering SBT. This would

vary the deposition and erosion pattern during sediment simulation. Thus, 1,593.5m, model has been considered for further analysis.

6.4.1 Simulation for without bed rise, 4cm and 8cm bed rise

Different simulation options as per section 5.3.1, with variable roughness height (k_s) have been carried out. The k_s value has been varied such that k_s becomes smaller than the minimum cell height. The minimum cell height at the river bank is 20mm whereas at the region of maximum depth is 14mm. This is due to the formation of only one vertical cell at river bank compared to other locations where the depth is divided into 10 vertical cells. To begin with, $k_s = 3*d_{90}$, i.e. 16.9mm has been considered, which is further reduced by 50% (8.49mm) and 80% (3.39mm).

In case of **Option 1: without bed rise** (Figure 6.6), magnitude of the surface velocities, compared to physical model, are lower. A relatively better magnitude can be observed for upstream section 3 and SBT sections. Similarly, upstream section 3, upstream section 2, SBT section 1 and SBT section 2 resembles pattern of physical model surface velocity (PMSV). Further, in upstream sections and SBT, velocity magnitude decreases with decrease in ks. Whereas in downstream section, it is just opposite. In case of upstream section 1 and downstream section 1, the velocity magnitude is higher on the left bank rather than right bank. Similarly, depressions in velocity magnitude can be observed for upstream section 3 and upstream section 2 at right and left side respectively. This may be due to the re-circulation zone at those locations. Likewise, a similar depression can be observed in PMSV at SBT section 3. This might be due to the vortex formation at SBT outlet as observed in physical model (Figure 6.7). However, no such vortex is seen in numerical model which might be attributed to the difference in outlet geometry. The SBT outlet at physical

model has a bottom outlet whereas in numerical model, it is free flow open end. A peculiar observation for this option is that, magnitude of the velocities is almost same as well as no shift in the flow or velocity pattern from left to right bank of river has been observed for decrease in k_s values.

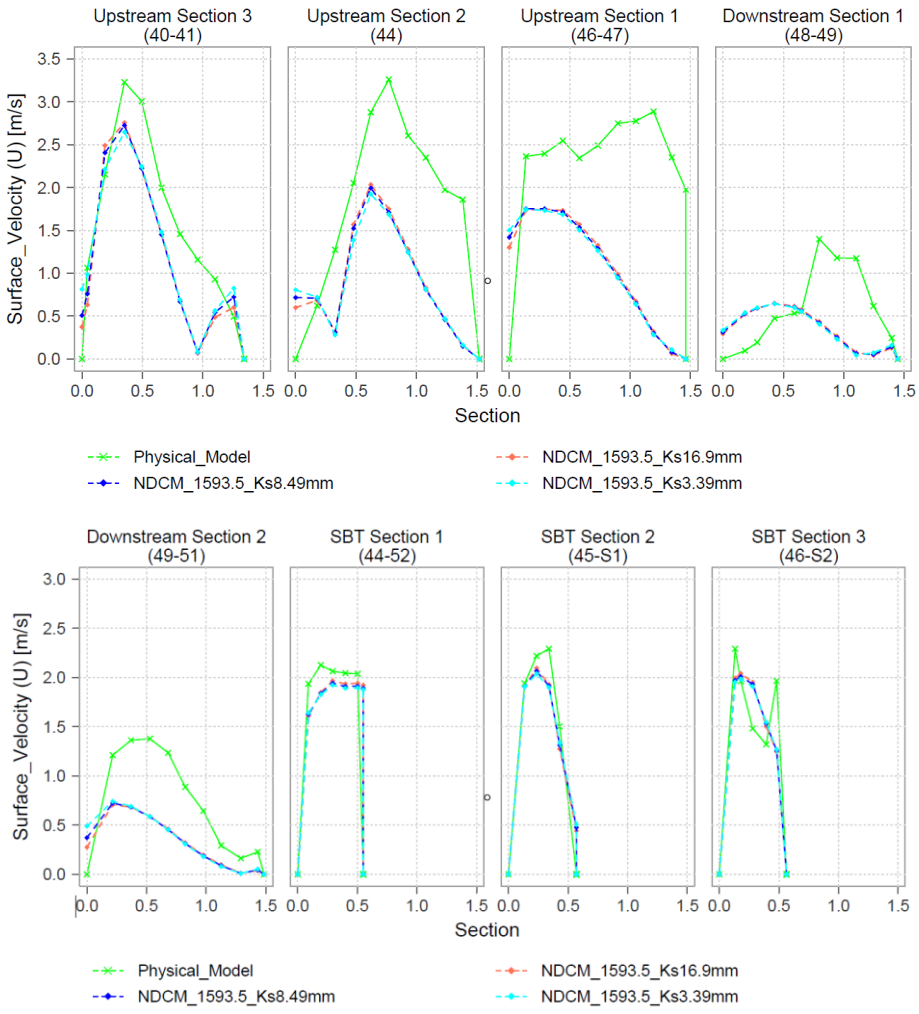

Figure 6.6 Comparison of surface velocities for Option 1: without bed rise

Figure 6.7 Typical flow pattern at SBT intake (left) and vortex formation at SBT outlet (right), seen from top (Adapted from report ANNEX H-3)

In case of **Option 2: 4cm bed rise** (Figure 6.8), the general observation is similar to Option 1. However, velocity magnitude has increased in all the sections. A noticeable observation is that, the flow or velocity pattern in upstream sections are shifting towards right side of river as k_s decreases.

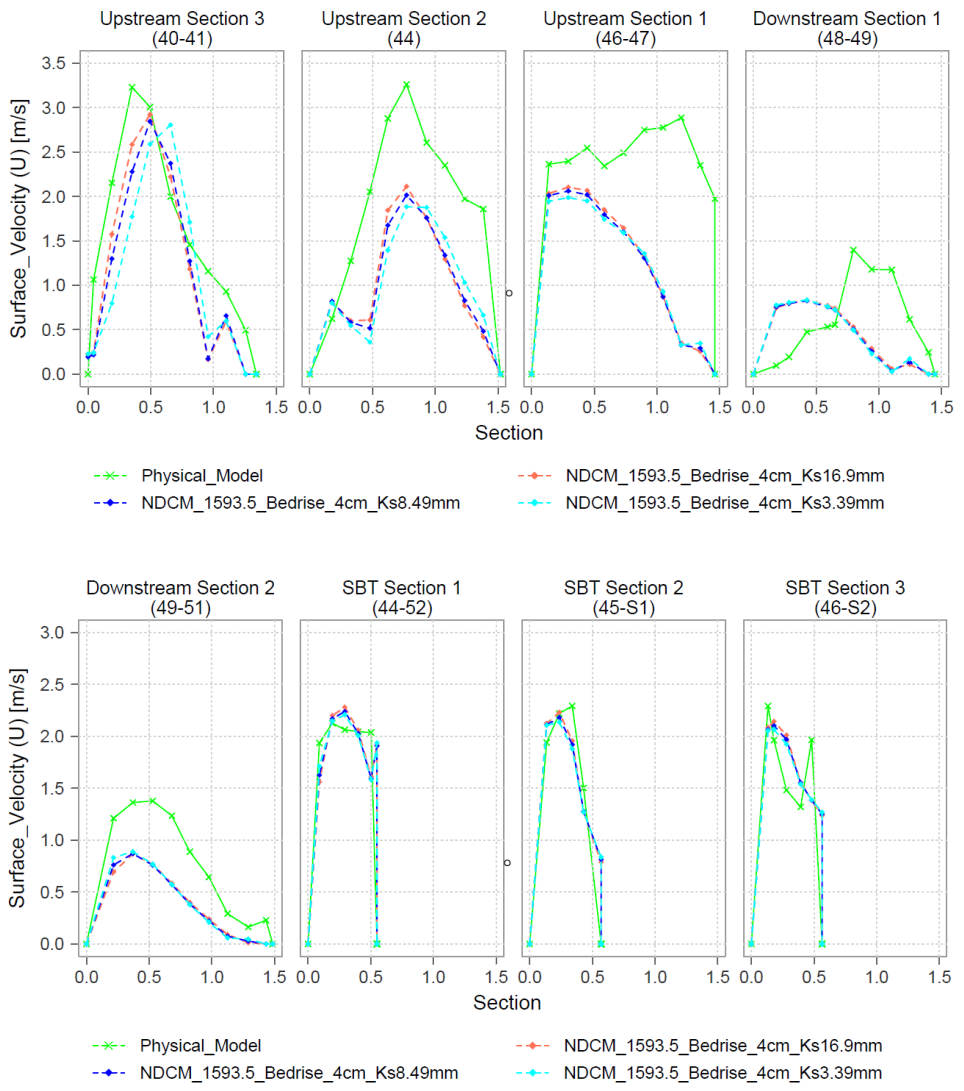

Figure 6.8 Comparison of surface velocities for Option 2:4cm bed rise

For the **Option 3: 8cm bed rise** (Figure 6.9), a vast difference at upstream sections can be observed. Velocity magnitude has increased drastically in all the sections. The flow or velocity pattern has shifted precisely to middle and right side of the river for upstream section 3 and upstream section 2 respectively. The shift in pattern can be observed in all the sections for decrease in k_s. Here, velocity magnitude for lowest k_s in upstream section 3 and 2 is higher in contrast to Option 1 and 2. Similar, for k_s 3.39mm, the upstream section 1 has a bit similar pattern with PMSV. Excluding high magnitude and shift in upstream section 3, other sections for k_s 3.39mm model resembles PMSV magnitude.

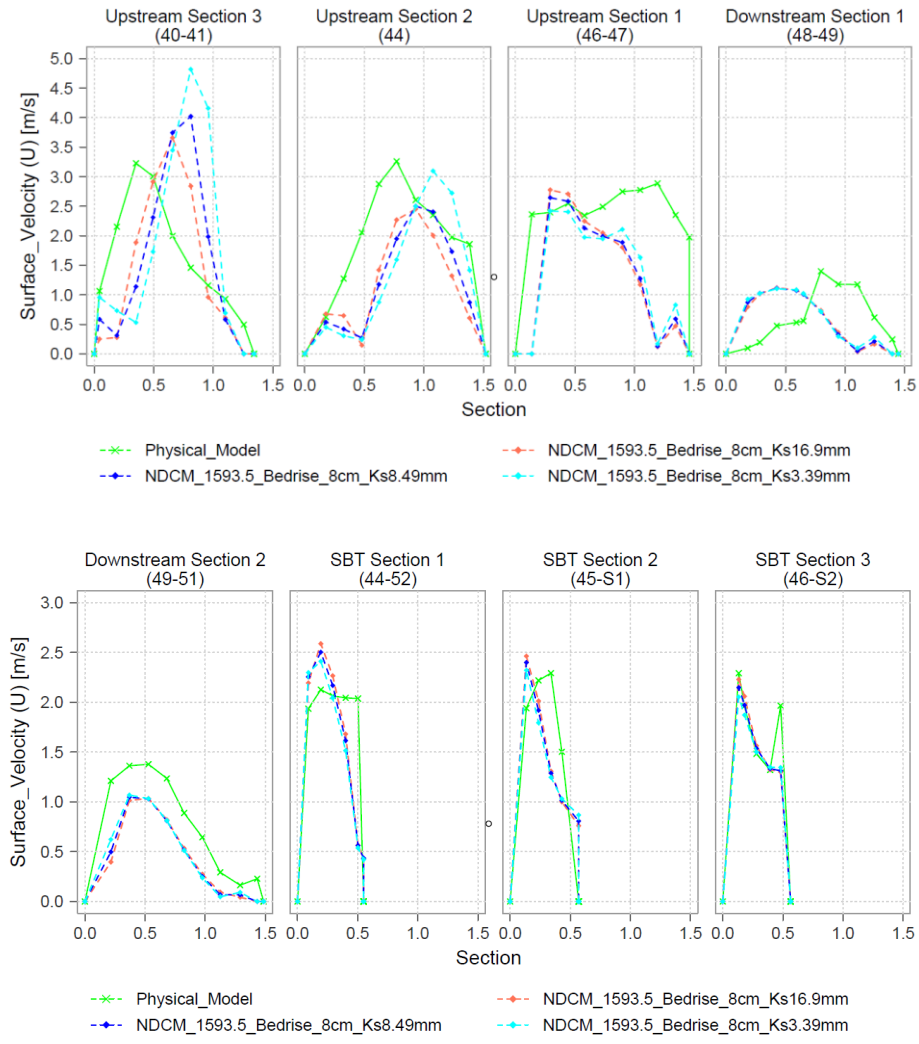

Figure 6.9 Comparison of surface velocities for Option 3: 8cm bed rise

While comparing all the three options, it has been observed that, as k_s decreases, the surface velocity magnitude for 8cm bed rise only, increases in such a way that it becomes nearly equal to PMSV value. Similarly, velocity patterns in upstream section 2 and upstream section 1 tries to resemble the PMSV pattern. On contrary, lowering of k_s shifts flow or velocity pattern towards the right side of river which is not desirable. Likewise, velocity magnitude at SBT becomes higher as well as the pattern deviates from PMSV. Besides this, it can be said that, the initial shifting of flow or velocity pattern from left towards right is due to the bed rise which is supplemented by lowering of k_s. A detailed inspection shows that, lowering of k_s, shifts top portion of the velocity graph, keeping the base nearly at same position, thereby causing the graph to lean towards right side.

Although, 8cm bed rise and lowering of k_s showed both positive and negative effect on velocity magnitude and pattern, it has been better than other options and opted for further analysis. Moreover, as the velocity in SBT increased due to lowering of k_s, a simulation by decreasing SBTs discharge with 10% has been put through. The result for this simulation (Figure 6.10) is better as it decreased the surface velocity at SBT, while increased at downstream section 1 and 2. Further, the velocity pattern at upstream section 1 resembles more to PMSV. Similarly, very small changes have been observed at upstream section 3 and 2. Therefore, 8cm bed rise with 10% decrement in SBT discharge has been considered for further analysis.

A graphical representation of surface velocities for Option 1, Option 2 and Option 3 without decrease in SBT's discharge can be referred in *Appendix D - Hydraulic Simulation - Graphical Representation of Surface Velocity*

for Hydraulic Simulation. Also, for decrease in SBT's discharge, the same appendix can be referred.

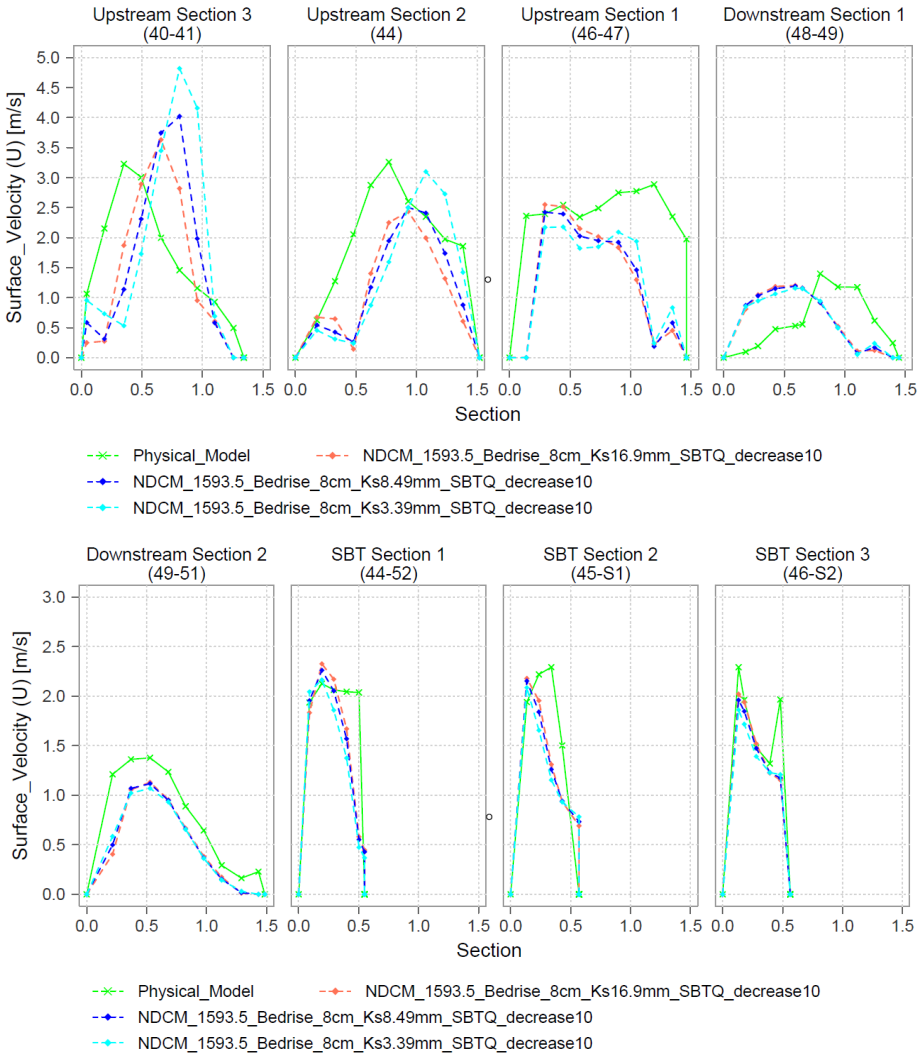

Figure 6.10 Comparison of surface velocities for Option 3: 8cm bed rise along with decrement of SBT discharge by 10%

6.4.2 Simulation combination of no bed rise and 8cm bed rise

As it is clear from the above analysis that, if bed rise is lowered, then the shifting as well as magnitude of flow or velocity pattern will reduce. Therefore, further analysis with decreased SBT discharge has been carried out for a combination of no bed rise and 8cm bed rise to decrease the magnitude and right shifting of upstream section 3 surface velocity. The bed deposition upstream of 1,363.3m away from dam is kept as it is. While, bed downstream till 1,321.5m from dam has been raised by 8cm. The portion in between these locations is left for smoothing during bed contour development.

The result of the simulation can be observed in Figure 6.11. The surface velocity magnitude for upstream section 3 has decreased as well as the flow pattern has shifted to left. In case of upstream section 2, velocity magnitude has decreased as compared to PMSV and previous models. Further, for other sections, velocity magnitude has increased and are nearly similar to PMSV. In this model also, the flow or velocity is higher along left side for upstream section 1 and downstream section 1 in contrast to PMSV.

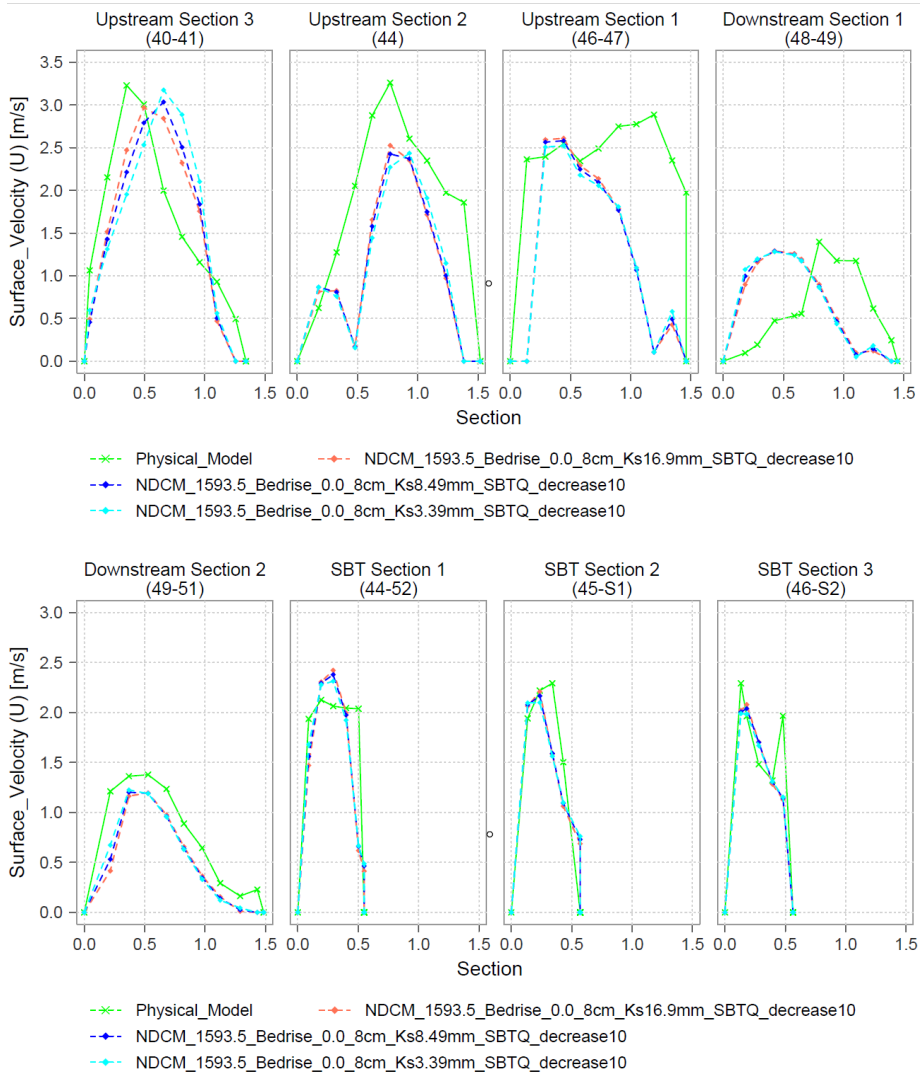

Figure 6.11 Comparison of surface velocities for Option 4: Combination of no bed rise and 8cm bed rise along with decrement of SBT discharge by 10%

6.4.3 Final simulation and grid parameters

After all these bed depositions, roughness height (k_s) and discharge variations, the best representative simulations are for Option 3: 8cm bed rise and Option 4: Combination of no bed rise and 8cm bed rise. These bed deposition models showed good results for k_s range from 16.9mm to 3.39mm. However, as the minimum cell height for all these models is 14mm, it has been decided to re-simulate the best models for 5 vertical cells. This will increase the minimum cell height in the model.

For 8cm bed rise with 5 vertical cells (Figure 6.12), increase in velocity magnitude in all the sections can be observed. Similarly, the surface velocity magnitude and pattern have become better for upstream section 1 and downstream section 2. Nevertheless, the velocity for upstream section 3 is very high as compared to PMSV.

Whereas, in case of Option 4 with 5 vertical cells (Figure 6.13), the simulation results are almost like 10 vertical cells simulation. Only very minimal surface velocity magnitude has increased.

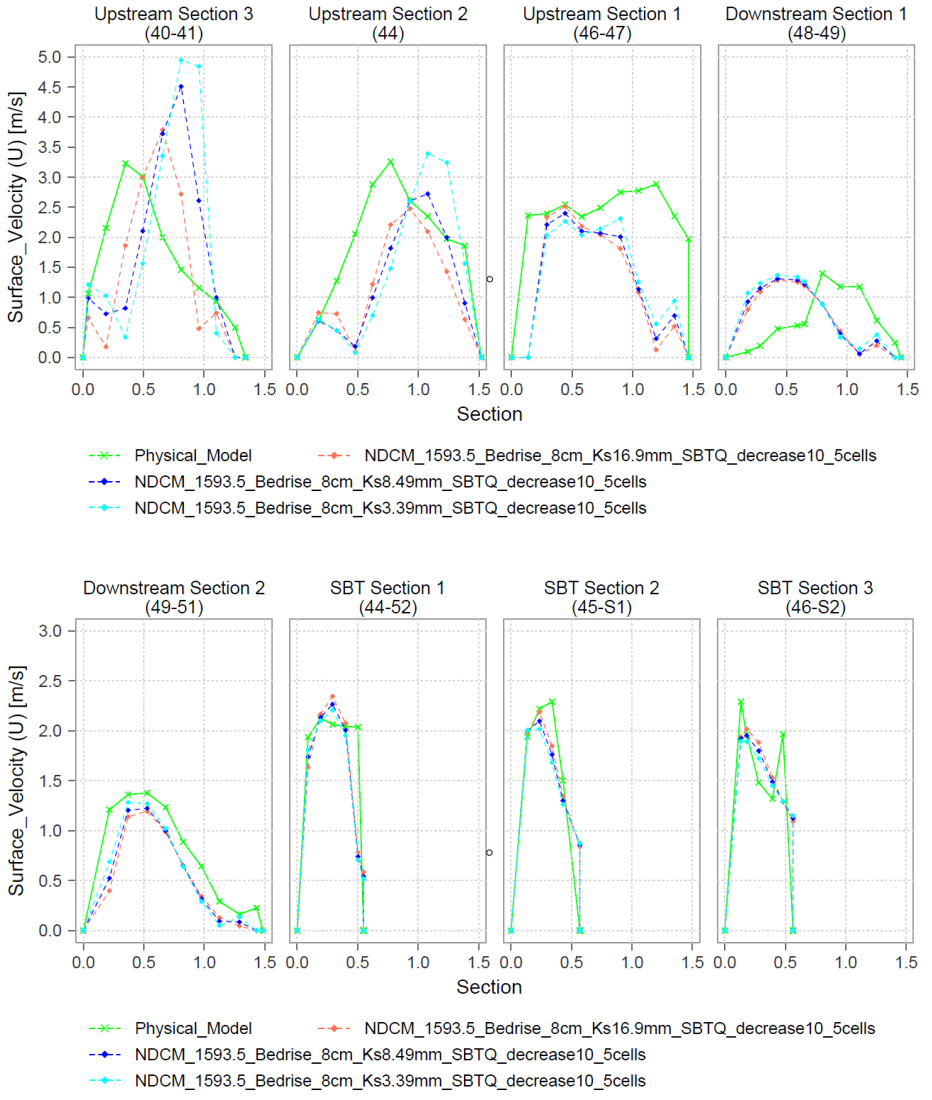

Figure 6.12 Comparison of surface velocities for Option 3: 8cm bed rise with 5 vertical cells along with decrement of SBT discharge by 10%

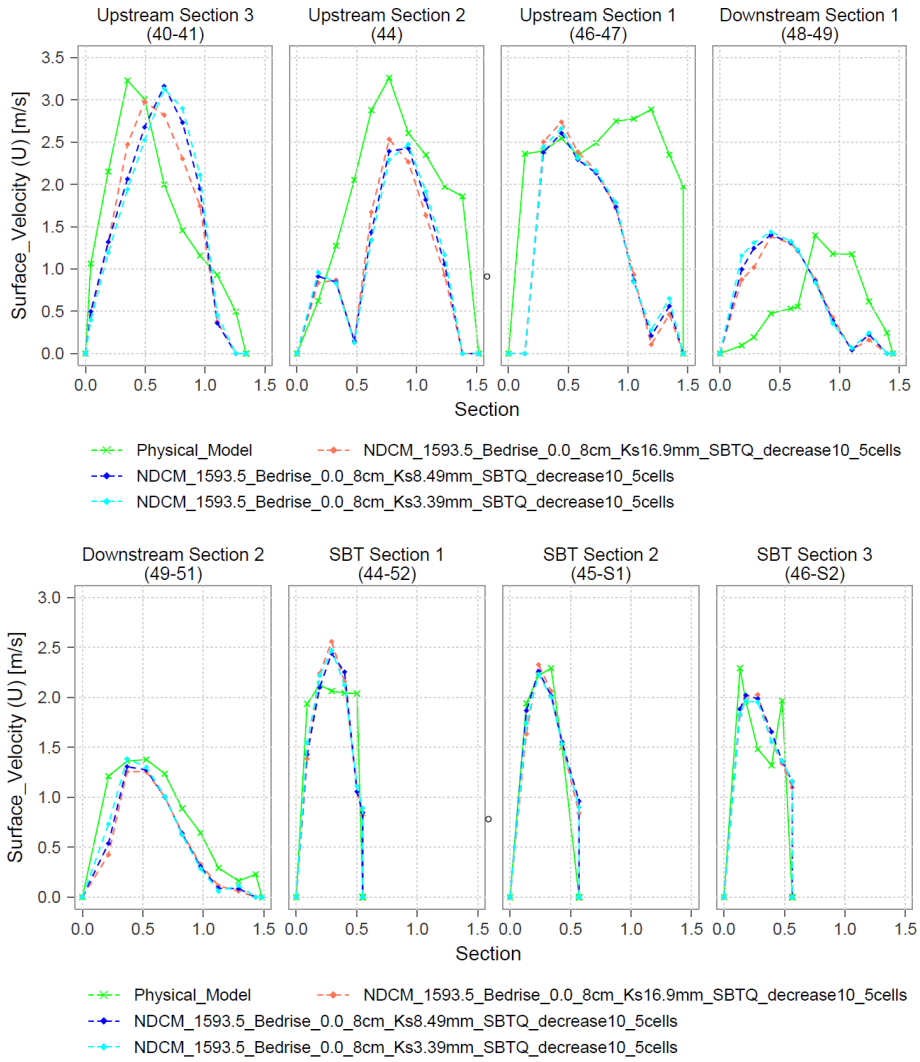

Figure 6.13 Comparison of surface velocities for Option 4: Combination of no bed rise and 8cm bed rise with 5 vertical cells along with decrement of SBT discharge by 10%

After all these model evaluations, the Option 4: Combination of no bed rise and 8cm bed rise has been considered for further analysis. The Option 3 model has been discarded since, the velocity magnitude at upstream section 3 is very high with greater shift to right side. Therefore, Option 4 model with 10% decrement in SBT discharge and 5 vertical cells with block size of 271 * 41 for main river and 13 * 19 for SBT is considered for sediment simulation. Roughness height (k_s) 3.39mm has been chosen based on the fact that, the upstream section 3 and other sections resemble better magnitude and pattern for this k_s with an exception to upstream section 1 and downstream section 1.

Furthermore, to choose the discretization scheme, second order upwind scheme for the selected model had been simulated but convergence couldn't be achieved. Therefore, as an alternative second order discretization scheme for 8cm bed rise model was simulated. The simulation resulted in higher velocity magnitude than PMSV and first order scheme; in all sections except upstream section 1 (Figure 6.14). As second order scheme doesn't seem to be stable for the selected model as well as higher velocity magnitude has been obtained for second best model i.e. Option 3, first order power law scheme has been considered for further analysis.

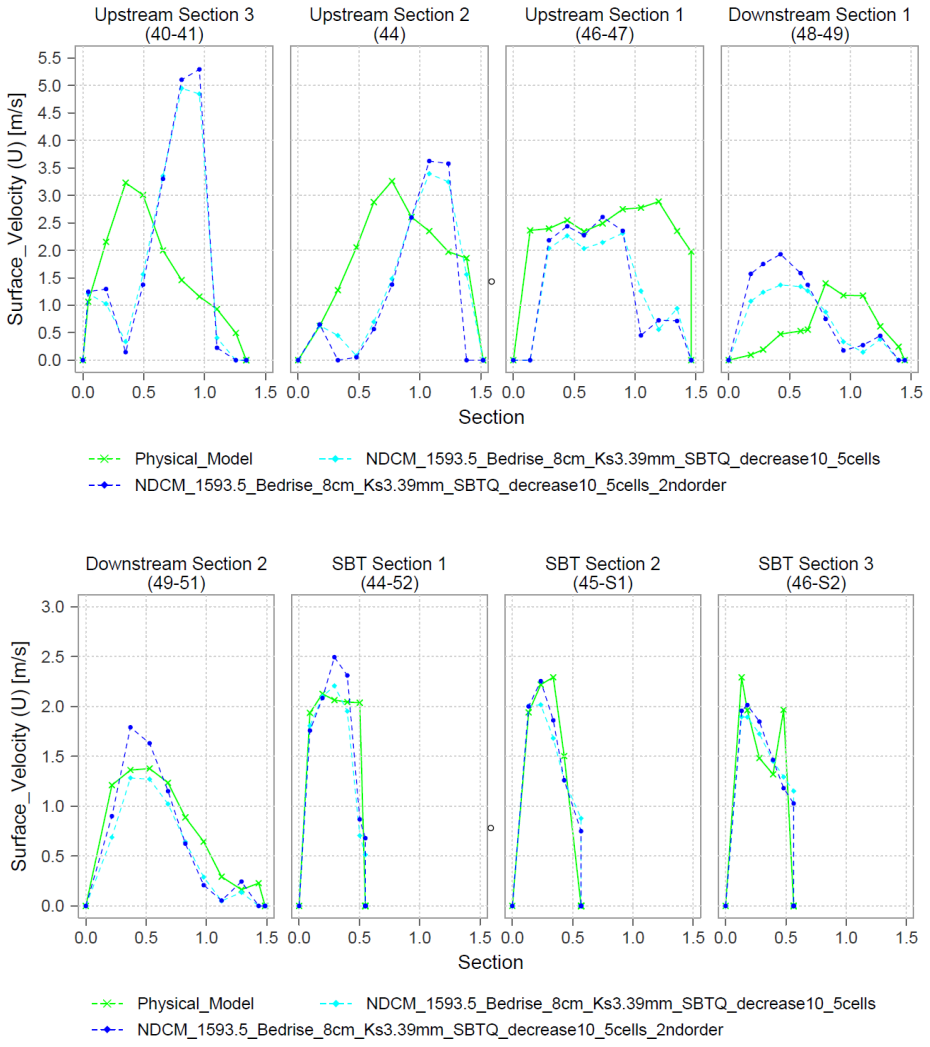

Figure 6.14 Comparison of surface velocities in 1st order and 2nd order scheme for selected 8cm bed rise model

Similarly, for the selected model, a much finer grid has been tested to see whether the results deviate from current coarser grid. The finer grid consists of 541 * 81 lines in x and y direction with 10 vertical cells. The results show lower velocity magnitude for downstream section 1 and downstream section 2. Whereas, higher for SBT sections (Figure 6.15). As both the grids i.e. coarser and finer, have almost similar simulation results, coarser grid has been adopted to save simulation time.

A graphical representation of surface velocities can be referred in *Appendix D - Hydraulic Simulation - Graphical Representation of Surface Velocity for Hydraulic Simulation.*

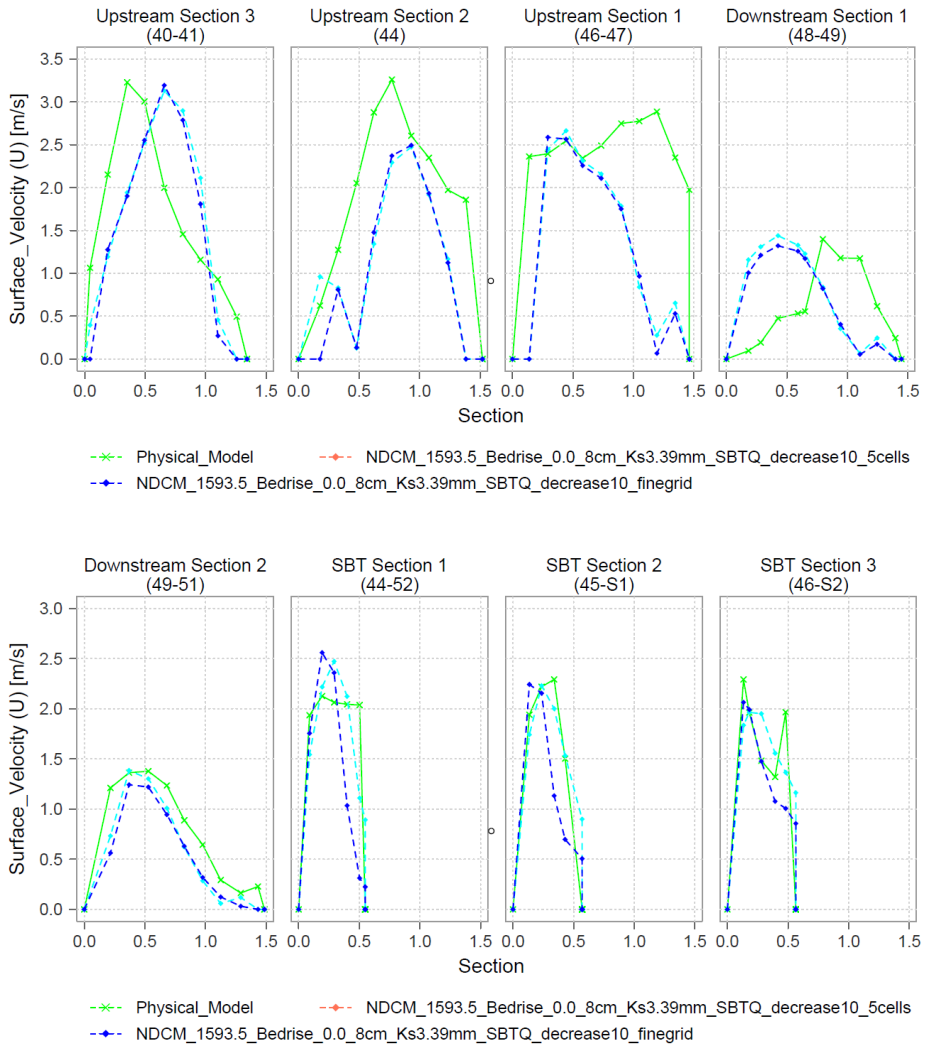

Figure 6.15 Comparison of surface velocities in coarse and finer grid scheme for final model

6.4.4 Problems faced

- As the velocity pattern differed with PMSV pattern, bed changes had to be carried out, to find the most probable bed deposition contour. With each bed change, the whole bed deposition contour

had to be regenerated in *Surfer* which was a very time-consuming problem.

- The bed level interpolation of SSIIM 2 had lots of error. Therefore, each time, the *koordina* file had to be checked and rectified. These rectifications were made looking at the *AutoCAD* drawings and plan map, longitudinal and transverse profiles of SSIIM. Similarly, continuity error for discharge like 0.000094 l/s were observed. This error was due to the wrong interpolation of boundary level by SSIIM. The boundary was fixed to 32.5masl, but the SSIIM interpolated 32.498masl in some locations.

7 Sediment Simulation

Based on the result from hydraulic simulation, sediment simulation has been carried out in SSIIM 2 with Option 4: combination of no bed rise and 8cm bed rise; k_s 3.39mm, 10% decrement in SBT discharge and 5 vertical cells. At first, sediment simulation for initial SBT location has been carried out (Figure 7.2). SBT outlet sediment concentration acquired from simulated model is then compared with the physical model value. After, SBT is shifted upstream by 130m (as per prototype scale) as the location seems to be more viable and effective in suspended sediment handling. Nevertheless, shifting of SBT has been carried out based on the description in physical model test report. In the physical model, new SBT has been proposed 100m upstream from the current/initial one. However, design of the new SBT is completely changed and physical model data on exact location, SBT dimensioning and test results are unavailable (Figure 4.10; Figure 4.11). Therefore, initial SBT design and dimensioning has been considered for shifted SBT such that results from initial and shifted can be compared based on location variability. The shifted location lies downstream of the outer bend whereas initial location lies in the inner bend (Figure 7.2). The location is also selected to observe the effect of outer bend on suspended sediment removal. Furthermore, sediment deposition on the left bank, just upstream of SBT can be observed in sediment simulation for initial location. This deposition is due to the formation of shadow area caused by protruding ridge on the left bank (Figure 7.1;Figure 7.3). Therefore, an intension on selecting the shifted location has also been to observe the effect on deposition. Similarly, shifting the SBT further upstream might increase the trapping of sediment due to reduced velocity

and increased reservoir trapping length. This will ultimately help in reducing the wear and tear of the turbines by decreasing the sediment concentration reaching the powerhouse. The Figure 7.2 shows the initial and shifted location of SBT intake.

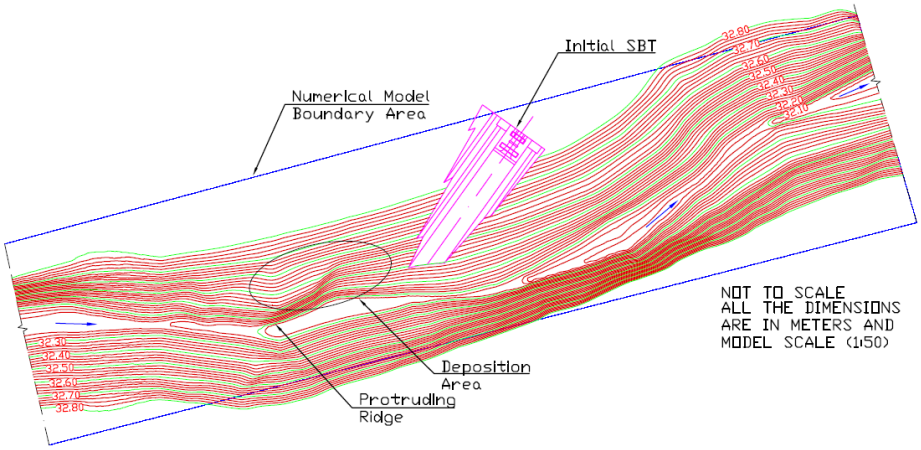

Figure 7.1 Deposition area during initial sediment simulation

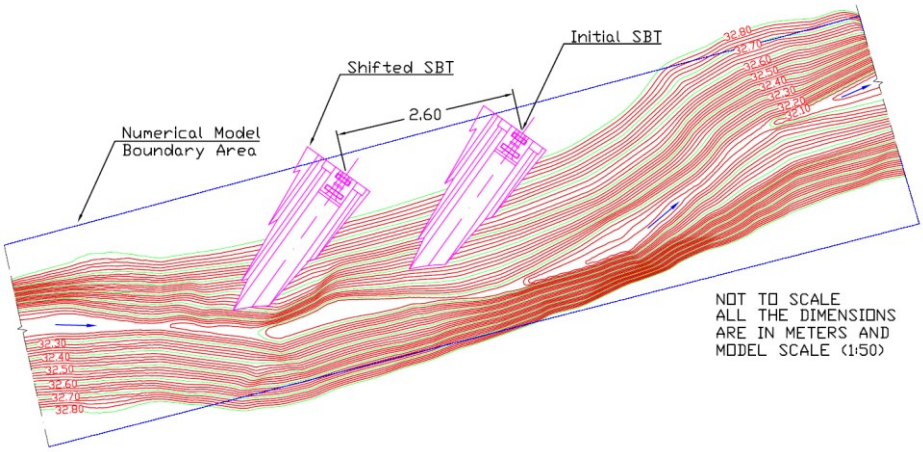

Figure 7.2 Position of SBT intake

7.1 Input Data

The data available in the document ANNEX H-3 Preliminary Results of the Sediment Physical Model, has been used for sediment analysis. As the physical model tests were carried out for 0.04961m^3/s (877m^3/s in prototype scale), nearly equivalent to 1-year return period flood at dam site, the same discharge has been considered for numerical model study. For simulating the sediment deposition, the water level has been fixed at 32.5masl (1,625masl in prototype), constant inflow discharge of 0.04961m^3/s and outflow discharges with 10% reduction in SBT discharge, 0.03230m^3/s (571m^3/s in prototype scale) and 0.01731m^3/s (306m^3/s in prototype scale) from SBT and main river outlets respectively for consecutive 6.788 hours (2 days in prototype scale) have been considered. The sediment simulation has been carried out only for the suspended sediments, as the SBT is designed to carry suspended sediments only. Furthermore, two different materials Zhuzhou coal (density 1,330kg/m^3) for suspended sediments and mixture of sand and pebbles (density 2,650kg/m^3) for bed load have been used in physical model test. In contrast to that, only one sediment density (1,330 kg/m^3) has been used in numerical model owing to the limitation of SSIIM on using different density materials. At different discharges, the bed deposition changes, which has been incorporated in the model as described in grid generation and hydraulic simulation section thereby favouring the use of suspended sediments only. As no bed load inflow have been considered for numerical model, the bed sediment of 3mm with density 1,330 kg/m^3 has been distributed all over the bed. It is considered to minimize the erosion from bed and limit the concentration at the outlets based on different sediment

simulation carried out for 1mm and 3mm. The 3mm bed sediment size will be 3.6mm in prototype scale.

In case of sediments, sediment sizes, sediment concentrations and fall velocities are the main input parameters. The sediment sizes are considered based on the grain size distribution of the suspended particles as shown in Figure 4.7 and Table 4-2. As 1mm and 0.8mm particles cover only 0.4% of the total volume, these have been excluded from the sediment group. The sediment sizes and their respective percentage have been shown in the Table 7-1. As per the Table 4-4, dated 1986.7.26 - 7.27, suspended sediment concentration of 5,005 ppm has been considered for 0.04961 m^3/s inflow. In physical model, a constant sediment inflow of 5,005ppm, equivalent to 5.0kg/m^3 is used throughout the simulation period. The volume fraction of the sediment concentration with 1,330kg/m^3 density is 0.003763m^3/m^3. Based on this and Table 7-1, the sediment concentration for 0.5mm model sand size is 1.37% * 0.003763 = 0.00005155m^3/m^3. The sediment concentration for each size fraction is shown in Table 7-2.

Table 7-1 Suspended sediment size fraction inflow

Suspended Sediment PSD in model scale (Dr (Dp/Dm) = 1.2)		
Prototype sand size	Model sand size	Sediment fraction in each group
(mm)	(mm)	(%)
0.60	0.5	1.37
0.15	0.125	14.99
0.058	0.048	33.64
0.030	0.025	18.41
0.018	0.015	12.26
0.008	0.007	8.07
0.004	0.003	11.26

Table 7-2 Suspended sediment size fraction concentration

Suspended Sediment Concentration in model scale (Dr (Dp/Dm) = 1.2)				
Model sand size	Density	Total sediment concentration	Total sediment concentration	Sediment concentration for each size fraction
(mm)	(kg/m^3)	(kg/m^3)	(m^3/m^3)	(m^3/m^3)
0.5	1,330	5.005	3.76E-03	5.16E-05
0.125	1,330	5.005	3.76E-03	5.64E-04
0.048	1,330	5.005	3.76E-03	1.27E-03
0.025	1,330	5.005	3.76E-03	6.93E-04
0.015	1,330	5.005	3.76E-03	4.61E-04
0.007	1,330	5.005	3.76E-03	3.04E-04
0.003	1,330	5.005	3.76E-03	4.24E-04

As the fall velocity of the natural particles will be lower than that of the spherical particles due to influence of grain shape, the formula developed by Nian Sheng Cheng has been used to calculate the fall velocities (Cheng, 1997). An explicit formula for the fall velocity of the natural particles can be expressed as:

$$V_s or\ \omega = \frac{\nu}{d}\left(\sqrt{25 + 1.2D_*^2} - 5\right)^{1.5} \quad (12)$$

$$D_* = \left(\frac{\rho_s - \rho}{\rho}\frac{g}{\nu^2}\right)^{1/3} \quad (13)$$

where, V_s or ω is terminal fall velocity m/s, ρ_s is density of sediments kg/m^3, ρ is density of water kg/m^3, ν is kinematic viscosity of water m^2/s, d is diameter of particle in m, g is acceleration due to gravity m/s^2 and D_* is the dimensionless grain diameter (Cheng, 1997).

The fall velocity depends on the viscosity of the fluid which further depends on the temperature. In the model, water at 10^o C has been

considered based on the hydrological report Annex B: Hydrology and Sediment Investigation Report (Draft) (Refer Section 4.2). The kinematic viscosity of water at this temperature is 1.306E-6m^2/s (Vennard, 1940). With increase in temperature, the kinematic viscosity decreases leading to increase in fall velocity. The fall velocities for the suspended particles at 10°C and 20°C are shown in Table 7-3.

Table 7-3 Fall velocities of sediment particles

Model sand size	Dimensionless grain diameter (D_*)	Settling velocity at 10°C	Settling velocity at 20°C	Difference in fall velocity
(mm)		m/s	m/s	
3	37.144	9.40E-02	9.68E-02	3%
0.5	6.191	1.65E-02	1.92E-02	16%
0.125	1.548	1.54E-03	1.98E-03	28%
0.048	0.594	2.35E-04	3.07E-04	30%
0.025	0.310	6.42E-05	8.39E-05	31%
0.015	0.186	2.31E-05	3.02E-05	31%
0.007	0.087	5.04E-06	6.59E-06	31%
0.003	0.037	9.27E-07	1.21E-06	31%

7.2 Simulation Time

Simulation for both the initial and shifted SBT have been conducted for 6.788 hours (2 days in prototype scale) which is approximately 24,440 seconds. As the SBT sediment concentration in physical model has been measured on both 1st day and 2nd day, the sediment concentration at the end of 1st day have also been acquired during the numerical simulation. However, only 2nd day data analysis has been carried out.

7.3 Simulation Criteria and Input files

For the hydraulic simulation, a steady state computation with fixed water surface and bed had been considered. Contrary to that, time dependent

computations for water flow and sediments with a moving water surface and bed has been considered in sediment simulation. This has been opted since, large suspended sediment deposition had been observed in the physical model test (Figure 7.3). As the bed deposition changes, the water surface and the flow velocities also change requiring time dependent computation.

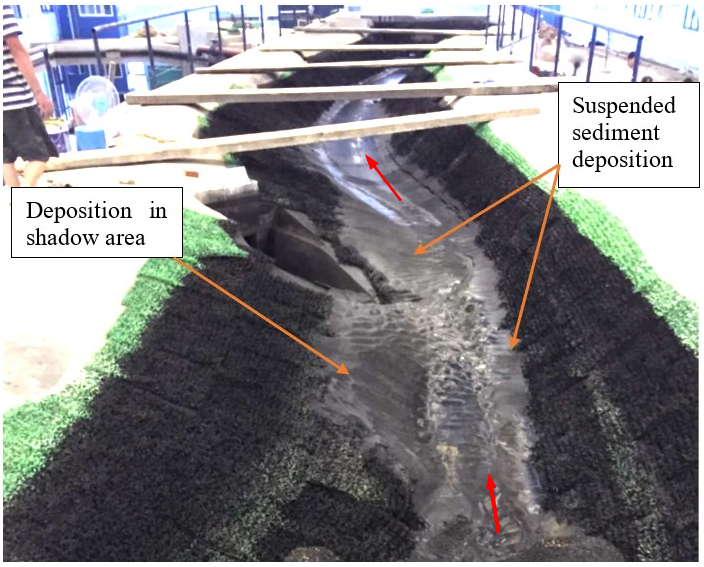

Figure 7.3 Suspended sediment deposition observed in physical model test

The same *control, koordina, geodata* and *unstruc* files from hydraulic simulation are used for sediment simulation. The *control* file is modified which includes extra data sets for sediments and time dependent simulation. These extra datasets are S, N, B and F data sets. Similarly, *timei* file for inputs of time, discharge, water levels and sediment concentrations is used in sediment simulation.

Control File

The algorithms in the *control* file are similar to that used in hydraulic simulation, with some new data sets. The sediment simulation is started using the F 2 UIS data set. The U term reads the *unstruc* file, I initialize the sediment concentration computation and S calculates the sediment concentration. For calculating the suspended sediment concentration, Van Rijn formula for suspended load has been used. This has been invoked by F 84 0 data set. For the transient water flow computations, F 33, F 36 2, F 68 0 and G 6 data sets have been used. Similarly, for transient sediment computation, F 37 2 data set is specified. The F 37 2 data set specifies the pick rate in the suspended sediment transport equation to put the sediments back into resuspension (Olsen, 2018).

The S data set gives sediment size and fall velocities of the sediments under consideration. The N data set gives information about different initial grain size distributions of the bed material and the B dataset tells where in the geometry the different distributions are. These data sets must be given with correct parameters. Whereas, the I data set gives the inflow of the sediments in kg/s in *control* file or m^3/m^3 in *timei* file (Olsen, 2018). A detailed description of the different used data set can be referred in the *Appendix E - Sediment Simulation.*

Timei File

The *timei* file is relevant for the time series calculations. It is an input file for time series of discharge, water level, sediment concentration and control for output. The *timei* file can read different types of data sets, which all begins with a capital letter. In the numerical model "I" data set has been used. The I data set contains five floats each indicating: the time for when the variables are used, upstream discharge, downstream discharge,

upstream water level and downstream water level. In case of the transient sediment calculation, additional floats are read representing the sediment concentration (volume fraction) of the inflowing sediments for each grain size.

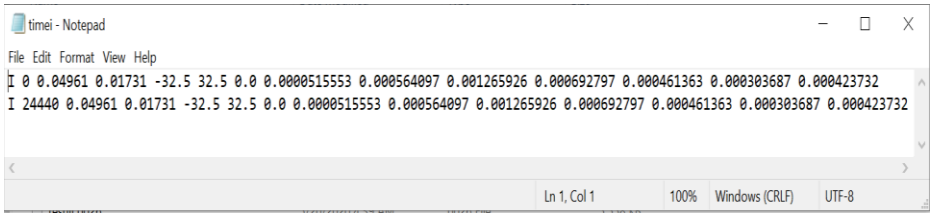

Figure 7.4 Timei file for Option 4 initial SBT location

7.4 Simulation and Results

The results from sediment simulation are described below in three sections: results based on velocity, bed shear and bed changes; results based on concentration at outlet and results of sensitivity analysis.

7.4.1 Results based on velocity, bed shear and bed changes

The velocity, bed shear stress and bed changes for both initial and shifted models are shown below. The negative number indicates erosion and positive number indicates deposition for bed changes. Refer Figure 7.5, Figure 7.6for velocity; Figure 7.7, Figure 7.8 for bed changes; and Figure 7.9, Figure 7.10 for bed level.

Initially at the beginning of simulation, velocity magnitude is similar in both models with higher velocity at shifted model's sediment bypass tunnel. The shifted model attains higher velocity in upstream inflow region, faster than initial model (Figure 7.5 for Time 16 and 21). However, velocity magnitude is nearly equal at the time of attaining highest velocity. This attainment occurs at different timeframe in two models. For initial model,

it occurs at Time 21 (i.e. 14,960 seconds) and at Time 16 (i.e. 11,560 seconds) for shifted model (Figure 7.5, Figure 7.6; the actual time changes with scale of the *ParaView* file). At the end of simulation, velocity upstream of SBT is higher for shifted model. Whereas, for the downstream section, the velocity is along left bank and higher for initial. The maximum velocity in shifted model is 0.6m/s whereas in initial is 0.58m/s for k_s 3.39mm. This leads to the fact that sediment erosion is higher upstream of SBT in shifted model which is also validated by the observed sediment concentration at SBT outlet. The same phenomenon and pattern can be observed for bed shear. The bed shear follows the occurrence of highest shear in two models exactly at similar period of occurrence of highest velocities. For bed shear *Appendix E - Sediment Simulation- Figure E. 2* can be referred.

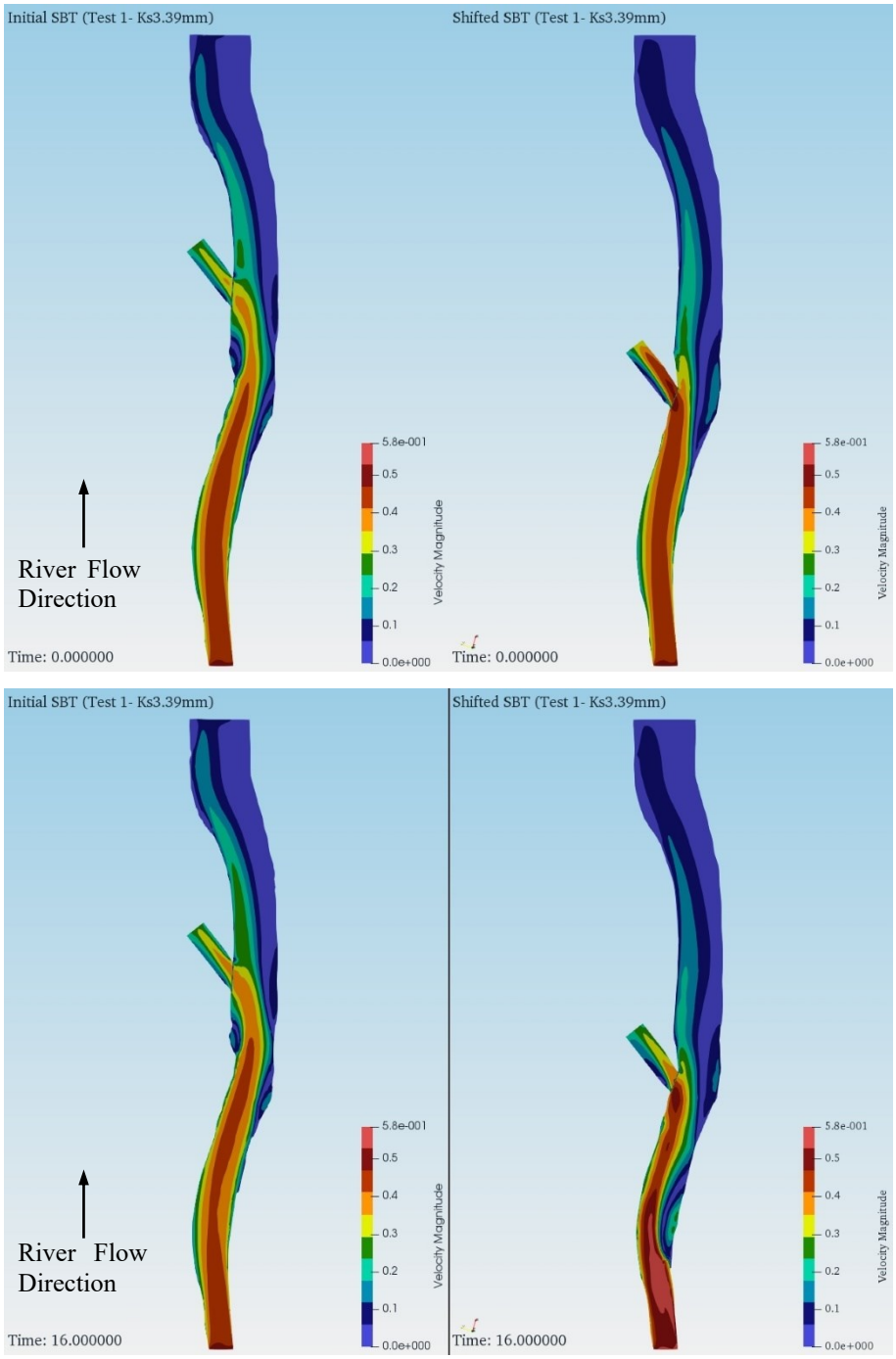

Figure 7.5 Velocity for SBT models at different timeframes

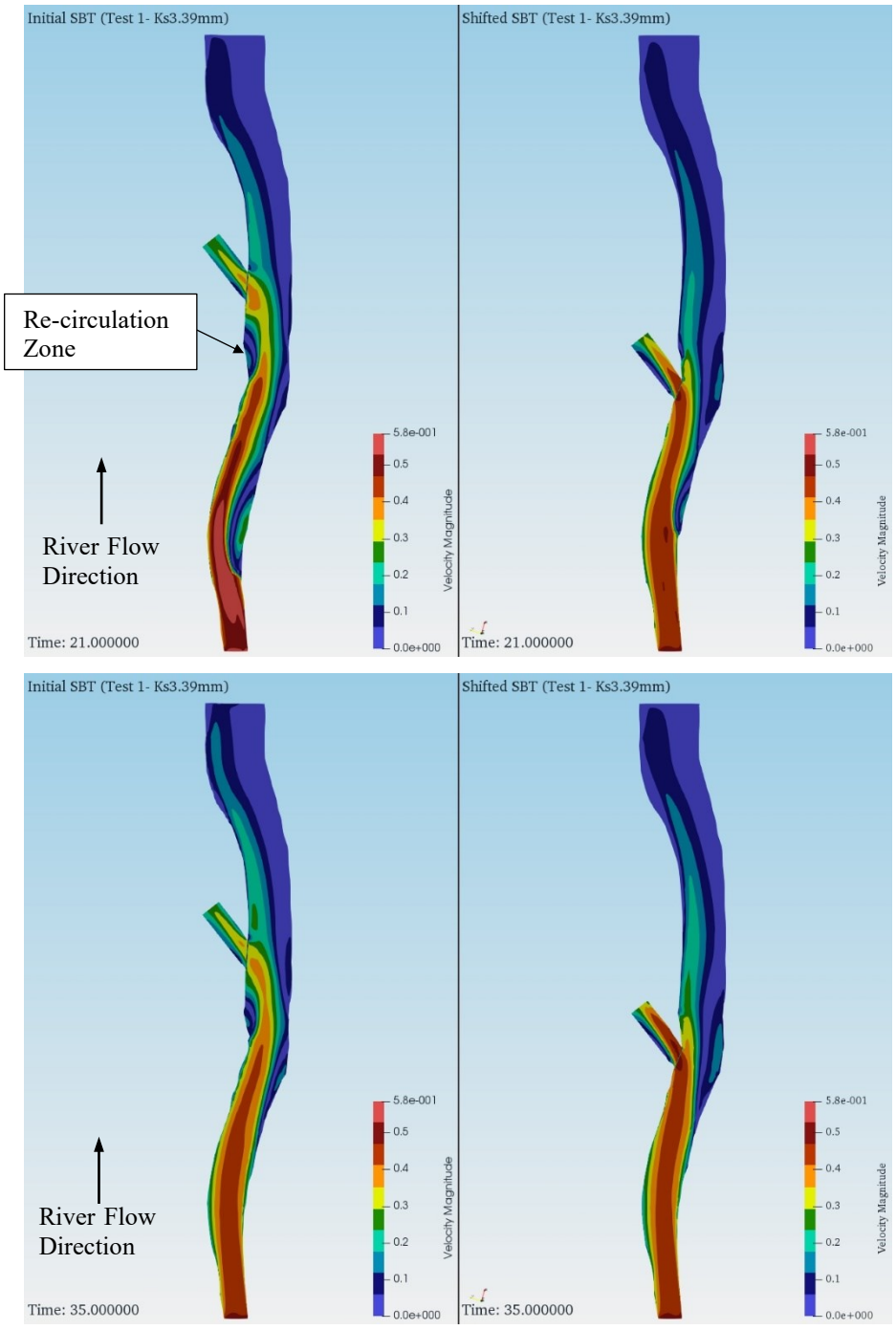

Figure 7.6 Velocity for SBT models at different timeframes

As similar bed shear pattern is observed in both models at same location but in different timeframes, the erosion and deposition also differ with the bed shear and its occurrence. However, the pattern of erosion and deposition are quite similar in both models. For both cases, erosion occurs at the right bank around inflow region, just upstream of the uppermost bend. Due to this bend, flow is directed towards left bank, which then erodes left bank. Further, erosion can also be seen in the vicinity of sediment bypass tunnel inlet. The eroded materials are carried by river and deposited just downstream of eroded location. The erosion and deposition are recurrent process, but deposition shifts downstream with time from river center to right bank in both models. Further, in case of initial model's left bank, eroded material gets deposited just downstream, in the shadow area of protruding ridge. While for the shifted SBT location, most of eroded material passes through the SBT and a small deposition beyond sediment bypass tunnel from river center to the left bank can be observed.

With passage of time, erosivity of flow has decreased and seems to erode the deposited material from right bank, which is further shifted downstream. At the end of simulation, high deposition along right bank, downstream of uppermost bend and in shadow area of initial model can be observed. Likewise, for the shifted model, deposition on left bank past SBT can be observed. Similarly, high erosion can be seen in left bank and inflow area. In both models, small deposition all along the reservoir downstream the SBT can be observed. Figure 7.7 and Figure 7.8 shows periodical bed changes from start to end of simulation.

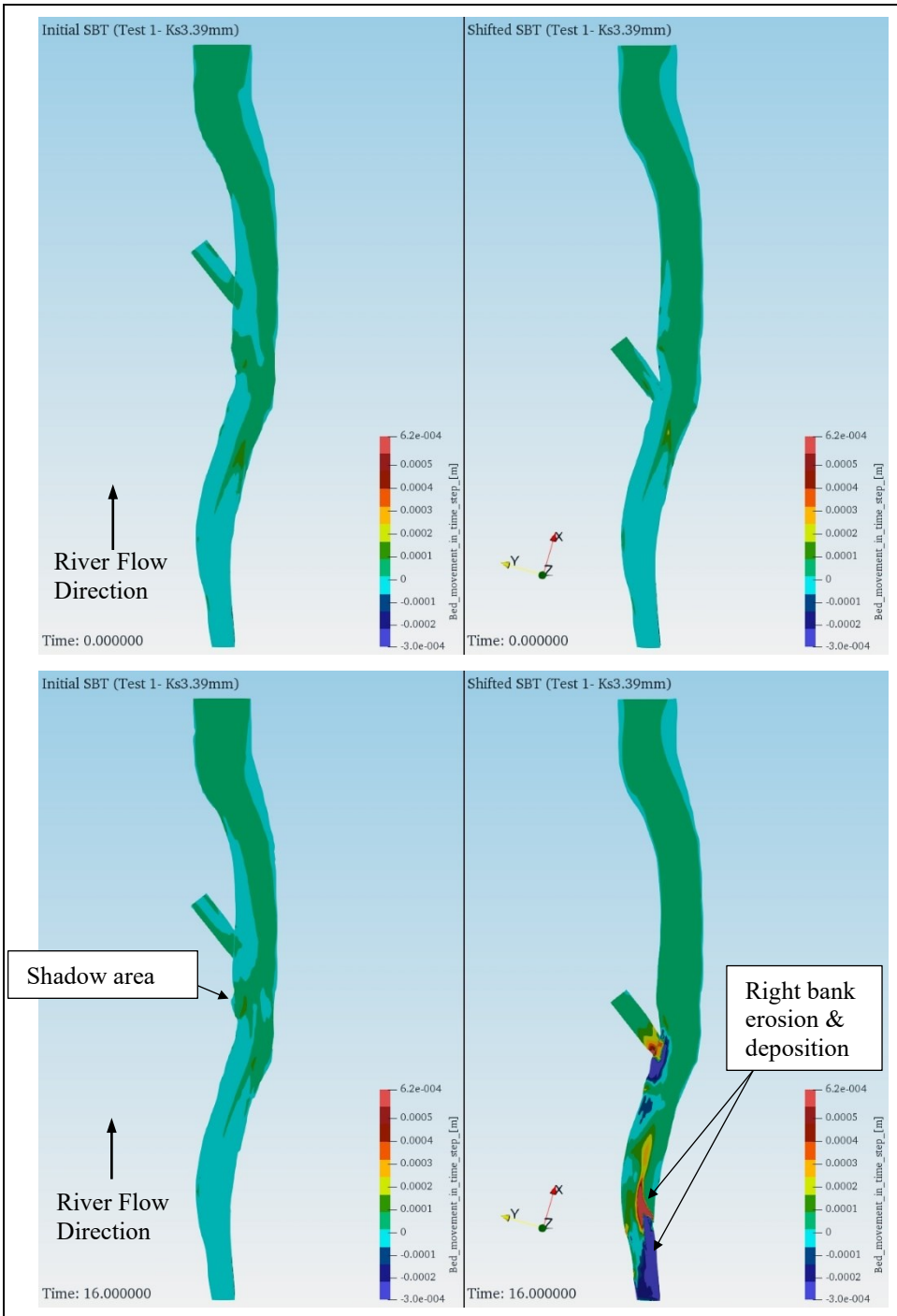

Figure 7.7 Bed changes for SBT models at different timeframes

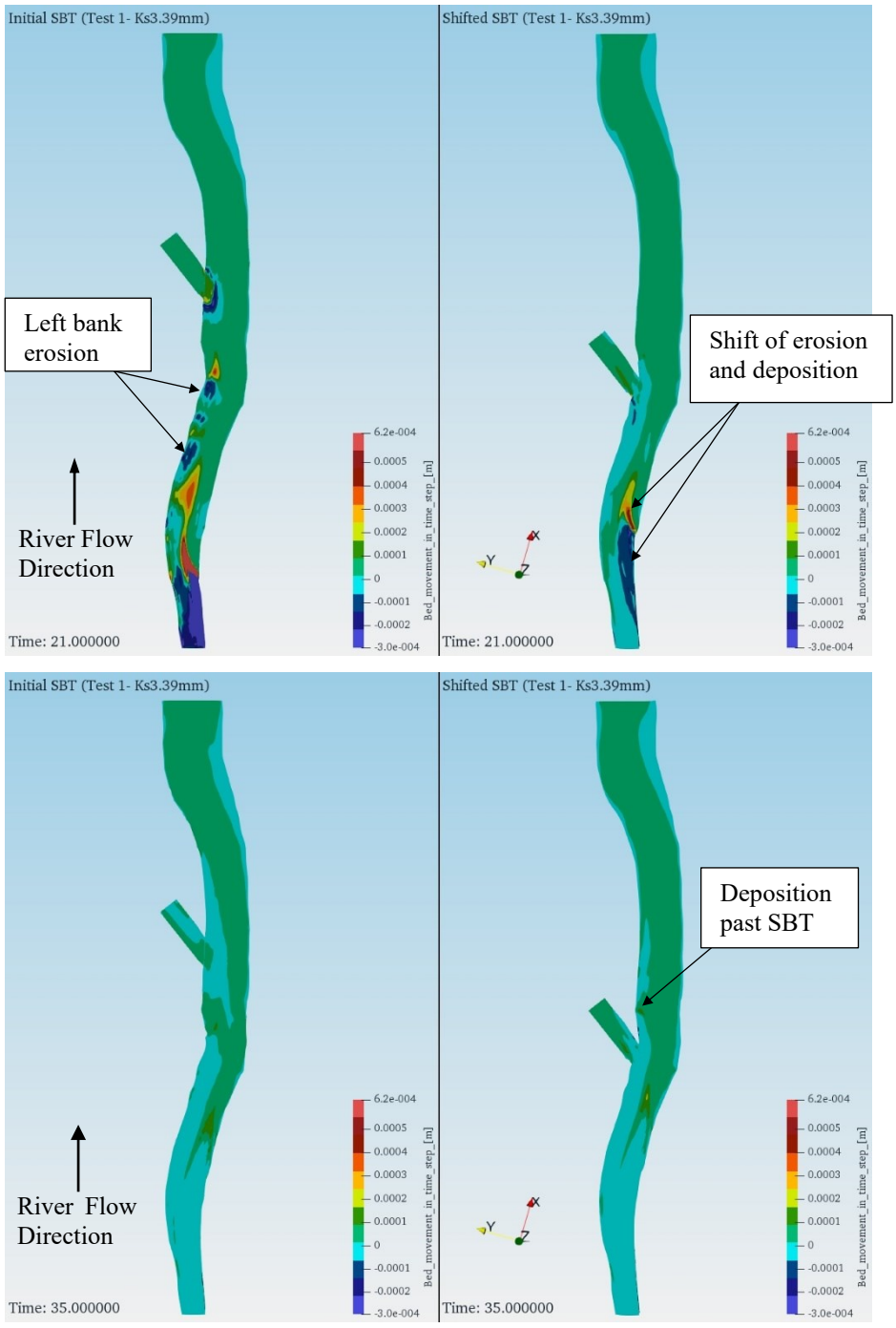

Figure 7.8 Bed changes for SBT models at different timeframes

Although, both the models look quite similar in velocity magnitude, bed shear, erosion and deposition pattern, the location of SBT seems to influence the bed level. In the shifted model, an increased bed just downstream of the SBT intake can be observed at Time 15 (Figure 7.9). This bed rise separates the riverbed into two parts. Moreover, the bed rise gets eroded in successive timeframe but eventually the overall river erosion and deposition pattern forms similar bed rise at the end of simulation (Figure 7.9 and Figure 7.10). However, such phenomenon is not observed in the initial model but were perceived during sensitivity analysis. In the sections below, this abrupt bed rise will be referred either as bed rise or bed wall.

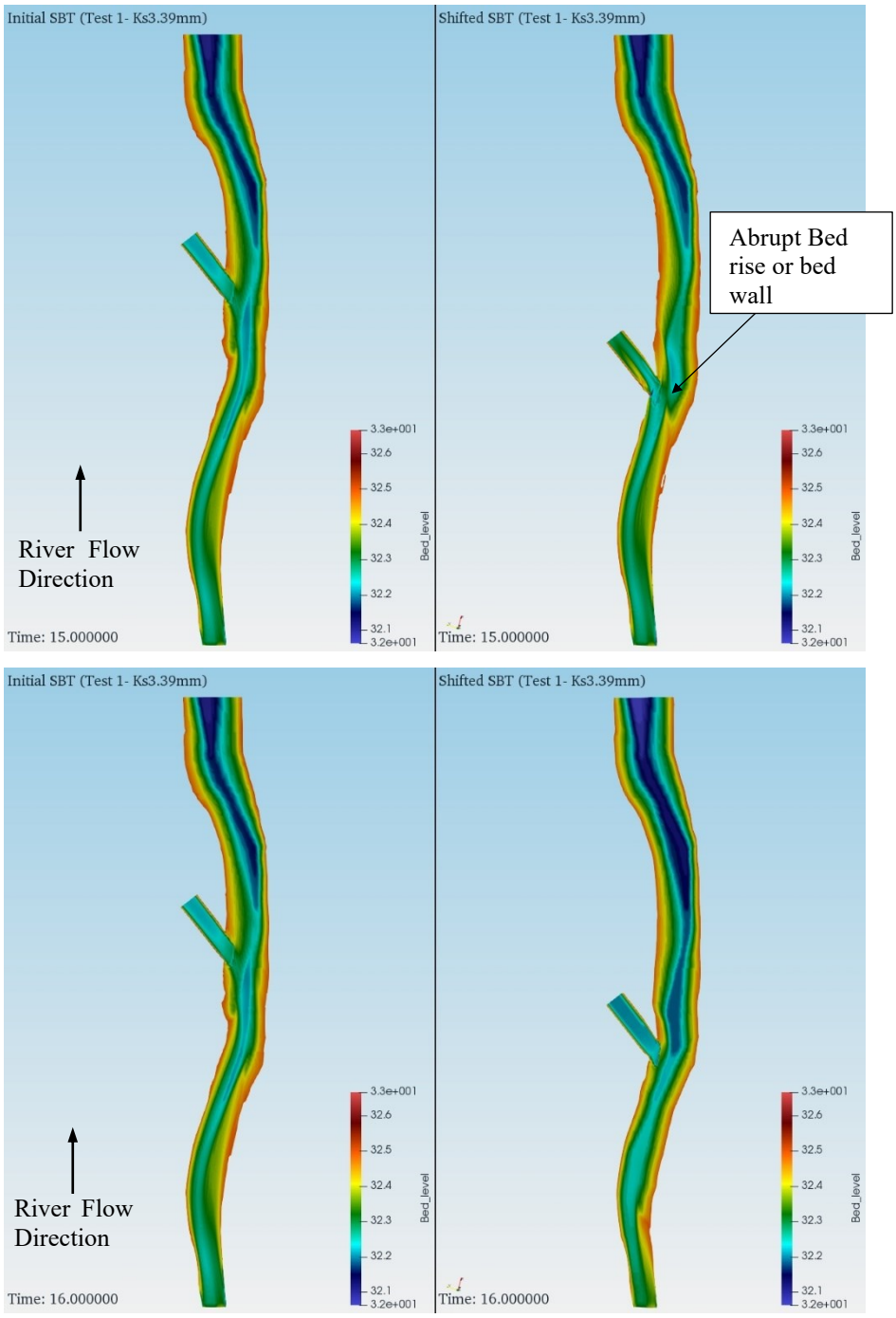

Figure 7.9 Bed level for SBT models at different timeframes

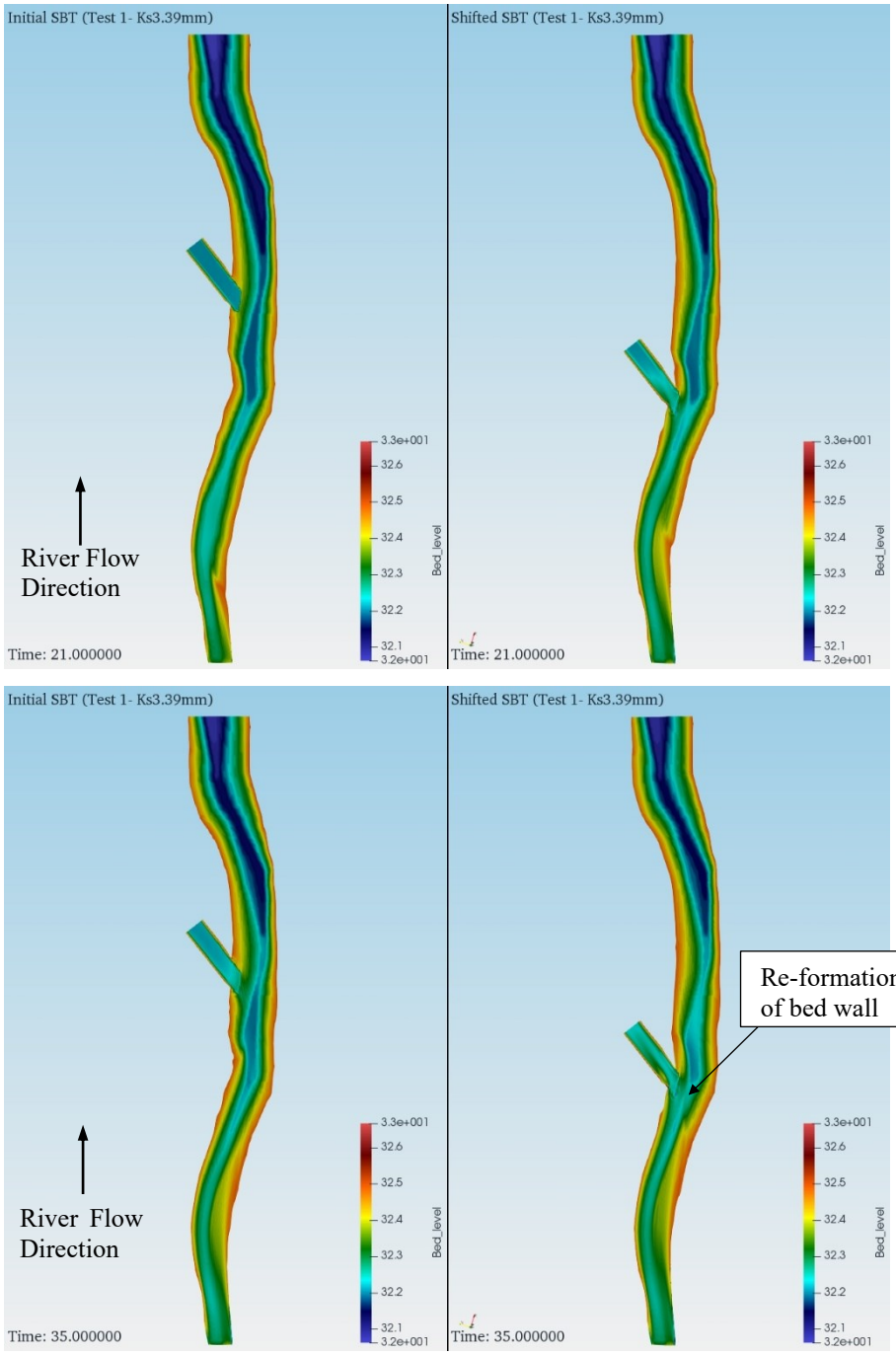

Figure 7.10 Bed levels for SBT models at different timeframes

7.4.2 Results based on sediment concentration at outlet

Sediment size concentrations at SBT and main river outlets for 6.788 hours (2 days in prototype scale) simulation have been obtained. The sediment concentration at SBT outlet for both models i.e. initial and shifted, have been compared with concentration measured in physical model. As the main river outlet in numerical model lies upstream of concentration measurement point in physical model, the available power intake sediment concentration couldn't be used. Similarly, concentration and trapped weight between the two models have been compared. The main river, herein means, river in which the dam has been built. The SBT and main river outlets are free-flowing open end in the numerical model.

The sediment concentration at SBT and main river outlets for initial and shifted models are 4.936 kg/m^3, 4.367 kg/m^3; and 4.943 kg/m^3, 4.177 kg/m^3 respectively. As per the physical model, the sediment concentration at the SBT outlet is 4.35 kg/m^3, which is lower than initial and shifted numerical models by 11.7% and 11.9% respectively (Figure 7.11). This exhibits the shifted model at SBT outlet has higher concentration thereby reducing the inflowing sediment volume into the reservoir. Similarly, sediment concentration at main river outlet is lower in shifted model signifying higher capability of the model to trap sediments in reservoir. In initial and shifted models, 4.52% and 5.47% of the total inflow sediments are trapped in reservoir respectively (Figure 7.13). The difference in the trapped sediment weight for consecutive 6.778 hours is 57.69kg in model scale.

In the figures below, the sediment weight passing through the outlets for 6.788 hours have been calculated based on the concentration obtained from numerical and physical models. The sediment weight percentage at SBT and main river outlet have been obtained based on the inflow to these

structures. Whereas, the trapped weight percentage has been calculated based on the total inflow and concentration to the model. The outflow weight per inflow also represents the concentration percentage for each outlet.

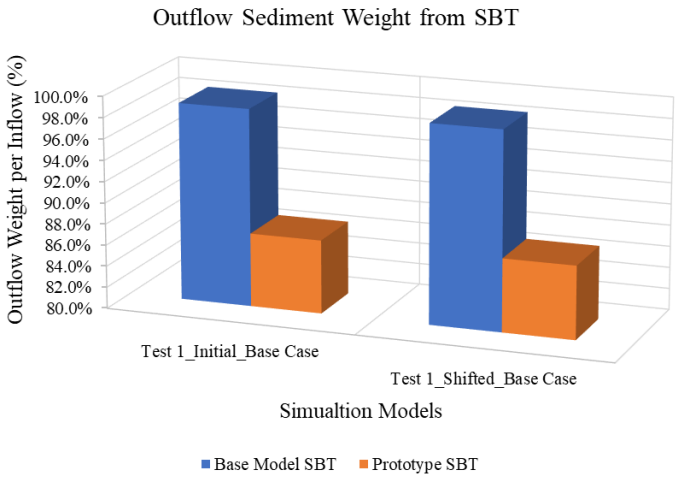

Figure 7.11 Comparison of the sediment outflow between physical model and numerical models at SBT outlet

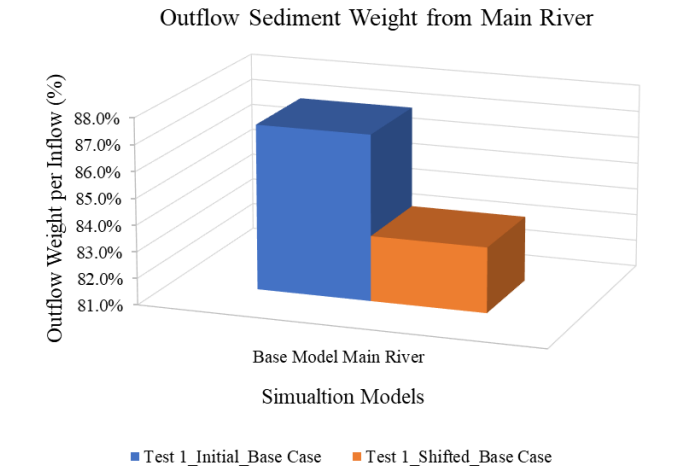

Figure 7.12 Comparison of the sediment outflow at main river outlet between two SBT numerical models

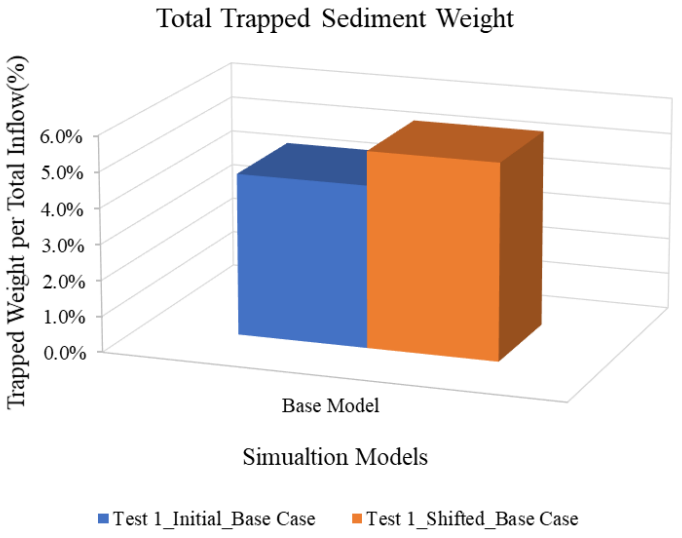

Figure 7.13 Comparison of the weight trapped in reservoir in two SBT numerical models

It has been observed that all the incoming sediments at SBT outlet are readily passed down. Therefore, concentration at SBT outlet is nearly equal to the inflowing concentration. However, incoming concentration for size 1 i.e. 3mm particle is relatively higher in shifted model (Figure 7.14 and *Appendix E - Sediment Simulation - Figure E. 4*). This suggests that higher bed erosion occurs in shifted model, as inflow concentration for this sediment size is zero. Similarly, at the main river outlet, sediment concentration for size 1 and 3 i.e. 3mm and 5mm; have not been observed. Also, all incoming sediment at main river outlet for size 6 (0.015mm), size 7 (0.007mm) and size 8 (0.003mm) are passed down. Among all, size 3 (0.125mm) and size 4 (0.048mm) are major sediments to be trapped in reservoir (Figure 7.15). Furthermore, shifted model traps higher sediment volume as compared to initial model.

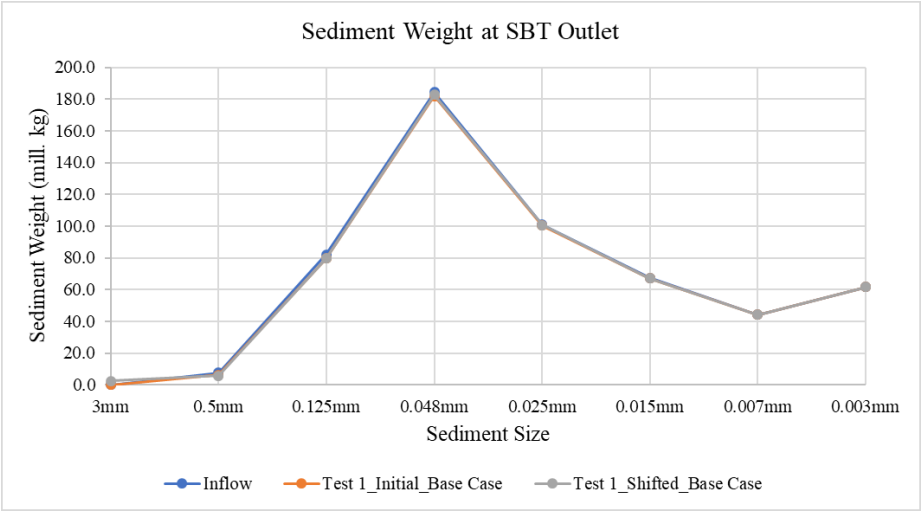

Figure 7.14 Comparison of inflow and outflow of different sediment sizes from SBT outlet

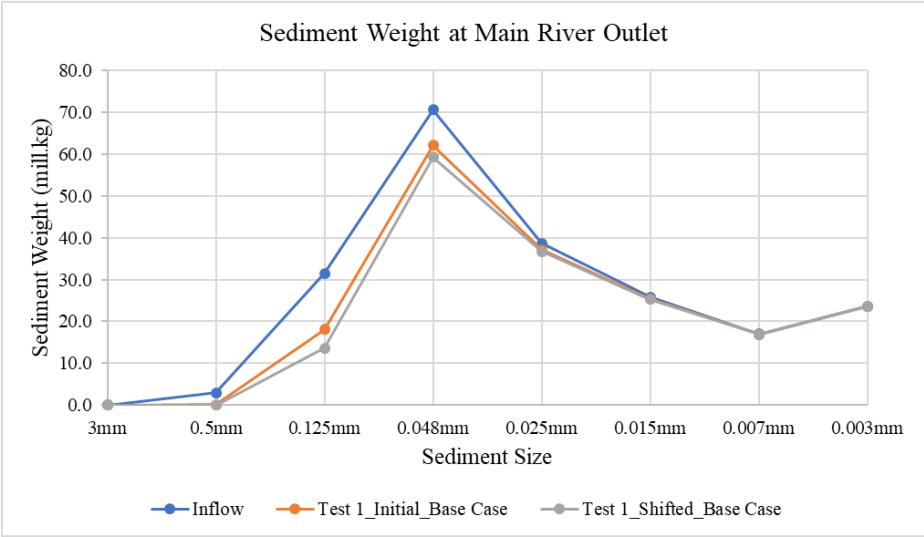

Figure 7.15 Comparison of inflow and outflow of different sediment sizes from main river outlet

7.4.3 Sensitivity analysis

To analyze the effect of various model parameters on the outflow concentrations, sediment trapping, velocity, bed changes etc. in comparison to the base case (Test 1), sensitivity analysis have been conducted. Further, this would also ensure that the model results are reliable and rigid. All together 18 parameters are analyzed and only those involving considerable changes have been mentioned here. Except these parameters, all other are represented in the *Appendix E - Sediment Simulation*. Table 7-4 Shows the different parameters used for the sensitivity analysis simulation for both initial and shifted models. The highlighted ones are the changed parameters for sensitivity analysis in each test case. Further, the concentrations or weight of sediment outflow from SBT and main river outlets for different sensitivity tests are represented in Figure 7.22 and Figure 7.23. The trapped sediment weight in reservoir is represented in Figure 7.24. The description of different bars and the horizontal lines in these figures are described just above the figures for better understanding.

Table 7-4 Parameters for sensitivity analysis

Test Number	Sensitivity Parameter	Corresponding Parameter Values										
		Minimum cell height (m)		Iteration	Discretization Scheme	Roughness (Ks) (mm)	Time step (sec)	Fall Velocity	Temperature (°C) and viscosity (m^2/s)	Sediment Formulae		Roughness Formula	Sediment Concentration (ppm)
		F 94 dataset								Type	Sediment Type		
Test 1	**Base Case**	**0.01**	**0.02**	**250**	**1st order**	**3.39**	**10**	**as caculated**	**10 ℃ & 1.306 E-6**	**Van Rijn**	**Suspended**	**F 90 0**	**5005**
Test 2	Minimum Cell Height	**0.001**	**0.01**	250	1st order	3.39	10	as caculated	10 ℃ & 1.306 E-6	Van Rijn	Suspended	F 90 0	5005
Test 3		**0.005**	**0.01**	250	1st order	3.39	10	as caculated	10 ℃ & 1.306 E-6	Van Rijn	Suspended	F 90 0	5005
Test 4	Iteration	0.01	0.02	**150**	1st order	3.39	10	as caculated	10 ℃ & 1.306 E-6	Van Rijn	Suspended	F 90 0	5005
Test 5		0.01	0.02	**10**	1st order	3.39	10	as caculated	10 ℃ & 1.306 E-6	Van Rijn	Suspended	F 90 0	5005
Test 6		0.01	0.02	**350**	1st order	3.39	10	as caculated	10 ℃ & 1.306 E-6	Van Rijn	Suspended	F 90 0	5005
Test 7	Discretization Scheme	0.01	0.02	250	**2nd order**	3.39	10	as caculated	10 ℃ & 1.306 E-6	Van Rijn	Suspended	F 90 0	5005
Test 8	Roughness	0.01	0.02	250	1st order	**8.49**	10	as caculated	10 ℃ & 1.306 E-6	Van Rijn	Suspended	F 90 0	5005
Test 9		0.01	0.02	250	1st order	**5.09**	10	as caculated	10 ℃ & 1.306 E-6	Van Rijn	Suspended	F 90 0	5005
Test 10		0.01	0.02	250	1st order	**1.69**	10	as caculated	10 ℃ & 1.306 E-6	Van Rijn	Suspended	F 90 0	5005
Test 11	Timestep	0.01	0.02	250	1st order	3.39	**30**	as caculated	10 ℃ & 1.306 E-6	Van Rijn	Suspended	F 90 0	5005
Test 12		0.01	0.02	250	1st order	3.39	**60**	as caculated	10 ℃ & 1.306 E-6	Van Rijn	Suspended	F 90 0	5005
Test 13	Fall Velocity	0.01	0.02	250	1st order	3.39	10	**10% increased**	10 ℃ & 1.306 E-6	Van Rijn	Suspended	F 90 0	5005
Test 14		0.01	0.02	250	1st order	3.39	10	**10% decreased**	10 ℃ & 1.306 E-6	Van Rijn	Suspended	F 90 0	5005
Test 15		0.01	0.02	250	1st order	3.39	10	**with temperature & viscosity**	**20 ℃ & 1.0 E-6**	Van Rijn	Suspended	F 90 0	5005
Test 16	Sediment Calcualtion Formula	0.01	0.02	250	1st order	3.39	10	as caculated	10 ℃ & 1.306 E-6	**Meyer Peter and Muller**	**Total load**	F 90 0	5005
Test 17	Roughness	0.01	0.02	250	1st order	3.39	10	as caculated	10 ℃ & 1.306 E-6	Van Rijn	Suspended	**F 90 2**	5005
Test 18	Formula	0.01	0.02	250	1st order	3.39	10	as caculated	10 ℃ & 1.306 E-6	Van Rijn	Suspended	**F 90 3**	5005

For minimum cell height and iteration test cases, the simulation results are similar to that of base case (Test 1). There are minor changes in the sediment concentration and outflow. This can be observed from the Figure 7.22, Figure 7.23, Figure 7.24 and figures in *Appendix E - Sediment Simulation - Figure E. 4 onwards*. Besides these, the Test 2 i.e. F 94 0.005 0.01; didn't converge in initial model. Various convergence options as described in manual like F 113 7, F 159, F 235 10 etc. were tried upon. However, convergence couldn't be achieved. In the section below, different observations and results are described based on the graphical representation.

For change in discretization scheme:

The higher order scheme reduces false diffusion thereby providing better simulation results. Whereas first order power law scheme provides stable simulation (Olsen, 2018; Hoven, 2010). Further, in some numerical simulation like for sand trap of Khimti HPP, the flow field varied significantly depending on the discretization scheme (Almeland *et al.*, 2019). Therefore, to access the effect of discretization scheme on simulation results, second order has been considered.

For initial model, the simulation results from Test 7 i.e. 2nd order discretization scheme, is similar to that of the base case. Whereas, differences in bed rise pattern have been noticed for shifted model. As discussed earlier in the section 7.4.1, a bed wall just downstream of SBT has been observed, that divides bed into two parts. Figure 7.16 shows the presence of initial bed wall in both cases which gets eroded in successive time. Similarly, Figure 7.17, i.e. at end of simulation, displays the formation of same bed wall for shifted base case and 2nd order test.

However, the bed wall in 2nd order forms faster and is wider in comparison to base case. Similarly, higher velocity at upstream and downstream of the SBT have been observed for 2nd order. The Figure 7.16 and Figure 7.17 shows the bed changes and velocity at different time frames for base case (Test 1) and Test 7 (2nd order) of shifted model.

The sediment concentration and trapping in 2nd order scheme, for the initial model is equal to the base case. Whereas for shifted model, concentration is higher at SBT outlet by 0.23%; nearly equal at main river outlet; and reservoir trapping is less by 0.22% in comparison to base case. The results can be referred in the Figure 7.22, Figure 7.23 and Figure 7.24.

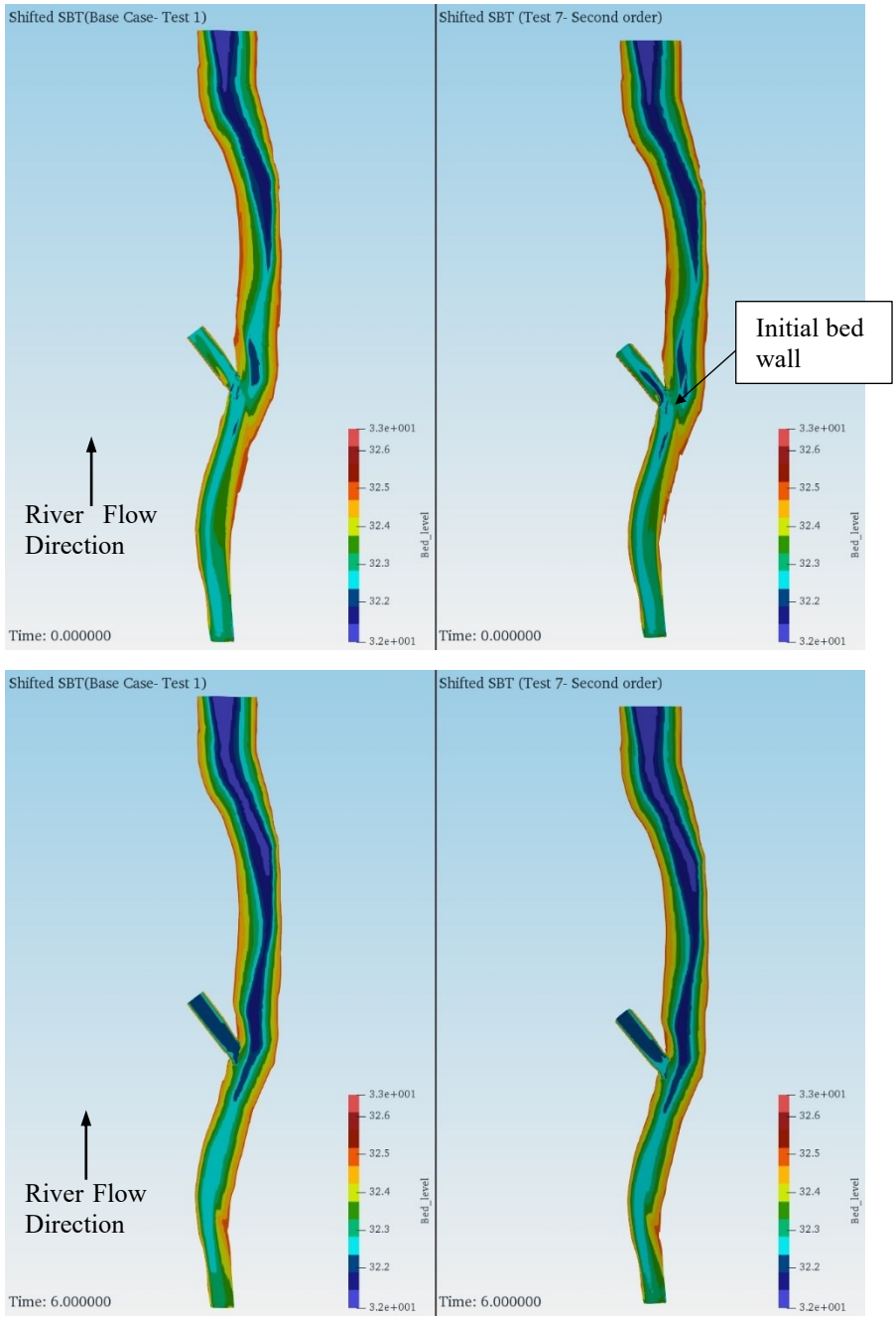

Figure 7.16 Bed changes at different timeframe

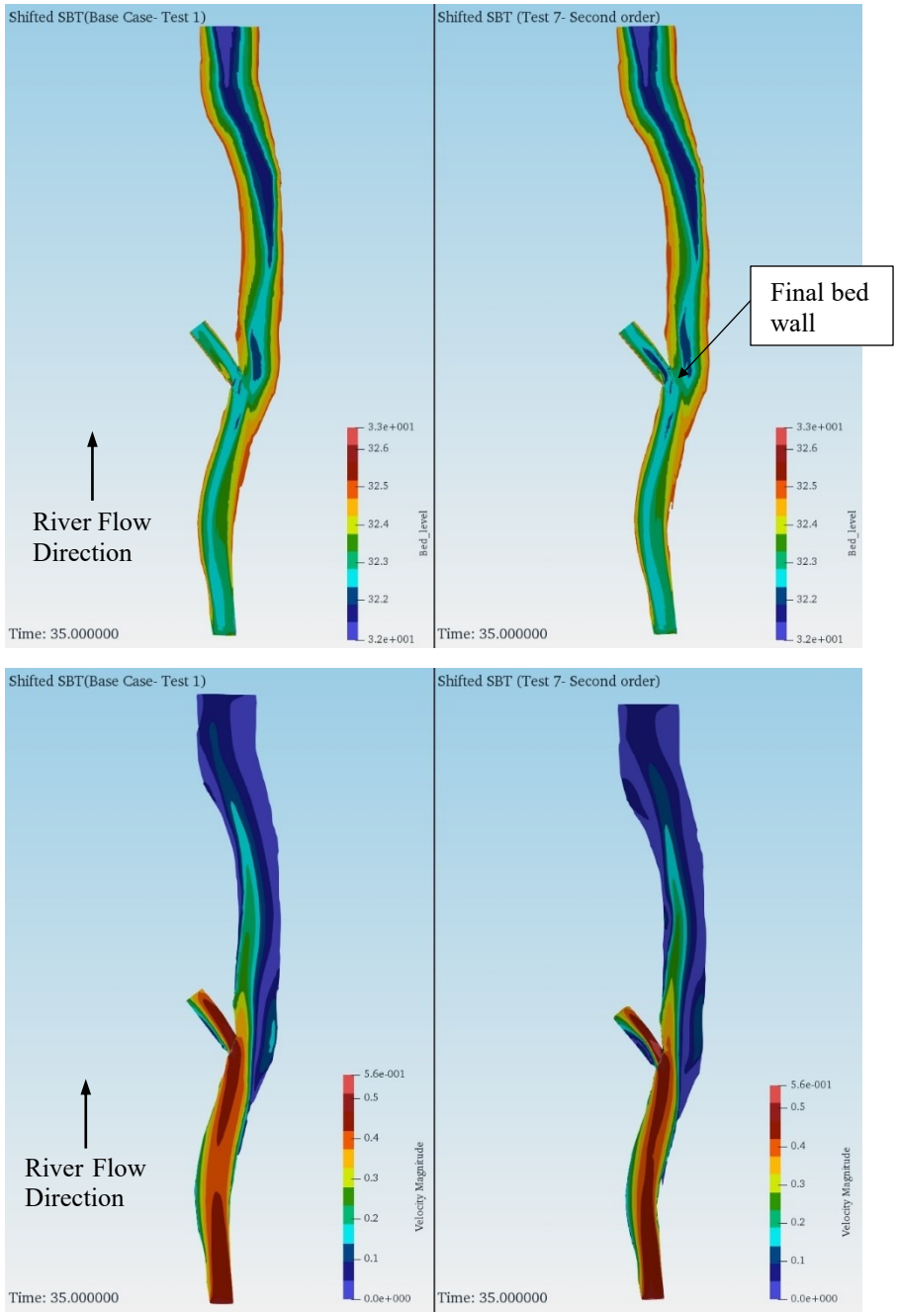

Figure 7.17 Bed changes and velocity at Time 35

For change in roughness height (k_s):

The roughness height plays a crucial role in determination of flow field. In this study, it has been observed that, with decrease in roughness height from 16.9mm to 3.39mm for hydraulic simulation, the flow field changed from left side to center or right side of the geometry. This would have much higher impact on the erosion and deposition pattern as well as concentration at outlets. Therefore, this parameter has been chosen to access its effect on the simulation results.

In both models, maximum velocity during simulation decreases with increase in k_s value at upstream of SBT and vice versa (Figure 7.18 and Figure 7.19). That means, highest velocity is for k_s 1.69mm whereas lowest for k_s 8.49mm. The velocities in initial model are 0.6m/s, 0.58m/s and 0.57m/s for k_s 1.69mm, k_s 3.39mm and k_s 8.49mm respectively. Similarly, for shifted model, the velocities are 0.63m/s, 0.6m/s and 0.57m/s respectively. However, the order of erosion for different roughness height differs in each model. In shifted model, initial major erosion takes place for k_s 8.49 (Test 8) followed by k_s 3.39mm (Test 1- Base case) and finally k_s 1.69m (Test 10). Whereas in initial model, erosion starts in k_s 1.69mm followed by k_s 8.49 and then on k_s 3.39mm.

After the initiation of erosion, rate of erosion and deposition is higher for model with higher k_s. This implies, although erosion starts late for k_s 8.49mm, sediment deposition and re-erosion process are much faster afterwards which might surpass the ongoing process for lower k_s. Likewise, at the end of simulation, velocity upstream of SBT is greater for the shifted model with higher k_s. While, the velocity is similar for the initial model. A similar phenomenon of bed wall formation as seen in Test 7 (2nd order

discretization scheme), has been observed for all the test cases in shifted model. These walls are generally seemed to be made by deposition of sediments when water is being discharge through SBT. Also, more prominent walls are seen before the major erosion. Moreover, the bed wall is more extended and elevated for greater k_s values. Further, no such change in flow field from one side of the geometry to other have been observed during sediment simulation. The results can be referred in Figure 7.18 and Figure 7.19.

Likewise, from sediment point of view, outflow from SBT outlet is higher for higher k_s, which decreases with lowering of k_s. Both the models have higher SBT outflow concentration for Test 8 (k_s 8.49mm) and Test 9 (k_s 5.09mm) whereas lower for Test 10 (k_s 1.69mm) as compared to base cases (Test 1- k_s 3.39mm). Similarly, the shifted model has higher outflow than initial model in case of SBT outlet.

For initial model, at main river outlet, Test 8 and Test 9 are nearly equal while Test 10 concentration is lower than base case. Similarly, for shifted model, all three tests are lower than the base case but among these tests, Test 9 has higher concentration than other two. For this outlet, initial model has higher outflow concentration than the shifted model. Further in case of sediment trapping, more sediment has been trapped for the smaller k_s and decreases with increase in k_s. The sediment trapping for Test 8 and Test 9 are lower whereas for Test 10 is higher than the base case in both models. However, the sediment trapping in shifted is greater than initial model for all the tests. The results can be referred in the Figure 7.22, Figure 7.23 and Figure 7.24.

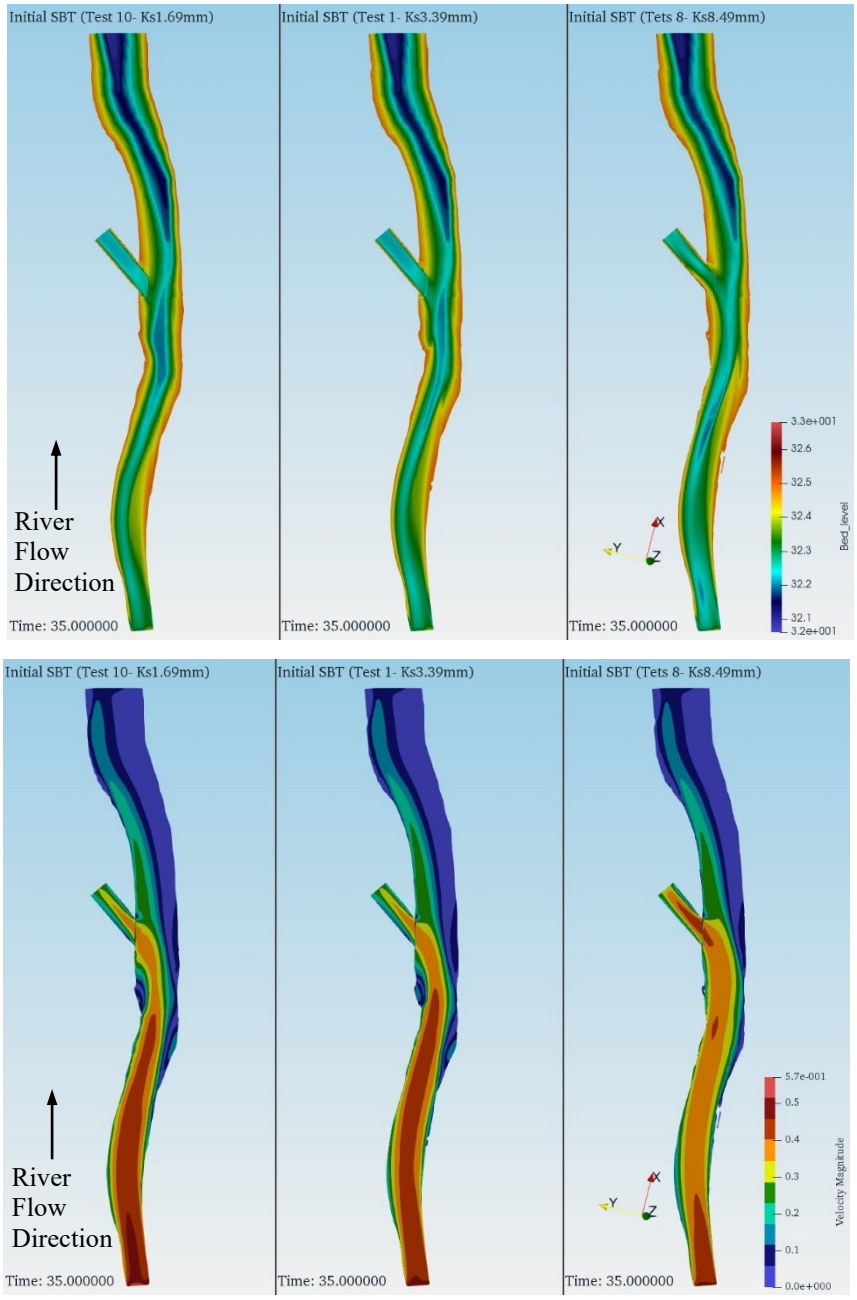

Figure 7.18 Bed changes and velocity for test 1, 8, 10 of initial model at time 35

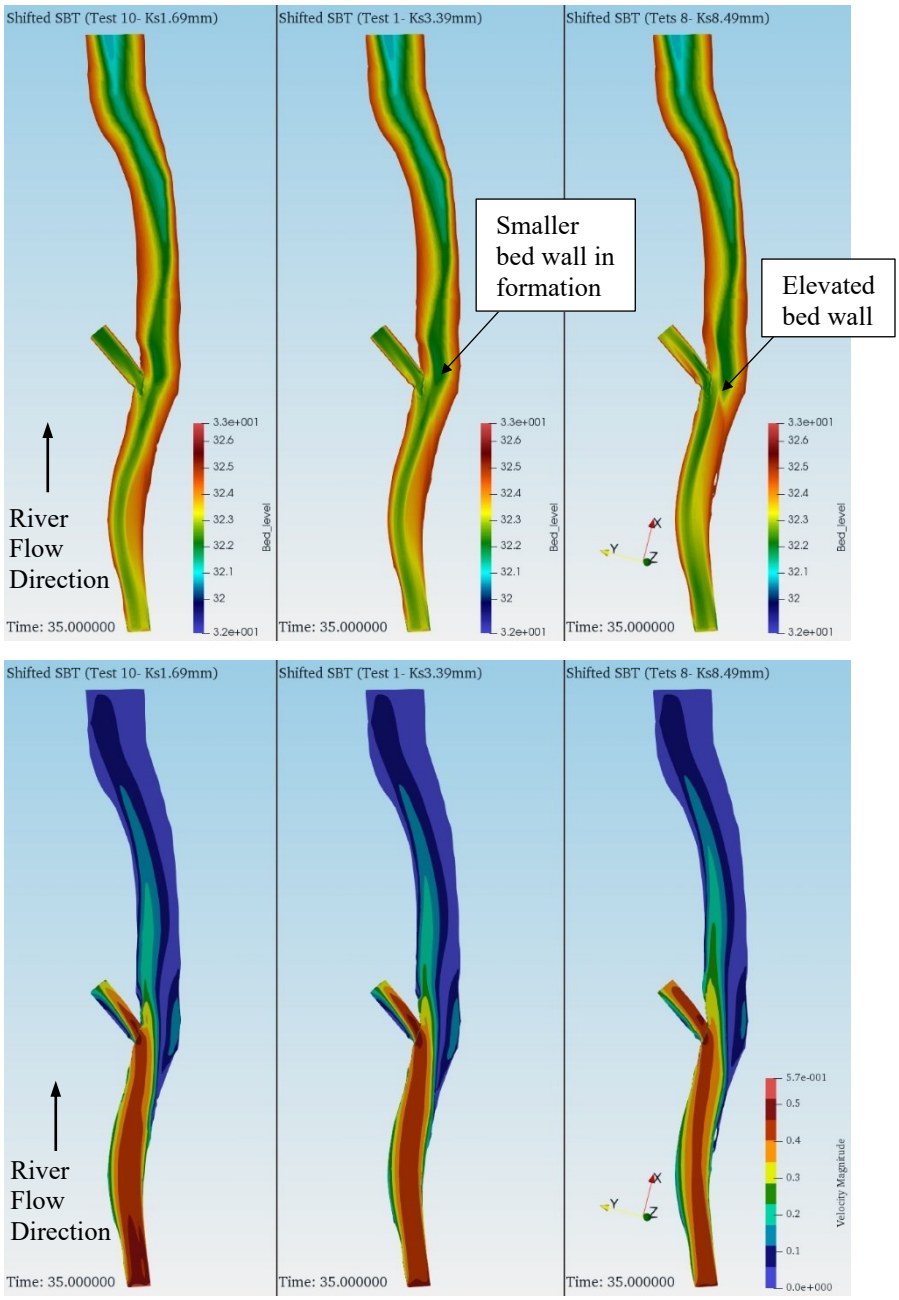

Figure 7.19 Bed changes and velocity for test 1, 8, 10 of shifted SBT at time 35

For change in Fall velocity and Temperature:

As the fall velocity of the sediments can change owing to the nature of their composition, sensitivity analysis for 10% increase (Test 13) and decrease (Test 14) in fall velocity of the particles have been carried out. Similarly, as water temperature of river fluctuates based on surrounding temperature, the effect of fluctuation on outflow concentration and trapped weight has to be observed. Therefore, simulation have been carried for 10°C (base case-Test 1) and 20°C (Test 15) water temperature.

When the fall velocity is increased, lower sediment concertation as compared to the base case or Test 1 have been observed at the outlet of SBT and main river. Similarly, in case of reservoir trapping, higher trapping has been observed. For the decrease in fall velocity, sediment concentration has increased at both outlets with lower reservoir trapping.

When the temperature is increased, sediment concentration at the outlets have decreased while trapped sediment weight has increased. The shifted model has higher outflow concentration at SBT outlet; and higher reservoir sediment trapping than initial model. Whereas in main river outlet, initial model has higher outflow than the shifted model. The results can be referred in Figure 7.22, Figure 7.23 and Figure 7.24.

For change in sediment transport formulae:

Van Rijn formula for suspended sediment transport has been considered in all simulation using the data set F 84 0. Although this formula works for suspended load, some concentration of Size 1 i.e. 3mm particles, bed sediments, have been observed at outlets. As both bed load and suspended load are obtained at the outlet, Meyer-Peter and Müller formula for total

load has been considered to see the effect on the sediment concentration. The formulae can be selected in SSIIM 2 only using data set F 84 5.

The sediment concentration at both outlets have decreased for Meyer-Peter Müller formula (Test 16). The total concentration at SBT and main river outlets have reduced by 0.95%, 0.67%; and 0.74%, 0.79% for initial and shifted models as compared to the base case (Test 1). Whereas, sediment trapping has increased in initial and shifted models by 0.88% and 0.76% respectively. The sediment concentration for each particle till size 6 i.e. 0.015mm has decreased. While, equal or slightly greater concentration for size 7 (0.007mm) and size 8 (0.003mm) have been observed at both the outlets. From the Figure 7.20 and Figure 7.21, it can be observed that, the bed changes are higher for the Van Rijn sediment transport formula rather than Meyer-Peter and Müller formula, for both the models. This also signifies, higher erosion and deposition for the Van Rijn formula. The sediment size concentration or total sediment weight for total simulation time can be referred in Figure 7.22, Figure 7.23, Figure 7.24 and *Appendix E - Sediment Simulation - Figure E. 4 onwards.*

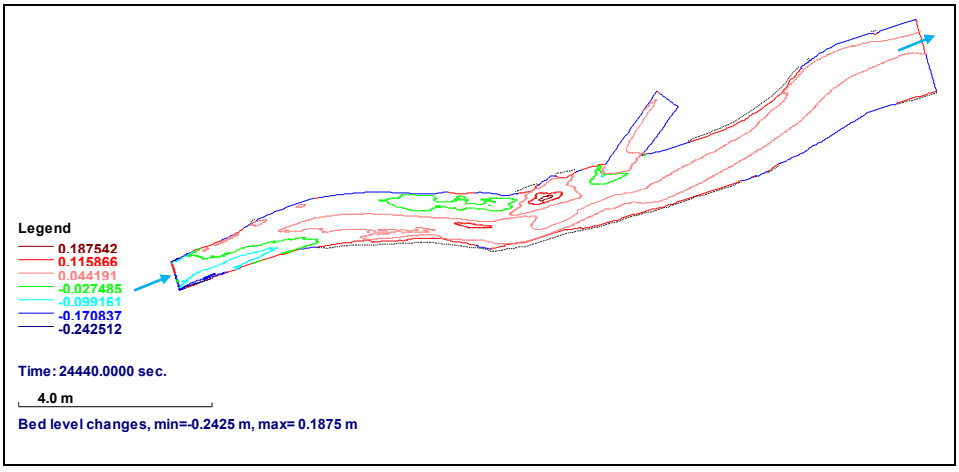

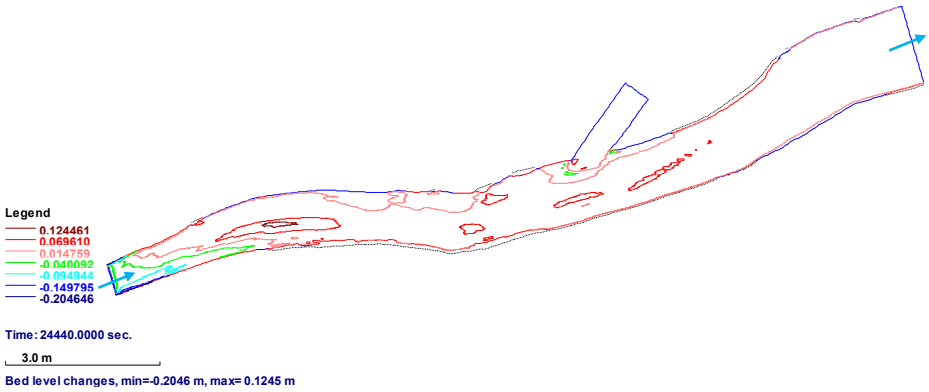

Figure 7.20 Bed level changes for Van Rijn (upper) and Meyer-Peter and Müller (lower) formula in initial model

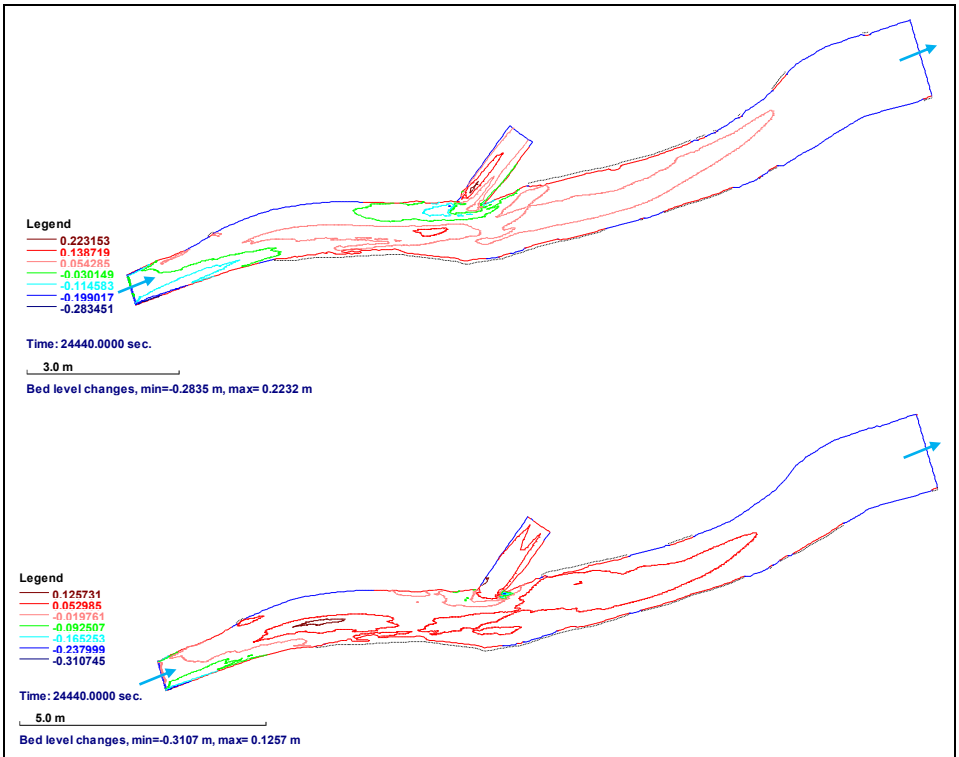

Figure 7.21 Bed level changes for Van Rijn (upper) and Meyer-Peter and Müller(lower) formula in shifted model

For different SSIIM algorithm in selecting roughness formulae:

As the simulated models uses the roughness provided either at W 1 or F 16 data sets, effect of the bed grain size distribution and bed form height has been ignored. Similarly, the roughness of bed might vary due to the deposition of suspended sediments leading to change in outflow concentrations and deposition in reservoir. Therefore, to observe the effect of these parameters on outflow concentration of sediments F 90 2 and F 90 3 data sets have been used. F 90 2 (Test 17) data set calculates the roughness based on bed grain size distribution (d_{90}) whereas F 90 3 (Test 18) dataset calculates based on d_{90} and bed form height.

Both tests show higher concentration at SBT outlet whereas lower at the main river outlet, compared to base case for initial model. Among these roughness parameter, Test 18 has higher concentration at both outlets. Likewise, in shifted model, Test 17 has less concentration than Test 18 at both outlets. Further, at SBT outlet, the concentration in nearly equal or higher than base case. While for the main river, the concentration is lower. The results can be observed in Figure 7.22, Figure 7.23 and Figure 7.24.

7.4.4 Problems faced

Convergence problem mainly in the shifted model has been encountered. These problems were due to the triangular cells and wetting/drying of the cells. The problems were solved by using F 235 10, F 113 7 and F 94 data sets.

Description for the Figure 7.22, Figure 7.23 and Figure 7.24

The vertical axis in the Figure 7.22 and Figure 7.23 represents the weight of sediment outflow from each outlets with respect to the inflow sediment weight. The sediment outflow weight at each outlet has been calculated based on the outflow concentration at the end of simulation. Whereas, the inflow sediment weight is calculated based on the inflow concentration provided to the numerical model. This can be also viewed as ratio of outflow concentration to inflow concentration at each outlet for the simulation period. Whereas, in Figure 7.24, it is the ratio of trapped sediment weight to inflow weight in the numerical model.

While, the horizontal axis represents the different sensitivity test as described in Table 7-4. The figures below have been compacted to compare the results of all the sensitivity test cases to the base case (Test 1) of initial as well as shifted model. Similarly, the results for the same test case between initial and shifted model can also be compared.

The blue bar graph represents the ratio of outflow sediment weight or concentration to inflow sediment weight or concentration of different sensitivity test cases at SBT (Figure 7.22)and main river (Figure 7.23) outlets for initial model. Similarly, the orange bar graph represents the results for shifted model. Whereas, the horizontal black and orange line represents the base case (Test 1) for initial and shifted model respectively. The same explanation for different bars and horizontal lines are valid for Figure 7.24, except that these are for trapped sediment weight in reservoir.

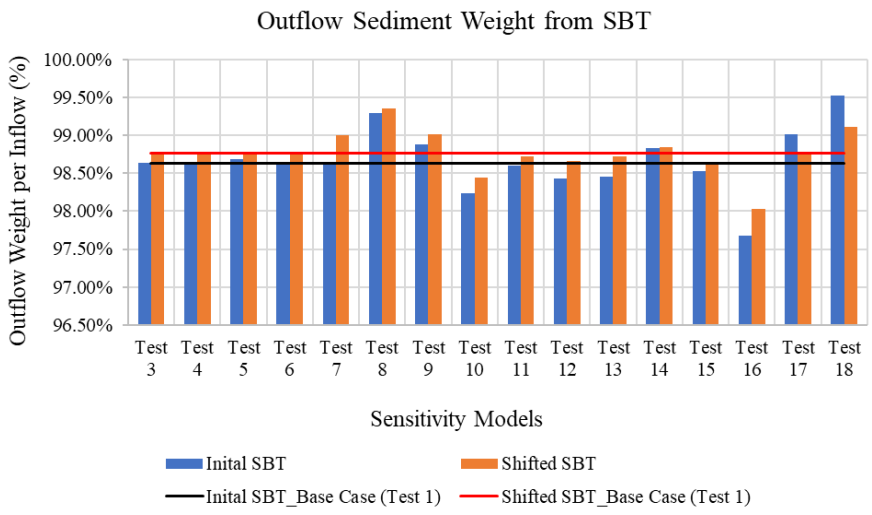

Figure 7.22 Comparison of sediment outflow from SBT outlet for different sensitivity parameters

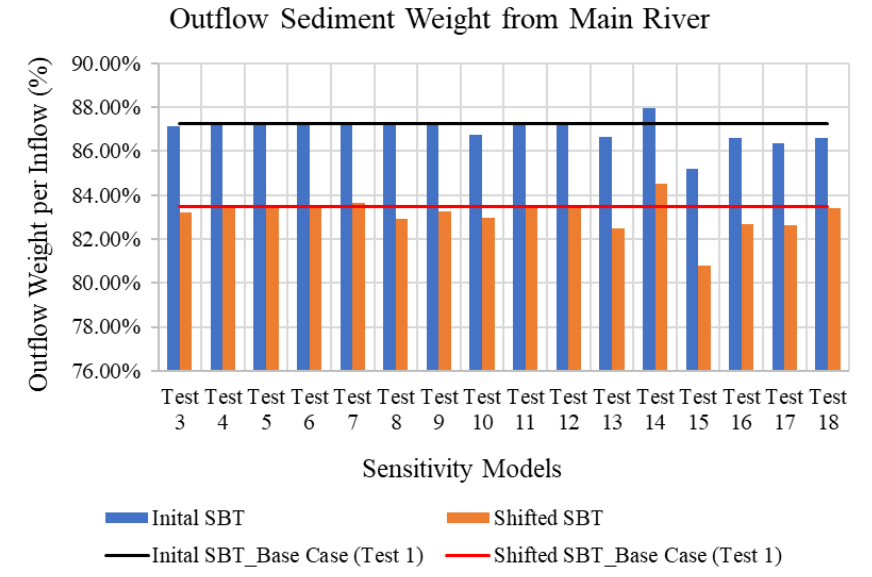

Figure 7.23 Comparison of sediment outflow from main river outlet for different sensitivity parameters

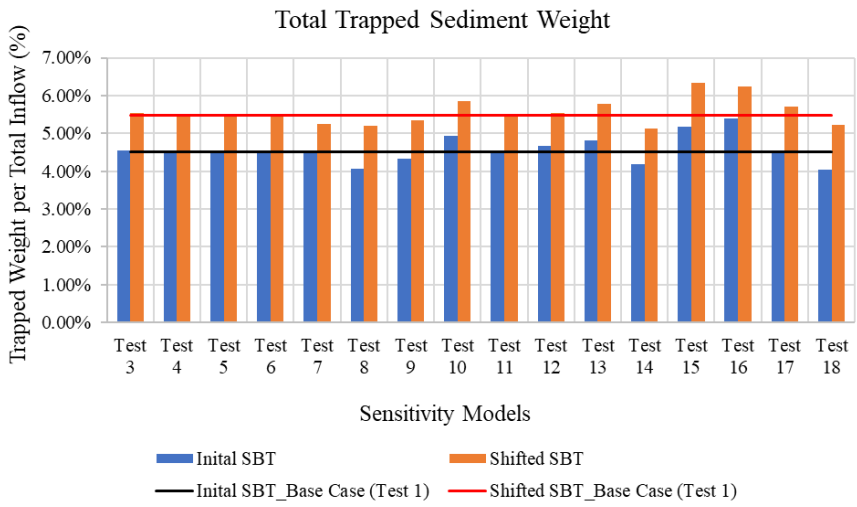

Figure 7.24 Comparison of trapped sediment weight in the reservoir for different sensitivity parameters

8 Discussion

This part comprises of discussion on various results that have been noticed during simulation and calculation. Mainly representing the deviation in results between the numerical and physical model; numerical model itself due to change in various parameters; and the limitations of the study and SSIIM 2 CFD model.

8.1 Discussion on Results and Study Objectives

Although hydraulic simulation flow pattern shows strong resemblance with physical model pattern, differences at upstream section 1 and downstream section 1 have been observed. These are mainly due to the difference in bed deposition geometry. As very few measured bed deposition cross sections were available for developing the whole riverbed contour, the bed geometry couldn't be properly replicated, thereby resulting the deviations at those sections. Therefore, it is very important to measure the bed deposition and velocities at many cross sections along the experimental river reach for proper numerical model development.

In numerical model, better surface velocity resemblance for SBT sections can be observed for higher k_s without bed rise (Refer *Appendix F - Discussion - Figure F. 1*). Whereas, for main river, bed rise with lower k_s values are better (Figure 6.11). This corresponds that these two structures have different roughness. It would have been better if different roughness could be utilized in SSIIM 2, which is a limitation for this CFD program. Therefore, a medial approach to obtain satisfactory result has been adopted.

Further, differences in flow field due to lowering of k_s have been observed in hydraulic simulation. As discussed in section 6.4.1, the flow field initially shifts from left to right due to the bed rise which is supplemented

by lowering of k_s (Figure 6.8; Figure 6.9). This shows the hydraulic model is sensitive to the roughness height for same bed rise. Similar phenomenon for discretization scheme and grid size was observed for Khimti and Tonstad HPP model (Almeland *et al.*, 2019) requiring verification from the physical model. Therefore, sensitivity for roughness has to be carried out and the simulated results have to verified from field data.

Likewise, the hydraulic model selected for simulating sediment (i.e. Option 4: combination of no bed rise and 8cm bed rise with k_s 3.39mm) has higher flow velocity skewed towards river centre or right side. Whereas, in sediment simulation, flow velocity is lower and along left side. This is probably due to sediment deposition along right bank which pushes the flow towards left bank during sediment simulation (Refer *Appendix F - Discussion - Figure F. 2*).

Looking at the hydraulics at the SBT region, the shifting has improved both hydraulics and sediment handling. The sediment deposition at the shadow area as previously present in initial model has highly reduced, although some small deposition past SBT can be seen (Figure 7.7; Figure 7.8). This suggests that the shifted SBT inlet location i.e. downstream of outer bend is more favourable for inlet position than inner bend. Similarly, the re-circulation zone in this area has also been reduced. Due to this reduction, the flow seems to be moving smoothly as well as the velocity had increased in the SBT region (Figure 7.6, Time 35). This has led to increase in the suction or erosion area near the SBT intake (Figure 7.8, Time 16 and 21).

Further, the velocity at downstream of the SBT in shifted model, compared at same location, has decreased leading to more trapping of the sediments. This decrease in velocity could be attributed to the formation of bed wall

in shifted model as discussed in Section 7.4.1. Although, it seems the velocity in downstream along left bank, at vicinity of SBT, has increased due to bed wall, the velocity all along the length of reservoir has decreased leading to higher trapping of sediments in reservoir (Figure 7.5; Figure 7.6). The fact of increased trapping has been confirmed by calculation for sediment trapping in Section 7.4.2. Besides, these, the phenomenon of forming the bed wall is quite interesting in numerical model. It seems that, due to the flow curvature at SBT intake, centrifugal force is being developed causing the sediments to be thrown tangentially forming this bed rise. Also, due to the backwater from dam, the velocity after SBT might be dampened causing more sediments to settle at that region. In the physical model report Annex H-3, no distinct remarks about the sediment deposition as such has been made. Yet, deposition of suspended load in the main river channel near the SBT intake has been mentioned (Changjiang Survey and Sinotech Engineering Consultants, 2019a). This phenomenon could have only arise in numerical model due to the difference in bed geometry as compared to physical model. Moreover, it seems to occur in the region (between upstream section 1 and downstream section 1) where the velocity pattern differs in comparison to physical model.

The sediment concentration at SBT outlet in numerical model is higher than physical model by 11.7% and 11.9% respectively for initial and shifted models (Figure 7.11). This might be due to the several factors like bed geometry, roughness, bed sediments etc. Among them, a clear factor that can be observed is the difference in composition of bed sediments on physical and numerical models. In physical model, sand and pebbles with density 2,650kg/m^3 have been used. Whereas, 3mm particle with same density as Zhuzhou coal (1,330kg/m^3) have been considered, for numerical

model. Therefore, higher erosion of these particles can be anticipated. As per the report, no any bed materials like pebbles have been observed at the SBT outlet (Changjiang Survey and Sinotech Engineering Consultants, 2019a). However, in numerical model, 3mm sediment concentration was observed at SBT outlet (Refer *Appendix E - Sediment Simulation - Figure E. 4*). This concentration increased for shifted model which also explains the increase in difference for shifted model than initial model. This difference could have been lowered if different density materials and most probably different roughness could be used in SSIIM 2.

Moreover, the sediment concentration at SBT outlet is slightly higher (i.e. by 0.14%) for shifted than initial model. Similarly, the concentration from main river outlet is 3.8% lower in shifted than initial implying more sediment being trapped in shifted model reservoir (i.e. higher by 0.95%). The increased concentration might be due to higher erosion corresponding to higher velocity in the upstream part of SBT for shifted model (Refer Section 7.4.1). Similarly, lower velocity in downstream part as well as increased length of reservoir might have provided optimum opportunity for the suspended sediments to settle in reservoir. Thereby trapping more sediments in the shifted model.

Looking at the overall results from simulation, the shifted model seems to work better than initial model. However, the cost for increased length of tunnel on shifting SBT by 130m upstream as well as the maintenance cost for abrasion have to be considered. This should be evaluated in comparison with the monetary values of increased sediment outflow from SBT and increased trapping in the reservoir which ultimately saves the maintenance cost for wear and tear of the turbines. Moreover, the monetary values for rate of decrement in efficiency of turbines due to sediment erosion have to

be included in the evaluation, as many reports have suggested that the loss due to efficiency decrement is higher than the maintenance cost (Rai, Kumar and Staubli, 2019).

In addition to this, the aim of this study is to see whether hybrid modelling i.e. inclusion of both numerical and physical model, functions better than individual models alone. The identical results for flow pattern and the outlet concentration at SBT support numerical model calibration and validation. The calibrated model can be further used to optimize different SBT intake locations as well as to investigate the effects of different parameters in the model. This would save a lot of time, energy and cost, that would otherwise be required for the physical model. As well as, the actual effects of scaling on using different materials like Zhuzhou coal than natural material is still a field of research. However, numerical models can be made in prototype scale thereby eliminating the scale effects. Therefore, the study here has helped to optimize the SBT intake location based on hydraulics and sediment handling, firmly supporting the hybrid modelling concept.

8.2 Discussion on Sensitivity Analysis

In case of minimum cell height for Test 2 (F 94 0.001 0.01) in initial model, the simulation didn't converge. This could be due to various factors like smaller cell height, roughness to depth ratio, shallow water problem, triangular cells etc in the model. As the cell height i.e. 1mm, is smaller than the used k_s value (3.39mm), the convergence problem could have arose. As per the SSIIM manual, the height of the bed cell should not be too much smaller than the roughness of the bed. When increasing the cell height to 5mm, the simulation keeping all the parameters same, converged which supports the above statement. Another reason could be the shallow/triangular cells during wetting/drying computation. As the map

graphics shows the simulation is being diverged at the side boundary with very high velocity, similar to description in the SSIIM manual (*Appendix F - Discussion - Figure F. 3*). This can be a flow separation point (Olsen, 2018) leading to divergence. Similarly, there might be other reasons too for the divergence in Test 2.

Further, in case of the roughness height, the velocity upstream of SBT decreases with increase in k_s and vice versa, as shown in Section 7.4.3. Similar decrease in velocity has been observed in the sensitivity of Binga reservoir (Nepal, 2019). However, the reason for it couldn't be found. The erosion sequence for initial model is as expected i.e. erosion for model with larger k_s followed by smaller. Since, the velocity deceases for increased k_s in the model, the decrease is smaller compared to increase in k_s value leading to increased bed shear. Thereby, initiating erosion earlier in model with higher k_s. However, for shifted model, the k_s 1.69 erodes first followed by k_s 8.49mm and then k_s 3.39mm. When the bed shear is checked at the major erosion simulation period, the bed shear is higher for higher k_s. However, the reason for such case couldn't be archived. Although the sequence of erosion may differ, the bed shear is higher for increased k_s depicting greater erosion. As the erosion has increased at upstream inflow region, the outflow concentration at SBT has also increased in model (Figure 7.22, Test 8). Similarly, velocity downstream of SBT in shifted model is higher for higher k_s, causing more sediments to outflow from the main river outlet, thereby decreasing the deposition in reservoir. This can be observed in the Figure 7.24, where deposition is greater for lower k_s value (Test 10 k_s 1.69mm) as compared to higher (Test 8 k_s 8.49mm).

In case of the fall velocity, the results same as anticipated have been observed in the numerical model. As fall velocity increase, the SBT outlet

concentration should decrease and reservoir trapping should increase; and vice versa. Whereas for, increase in temperature, the fall velocity increases owing to the fact that the kinematic viscosity of the water decreases. As the fall velocity increases, the sediment concentration at outlet decreases as well as trapping increases, which has been observed in the numerical model.

As there are lots of formula for bed load and suspended load transport, it is very difficult to find the most suitable sediment transport formula for numerical model. Similarly, it is also difficult to distinguish between the bed load and suspended load to apply the transport formula. As discussed in Section 7.4.3, the presence of bed sediment at the SBT outlet in numerical model, suggested to consider the total load formula provided by Meyer-Peter and Müller. However, the results showed that, the concentration at SBT outlet has decreased for Meyer-Peter and Müller than the base case or the Van Rijn formula for suspended load. As the Van Rijn formula is developed for sandy rivers compared to Meyer-Peter and Müller which is developed for gravel bed rivers, Van Rijn might be more reliable for suspended sediment calculation. Also, the results for Van Rijn may be more accurate. Similarly, in experiments with gravel bed rivers also, the Van Rijn formula have showed better performance in comparison to Meyer-Peter and Müller formula (Mineault-Guitard, Rennie and Williams, 2016). Moreover, Meyer-Peter and Müller has been found to significantly underestimate transport of large gravels in several studies (US Army Corps of Engineers, 1995).

While looking into the roughness algorithm options, both the tests i.e. Test 17 (F 90 2) and Test 18 (F 90 3), the outflow from the SBT is nearly equal or higher than the base cases. For Test 17, the roughness algorithm uses

bed grain size distribution (d_{90}) to calculate the roughness as $k_s = 3*d_{90}$. The bed sediment provided for the numerical model is 3mm which means the ks value will be 9mm. Similarly, in Test 18, the roughness is calculated as

$$k_{s+\Delta} = 3 * d_{90} + 1.1\Delta\left(1 - e^{25\Delta/\lambda}\right) \quad (14)$$

where, Δ is bed form height and λ is bed form length.

In the above equation, $3* d_{90}$ will be equal to 9mm as pervious Test 17. Further addition of bedform effect will increase the roughness. As the roughness increases, increase in sediment concentration at SBT outlet has been observed during the sensitivity analysis for roughness height. Therefore, in both the cases the sediment concentration at SBT outlet should increase. Similarly, the outflow from the main outlet should decrease promoting higher reservoir trapping. In the simulation for both the tests, the described phenomenon has been observed.

8.3 Limitation for the Input Data and SSIIM 2

There have been various limitations for input files due to unavailability of data as well as the SSIIM 2 has its own limitations and problems. These have been discussed briefly.

8.3.1 Problems and limitations for input data

This whole study has been conducted based on the draft reports of UAHEP. The Client or Upper Arun Hydro Electric Limited had assured to provide final reports of the physical model with all the data around end of January 2020. However, due to the outbreak of Corona Virus, the reports from the consultants conducting the physical hydraulic test at Yangtze River Science Academy in Wuhan had been delayed. Therefore, no any further supporting

documents were received, and all the works had to be carried out on limited data. Mainly the measured bed deposition data, sediment concentrations, surface velocities, time of measurement etc were very limited as well as the explanations on different aspects were insubstantial. All the bed deposition and the PMSV data had to be interpolated or extrapolated from the graphical plots present in the reports.

8.3.2 Problems and limitations in SSIIM 2

Various problems have been encountered during simulation in SSIIM 2. Some relate to the limitation of the program itself whereas some seem to be bug. A typing error for printing the concentration has been found in the description of interpol and interres file of SSIIM's user manual. For printing the concertation, integer 6 should be used rather than 3 in F 48 data set.

Limitations:

- In SSIIM 2, different sediment densities can't be specified. Due to this, only suspended sediments have been modelled. Although different densities materials were used as suspended and bed sediments in physical model.
- Although roughness editor is present in SSIIM 2, different roughness can't be specified. The editor doesn't function. Therefore, same roughness value has been used for main river and SBT section.
- Concrete structures can't be made or specified in SSIIM 2. Due to this, pressurized bottom outlet for SBT can't be modelled. Therefore, the SBT and main river outlets are assumed to be free flowing open ends.

Probable Bugs:

- Although out blocking option in SSIIM 2 have been revealed during the study, the function doesn't work properly. The same data set can be used in SSIIM 2 as specified for SSIIM 1; however, the out blocking occurs for the whole grid section rather than just specified part. For example, if an out blocking is specified from i = 3 to 5 , j = 3 to 5 and k = 3 to 5 for a block of i * j* k = 7 * 7* 7, then the out blocking function will out block the whole section i = 3 to 5, j =3 to 5 and k = 1 to 7.
- A probable bug can be associated with the F 48 5 data set. The integer 5 used in data set prints the surface velocity as specified in description of F 48 data set in SSIIM manual. While using this integer, zero velocity for some locations were returned in the interres file. When this was rechecked using F 48 2 data set, velocity magnitude was present at that location. However, it couldn't be ascertained how F 48 5 data set works or from which depth the velocity magnitude is written in the interres file.

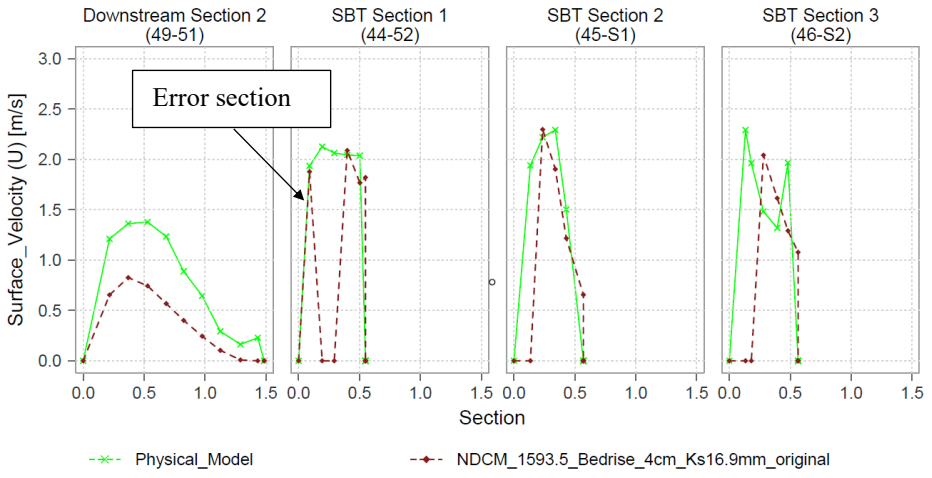

Figure 8.1 F 48 5 data set error representation

```
N 633.009000 646.884000 0.000000
N 633.089000 646.826000 0.000000
```

```
M 633.009000 646.884000 61011 60905 61004 60898 10.934019 67.744302 14.911880 31.016676
32.478571 0.162333 0.270799 -0.005844 0.003024 0.000587
32.435714 0.161060 0.270521 -0.011874 0.002937 0.000581
32.392857 0.160510 0.265499 -0.018490 0.002768 0.000568
32.350000 0.158346 0.254948 -0.020795 0.002581 0.000566
32.307143 0.152865 0.237974 -0.019718 0.002406 0.000573
32.264286 0.142544 0.216657 -0.014891 0.002257 0.000634
32.221429 0.118549 0.182161 -0.005860 0.001805 0.001472
M 633.089000 646.826000 60926 60820 60919 60813 11.403760 66.851147 16.349754 31.428764
32.478571 0.142526 0.297425 -0.007880 0.003871 0.000903
32.435714 0.145790 0.295511 -0.016819 0.003739 0.000875
32.392857 0.152370 0.287989 -0.026075 0.003392 0.000785
32.350000 0.157717 0.274335 -0.028042 0.002987 0.000703
32.307143 0.158879 0.253132 -0.025266 0.002642 0.000656
32.264286 0.154745 0.226528 -0.018471 0.002400 0.000682
32.221429 0.138757 0.185924 -0.007121 0.002014 0.001734
```

Figure 8.2 Interres values of error location for F 48 5 (upper) and F 48 2 (lower) data sets

8.4 Reasons for Inaccuracies

The errors and uncertainties mentioned in Section 2.3.2 are relevant in this case. They are discussed as follows:

- Errors in numerical approximations: As first order power law scheme is used as the discretization scheme, false diffusion can be a numerical approximation error for this study.
- Modelling errors: This can be relevant in this study. An example can be modelling the sediment transport using suspended load transport formula only. Whereas in real, both bed load and suspended load are used. So proper mathematical representation of the phenomena couldn't have been achieved.
- Errors due to not complete convergence: The time-dependent computations are used, and convergence has not been reached for every time step. To achieve complete convergence, the simulations would be very time-consuming. Therefore, there is a risk of inaccurate result due to incomplete convergence.
- Round- off errors: 64 bits floating point numbers with 12 digits accuracy is used by SSIIM. So, rounding- off error should not be a problem in this case.
- Errors in input data: There are uncertainties in the bed deposition geometry and input for the bed sediments. As well as some assumptions have been made during sediment simulation which might cause error in results.
- Programming errors: SSIIM has not been tested widely and has been used by a limited number of people, so there might be many bugs which can produce inaccurate results.

Other reasons for error can be reduced number of cells due to deposition especially in case of sediment simulation. The F 94 data set can eliminate many cells at the boundary resulting in different solution. Further, during sensitivity analysis, the change in parameters have influenced the model results which itself can be questionable. One of the errors could be the interpretation error, based on the thesis candidate's interpretations. However, candidate have tried to minimize this error as much as possible.

9 Conclusion

The SSIIM 2 numerical model has been successful in replicating the flow pattern and the surface velocities of the physical model. Similarly, the sediment concentration at SBT outlet is slightly higher than that measured in physical model. The deviation from physical model is about 11.7% and 11.9% for initial and shifted models respectively. Some discrepancies in flow pattern at sections upstream section 1 and downstream section 1 as well as deviation in concentrations at SBT outlet have been observed. However, those mainly relate to the problem in input files for bed deposition geometry and bed sediments. Therefore, more emphasis and focus must be provided to obtain the input data as these are the back bones of numerical model. Thus, proper measurement guidelines have to be made and carried out either for field data or physical model data measurement. This would ensure better numerical model development.

Further, the models are sensitive to various parameters which might affect the result accuracy. Therefore, sensitivity analysis of the important parameters is very essential and should be carried out. In this study, the roughness height and the sediment transport formula showed slight discrepancy with the base model results, which has to be further analyzed.

The optimization study on shifting the SBT inlet location showed positive results for both hydraulic and sediment point of view. The hydraulics near the SBT inlet location improved as the re-circulation zones and deposition at the shadow region disappeared. This supports the shifted SBT inlet location, downstream of the outer bend, to be more favorable than the initial SBT inlet position in inner bend. Similarly, higher velocity at upstream and lower downstream of SBT have been confronted for the shifted model. This

has led to the fact of higher erosion upstream and deposition downstream of the SBT. Therefore, providing ample or better solution for sediment handling in comparison to initial SBT location. However, no any monetary evaluation between increased tunnel length and higher sediment removal either from SBT or as deposition in reservoir itself has been carried out to decide whether the initial SBT location or the shifted is better. Therefore, this factor has to be taken into account when analyzing the SBT inlet locations.

Moreover, the replication of the physical model provides a better ground for various modifications in numerical model as such done in this study. Also, the sensitivity of various parameters can be analyzed providing a better understanding on the effect of these parameters and modifications. This would save a lot of time and cost in comparison, if all these replications have to be carried out in physical model. Therefore, this adds value to the concept of hybrid modelling where the numerical model can be calibrated and validated using the physical model and appropriate optimized results can be obtained from the numerical model. This optimized result can further be analyzed in the physical model to eliminate the limitations of the numerical model as seen for SSIIM 2, saving time, energy and cost.

From the sediment management perspective, evaluation of such arrangement i.e. bypassing of suspended sediments during high flows, utilizing the reservoir pond to settle particles and flushing through the bottom outlets; could be an alternative for the settling basins in a difficult and challenging topography as seen in UAHEP (Morris, 2020). Also, as this is a high head project, sediments finer than 0.2mm (most probably 0.01mm to 0.05mm) has to be settled to protect the wear and tear of the

turbines (Mosonyi, 1991). To do so, very large settling basins are required which are confined due to topography and cost itself. As well as these sediments are mainly concentrated for specific time period, generally 3 months, in these regions of world, therefore, monetary evaluation on whether constructing costly settling basin for 3 months operation or applying such innovative new arrangements could be assessed. For such assessment, numerical models can be very effective tool in aiding the decisions.

In overall, the objectives of the study have been fully covered as well as the shifted SBT location has been recommended based on the available data for further analysis in the physical model.

10 Recommendation

To improve the results of the numerical model, various further works can be done. Firstly, the simulation has to be verified using the final physical model measured data rather than the interpolated data (draft report) used in this study. This would increase the accuracy of the numerical model.

As the suspended sediments have only been simulated on the interpolated bed deposition geometry, it is recommended to carry out the bed deposition simulation for the whole reservoir and calibrate the model for the required deposition pattern in case of initial SBT location. Then, finally use this calibrated model for various modifications and validate the results. Further, the model can be simulated for the prototype scale overcoming the limitation of the program for different density materials as well as scale effects.

Moreover, this study has been conducted for only one operating condition i.e. water level at 1,625masl and discharge of 877m^3/s. However, the reservoir operation has many operating conditions which can be simulated for further analysis and the results can be interpreted.

Similarly, the position of SBT can be shifted further upstream i.e. to reservoir head, to handle bed sediments, thereby prolonging the reservoir life. However, the effectiveness as compared to proposed design should be analyzed. Further, the angle of the SBT intake can be modified to see its effect on the sediment concentration through SBT outlet.

References

Agrawal, A. K. (2005) *Numerical Modelling of Sediment Flow in Tala Desilting Chamber*, Norwegian University of Science and Technology (NTNU).

Almeland, S. K. *et al.* (2019) Multiple solutions of the Navier-Stokes equations computing water flow in sand traps, *Engineering Applications of Computational Fluid Mechanics*, 13(1), pp. 199-219. doi: 10.1080/19942060.2019.1566094.

Annandale, G. (2013) Quenching the Thirst: Sustainable Watr Supply and Climate Change. North Charleston, S.C.: CreateSpace.

Annandale, G. W. *et al.* (2003) *Reservoir conservation : economic and engineering evaluation of alternative strategies for managing sedimentation in storage reservoirs : RESCON approach (English)*. (34954). Washington, DC.

Annandale, G. W., Morris, G. L. and Karki, P. (2016) *Extending the Life of Reservoirs : Sustainable Sediment Management for Dams and Run-of-River Hydropower*. Washington, DC: World Bank.

Auel, C. and Boes, R. (2011) Sediment bypass tunnel design - review and outlook. pp. 403-412.

Auel, C. *et al.* (2011) Design and construction of the sediment bypass tunnel at Solis, *International Journal on Hydropower and Dams*, 18, pp. 62-66.

Auel, C., Kantoush, S. and Sumi, T. (2016) *Positive effects of reservoir sedimentation management on reservoir life - examples from Japan*.

Auel, C. *et al.* (2017) Abrasion prediction at Mud Mountain sediment bypass tunnel. doi: 10.3929/ethz-b-000185304.

Boes, R., Müller-Hagmann, M. and Albayrak, I. (2019) *Design, operation and morphological effects of bypass tunnels as a sediment routing technique*.

Changjiang Survey, P., Design and Reserch Co., Ltd., and Sinotech Engineering Consultants, L., Soil Test (P) Ltd., (2019a) *Annex H-3 Preliminary Results of the Sediment Physical Model*. (Phase I: Project Optimization and Updated Feasibility Study Report).

Changjiang Survey, P., Design and Reserch Co., Ltd., and Sinotech Engineering Consultants, L., Soil Test (P) Ltd., (2019b) *Annex H-1 Sediment Numerical Simulaton*. (Phase I: Project Optimization and Updated Feasibility Study Report).

Cheng, N.-S. (1997) Simplified Settling Velocity Formula for Sediment Particle, *Journal of Hydraulic Engineering-ASCE*, 123, pp. 149-152. doi: 10.1061/(ASCE)0733-9429(1997)123:2(149).

Einstein, H. A. (1964) *River Sedimentation*. New York: McGraw-Hill.

Haun, S. and Olsen, N. R. B. (2012) Three-dimensional numerical modelling of the flushing process of the Kali Gandaki hydropower reservoir, *Lakes & Reservoirs: Research & Management*, 17(1), pp. 25-33. doi: 10.1111/j.1440-1770.2012.00491.x.

Haun, S. *et al.* (2013) Three-dimensional measurements and numerical modelling of suspended sediments in a hydropower reservoir, *Journal of Hydrology*, 479, pp. 180-188. doi: .

Hoven, L. E. (2010) *Three dimensional numerical modelling of sediments in water reservoirs*, Norwegian University of Science and Technology (NTNU).

ICOLD (2009) Sedimaentation and sustainable use of reservoirs and river Systems *Bulletine 147*.

ICOLD (2020) *Genearal Synthesis* (Accessed: 9th May 2020).

IPCC (2007) *Climate Change 2007: Synthesis Report*. Geneva,Switzerland.

Kobus, H. and Abraham, G. (1984) *Wasserbauliches Versuchswesen*. Hamburg; Berlin: Parey.

Kondolf, G. M. (2013) Sustainable sediment management in reservoirs and regulated rivers: Experiences from five continents, Earth's Future, 2, doi: 10.1002/2013EF000184: Received.

Lai, Y. and Wu, K. (2018) A numerical modeling study of sediment bypass tunnels at shihmen reservoir, Taiwan, *International Journal of Hydrology*, 2. doi: 10.15406/ijh.2018.02.00056.

Mineault-Guitard, A., Rennie, C. and Williams, R. D. (2016) Validation of observed bedload transport pathways using morphodynamic modeling.

Mohammad, E. M. *et al.* (2020) A Computational Fluid Dynamics Simulation Model of Sediment Deposition in a Storage Reservoir Subject to Water Withdrawal, *Water*, 12(959), pp. 959. doi: 10.3390/w12040959.

Morris, G. (2020) Classification of Management Alternatives to Combat Reservoir Sedimentation, *Water*, 12, pp. 861. doi: 10.3390/w12030861.

Morris, G. L. and Fan, J. (1998) *Reservoir sedimentation handbook : design and management of dams, reservoirs, and watersheds for sustainable use*. New York: McGraw-Hill.

Mosonyi, E. (1991) *Water power development. with 640 figures and 4 supplements Volume II/A-B, Volume II/A-B*. Translated by Szilvassy, Z., Nagy, E. and Palotay, P. 3rd edn. Budapest: Akadémiai Kiadó.

Nepal, D. (2019) *3D CFD Simualtion of flow structures and bed load movement at Binga HPP*, Norwegian University of Science and Technology (NTNU).

Olsen, N. (2017) Numerical Modelling and Hydraulics (5th edn.). Trondheim.

Olsen, N. (2018) SSIIM User's Manual. Trondheim.

Olsen, N. R. B. (2010) *Result assessment methods for 3D CFD models in sediment transport computations*. Unpublished paper presented at 1st Conference of the European section of the IAHR. Edinburgh, Scotland.

Rai, A., Kumar, A. and Staubli, T. (2019) Financial analysis for optimization of hydropower plants regarding hydro-abrasive erosion: A study from Indian Himalayas, *IOP Conference Series: Earth and Environmental Science*, 240, pp. 022025. doi: 10.1088/1755-1315/240/2/022025.

Sumi, T. and Kantoush, S. A. (2011) Comprehensive sediment management strategies in Japan: Sediment bypass tunnels, *Proceedings of the 34th World Congress of the International Association for Hydro-Environment Research and Engineering: 33rd Hydrology and Water Resources Symposium and 10th Conference on Hydraulics in Water Engineering*. Engineers Australia, pp. 1803.

US Army Corps of Engineers (1995) *Engineering and Design-Sedimentation Investigations of Rivers and Reservoirs*.

Vennard, J. K. (1940) *ELEMENTARY FLUID MECHANICS*. New York, USA: John Wiley And Sons Inc.

Wang, H. *et al.* (2018) *Sediment Management in Taiwan's Reservoirs and Barriers to Implementation*.

Wendt, J. F. (2009) *Computational Fluid Dynamics AN INTRODUCTION*. Heidelberg, Berlin: Springer.

Appendix A - Task Description

NTNU

M.Sc. THESIS IN HYDRAULIC ENGINEERING

Candidate: Mr. Nitish Sapkota

Title: Numerical Modelling of hydraulics and sediment at the inlet location of Sediment Bypass Tunnel (SBT) – Test Case: Upper Arun Hydroelectric Project, Nepal

1. Background

Hydropower being realized as the most crucial renewable energy source in today's world, faces high risk from sediments. Sediments pose risks from reservoir storage depletion to high erosivity of turbines and its accessories. These risks add economic burden to the project and raise questions on its sustainability. To deal with these problems, various sediment handling techniques have been developed and utilized. Among them, where applicable, sediment bypass tunnel has been considered as a promising measure to handle the bed load sediments. For its proper functioning, the hydraulics and location of inlet plays a vital role. Generally, to study and optimize the most favorable location, physical hydraulic models are sought for. However, due to limitations concerned mainly with time and cost, it may not be possible to investigate every inlet location in the model. Therefore, as a substitute, numerical models can play an important role in accessing and understanding the suitability of locations. This further aids developers, designers and physical model engineers to access the next best favorable location for optimum operation of sediment bypass tunnel. Therefore, this study aims at comparing and evaluating the inlet location and strategies proposed by physical hydraulic modelling; numerically and provide any recommendations for a test case of peaking hydroelectric project in Nepal.

As a test case, Upper Arun HEP (UAHEP), Nepal, under detail design phase has been considered. The project utilizes gross head of 545m and 235.44 m^3/s flow of Arun river to generate 1040MW. As the river is a glacial fed with high sediment concentration, it has been proposed to settle the sediments utilizing a part of reservoir and evacuate bed load through a sediment bypass tunnel. In this regard, UAHEP, under Nepal Electricity Authority (NEA), has been conducting physical hydraulic modelling at River house of Yangtze River Science Academy, Wuhan. Similarly, as UAHEP is the first of its kind in Nepal i.e. with sediment bypass tunnel, NEA wants to verify the proposed inlet location and sediment management strategy numerically. Therefore, this study will evaluate the reliability and if possible, optimize the inlet location and sediment strategies proposed by physical hydraulic modelling and further provide any recommendations/inputs using numerical models

2. Work description

The thesis shall cover, though not necessarily be limited to the main tasks listed below.
The candidate must collect available documents such as reports, relevant studies and maps. Based on the available documentation the following shall be carried out:

1 Literature review of the sediment handling techniques at headworks and 3D CFD Numerical Modelling for suspended and bed load sediments.
2 Numerical modelling of hydraulics and sediment at the proposed inlet location of a SBT in model scale
3 Optimization study of the SBT inlet location.

NTNU

4 Sensitivity Analysis
5 Conclusions
6 Proposals for future work
7 Presentation of the work

The literature review should outline the previous contributions in a condensed manner and result in the motivation for the current study.

3 Supervision

Associate Prof. Nils Ruther will be the main supervisor. Mr. Diwash Lal Maskey (PhD Candidate) and Adjunct Associate Prof. Siri Stokseth will be co-supervisors. The supervisors shall assist the candidate and make relevant information available. The contact person at Upper Arun Hydroelectric Project (UAHEP), NEA will be Mr. Ram Chandra Poudel, Project Director and Mr. Surya Narayan Shrestha, Assistant Manager. The contact person will coordinate the field work and provide relevant documents and data.

Discussion with and input from other research or engineering staff at NTNU or other institutions are recommended. Significant inputs from others shall be referenced in a convenient manner.

The research and engineering work carried out by the candidate in connection with this thesis shall remain within an educational context. The candidate and the supervisors are free to introduce assumptions and limitations which may be considered unrealistic or inappropriate in a contract research or a professional/commercial context.

4 Report format and submission

The report should be written with a text editing software. Figures, tables and photos shall be of high quality. The report format shall be in the style of scientific reports and must contain a summary, a table of content, and a list of references.

The report shall be submitted electronically in B5-format .pdf-file in Blackboard, and three paper copies should be handed in to the institute. Supplementary working files such as spreadsheets, numerical models, program scripts, figures and pictures shall be uploaded to Blackboard. The summary shall not exceed 450 words. The Master's thesis should be submitted within 11th of June 2020.

The candidate shall present the work at a MSc. seminar towards the end of the master period. The presentation shall be given with the use of PowerPoint or similar presentation tools. The date and format for the MSc. seminar will be announced during the semester.

Trondheim, 15. January 2020

Nils Ruther
Associate Professor
Department of Civil and Environmental Engineering
NTNU

Appendix B - Project Description

Table B. 1 Model test elements extended

Time	Days	Inflow	SCC	Bed load	Reservoir level	SBT	Intake	LLOs	Ecological
		m^3/s	kg/m^3	kg/s	masl	m^3/s	m^3/s	m^3/s	m^3/s
1985.9.18 - 9.21	4	557	2.41	228.2	1625	313.75	237.84	0	*5.41*
1985.9.22 - 9.30	9	442	1.67	125.48	1625	198.75	237.84	0	*5.41*
1985.10.1 - 10.17	17	251	0.69	29.44	1637.72	75.14	170.45	0	*5.41*
1985.10.18 -10.19	2	534	3.02	274.16	1640	0	0	528.59	5.41
1985.10.21 - 10.25	6	232	0.59	23.27	1637.72	56.14	170.45	0	*5.41*
1985.10.26 - 11.15	21	125	0.18	3.83	1635.89	0	119.59	0	*5.41*
1985.11.16 - 12.31	46	76	0.08	1.03	1634.73	0	70.59	0	*5.41*
1986.1.1 - 5.31	151	66.7	0.058	0.66	1634.25	0	61.29	0	*5.41*
1986.6.1 - 6.7	7	112	0.18	3.43	1635.57	0	106.59	0	*5.41*
1986.6.8 - 6.12	5	226	0.558	21.44	1639.56	0	220.59	0	*5.41*
1986.6.13 - 6.16	4	284	0.81	39.11	1625	40.75	237.84	0	*5.41*
1986.6.17 - 6.23	7	444	1.68	126.81	1625	200.75	237.84	0	*5.41*
1986.6.24 -6.25	2	546	2.33	216.27	1625	302.75	237.84	0	*5.41*
1986.6.26 - 6.27	*2*	*623*	*2.885*	*305.55*	*1595.28*	*0*	*0*	*617.59*	*5.41*
1986.6.28 - 6.30	3	760	3.99	515.51	1625	516.75	237.84	0	*5.41*
1986.7.1 -7.14	14	467	1.822	144.66	1625	223.75	237.84	0	*5.41*
1986.7.15 - 7.16	*2*	*726*	*3.7*	*456.65*	*1595.85*	*0*	*0*	*720.59*	*5.41*
1986.7.17 - 7.18	2	653	3.105	344.69	1625	409.75	237.84	0	*5.41*
1986.7.19 -7.23	5	742	3.814	481.1	1625	498.75	237.84	0	*5.41*
1986.7.24 - 7.25	*2*	*794*	*4.26*	*575.01*	*1596.21*	*0*	*0*	*788.59*	*5.41*
1986.7.26 - 7.27	**2**	**877**	**5.005**	**746.2**	**1625**	**633.75**	**237.84**	**0**	***5.41***
1986.7.28 - 8.1	5	754	3.928	503.49	1625	510.75	237.84	0	*5.41*
1986.8.2 - 8.3	*2*	*770*	*4.065*	*532.11*	*1596.08*	*0*	*0*	*764.59*	*5.41*
1986.8.4 - 8.17	14	488	1.96	162.6	1625	244.75	237.84	0	*5.41*
1986.8.18 - 8.19	2	552	2.37	222.4	1625	308.75	237.84	0	*5.41*
1986.8.20 - 8.21	*2*	*605*	*2.755*	*283.35*	*1595.18*	*0*	*0*	*599.59*	*5.41*
1986.8.22 - 8.25	4	558	2.413	228.9	1625	314.75	237.84	0	*5.41*
1986.8.26 - 8.27	2	607	2.76	284.8	1625	363.75	237.84	0	*5.41*
1986.8.28 - 9.11	15	454	1.732	133.68	1625	210.75	237.84	0	*5.41*
1986.9.12 - 9.13	*2*	*610*	*2.785*	*288.8*	*1595.21*	*0*	*0*	*604.59*	*5.41*

Appendix C - Grid Generation for Models

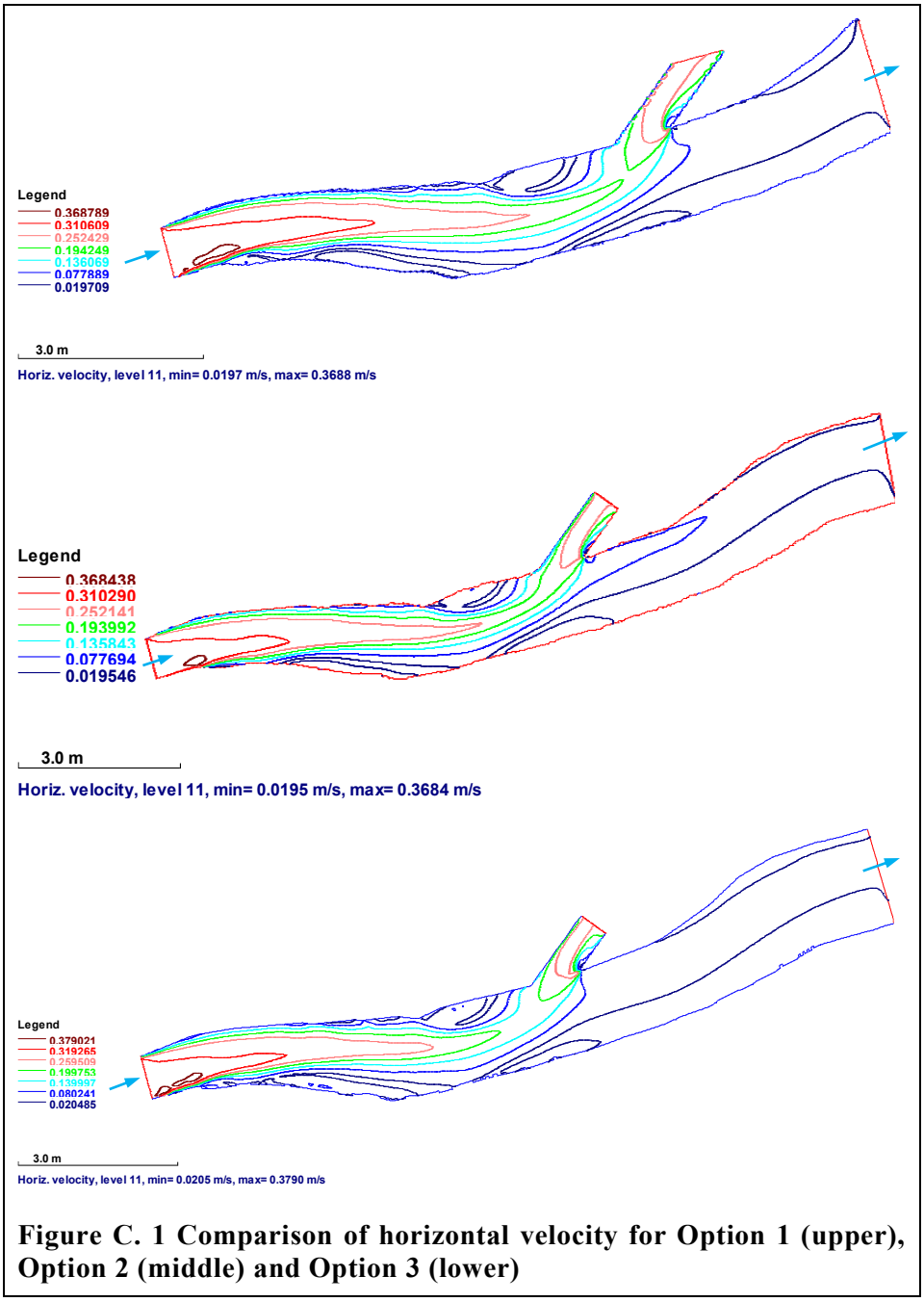

Figure C. 1 Comparison of horizontal velocity for Option 1 (upper), Option 2 (middle) and Option 3 (lower)

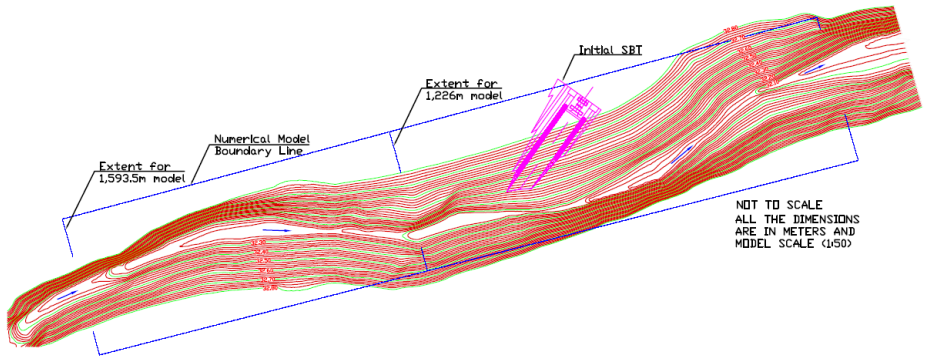

Figure C. 2 Extent of numerical model for various options

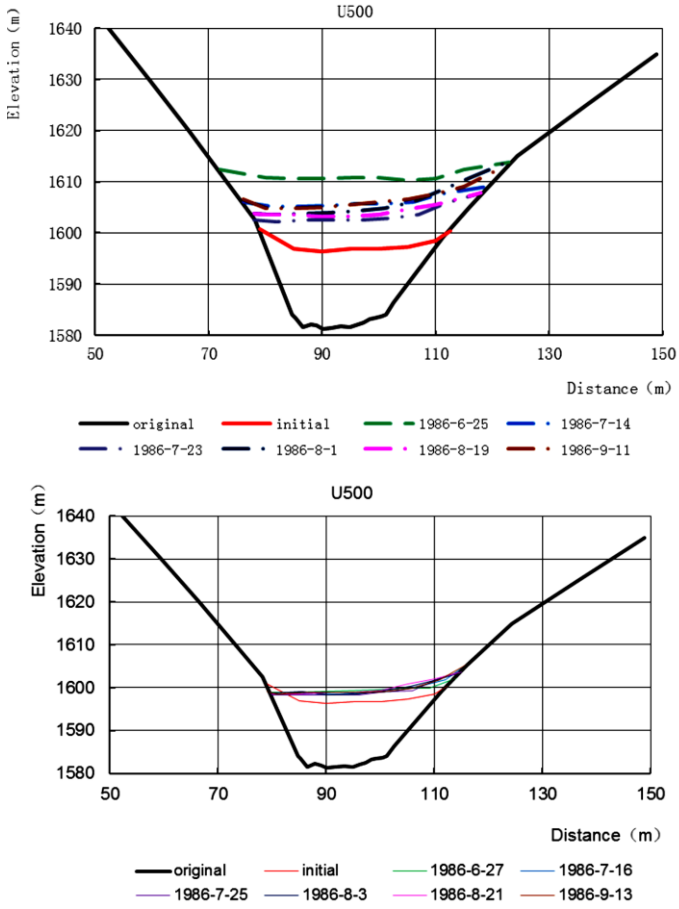

Figure C. 3 Before (left) and after (right) flushing cross section at 500m from dam

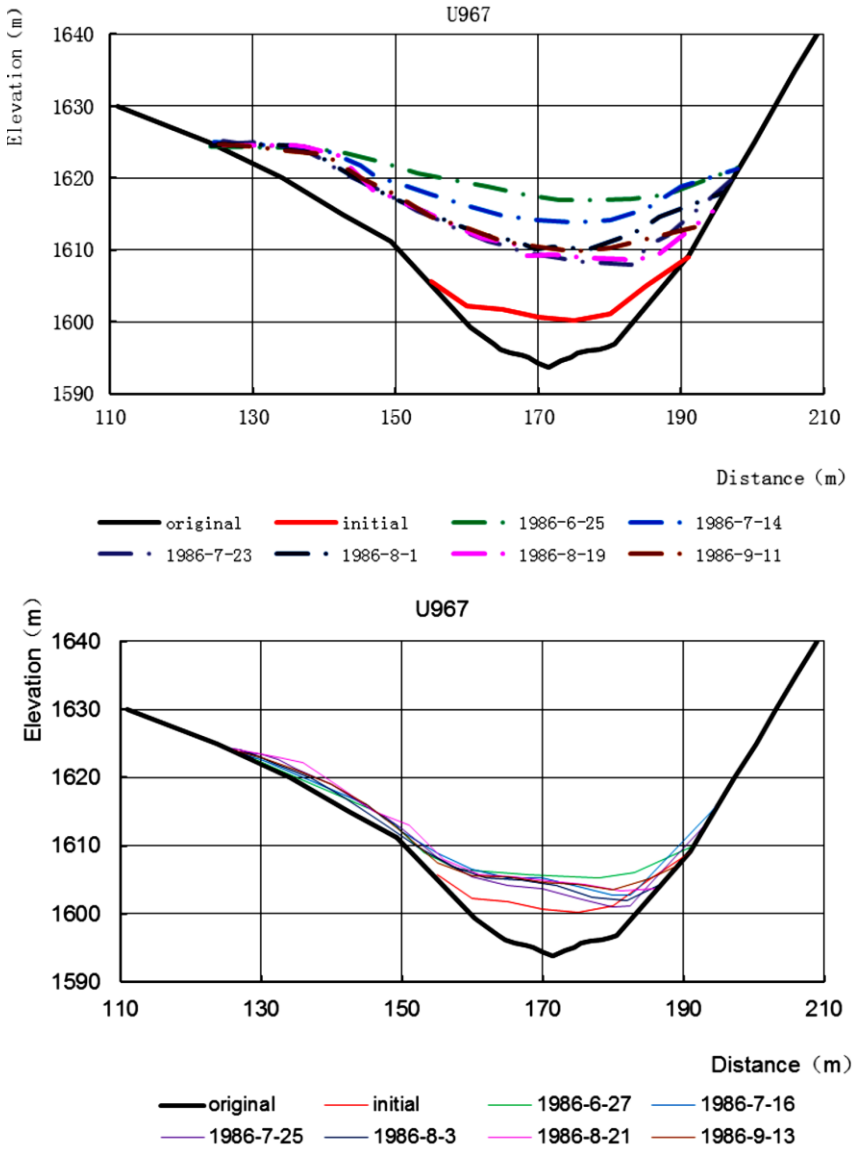

Figure C. 4 Before (left) and after (right) flushing cross section at 967m from dam

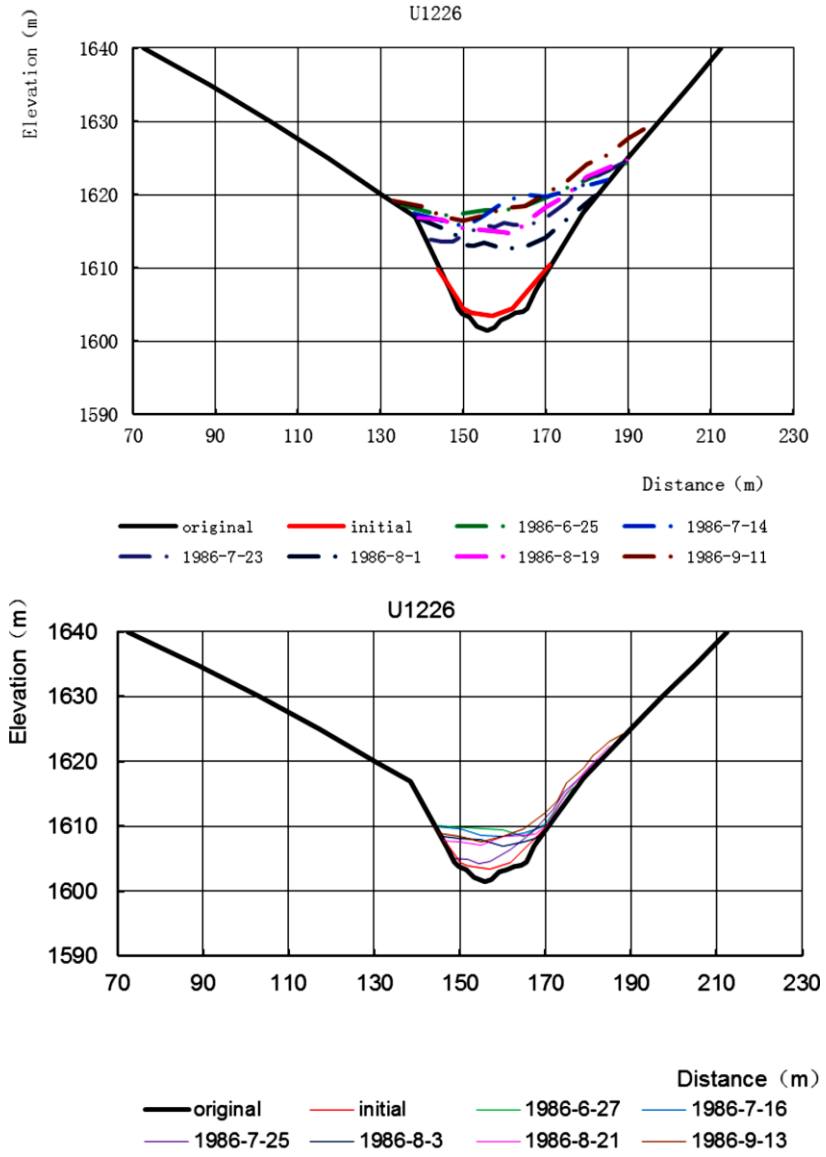

Figure C. 5 Before (left) and after (right) flushing cross section at 1226m from dam

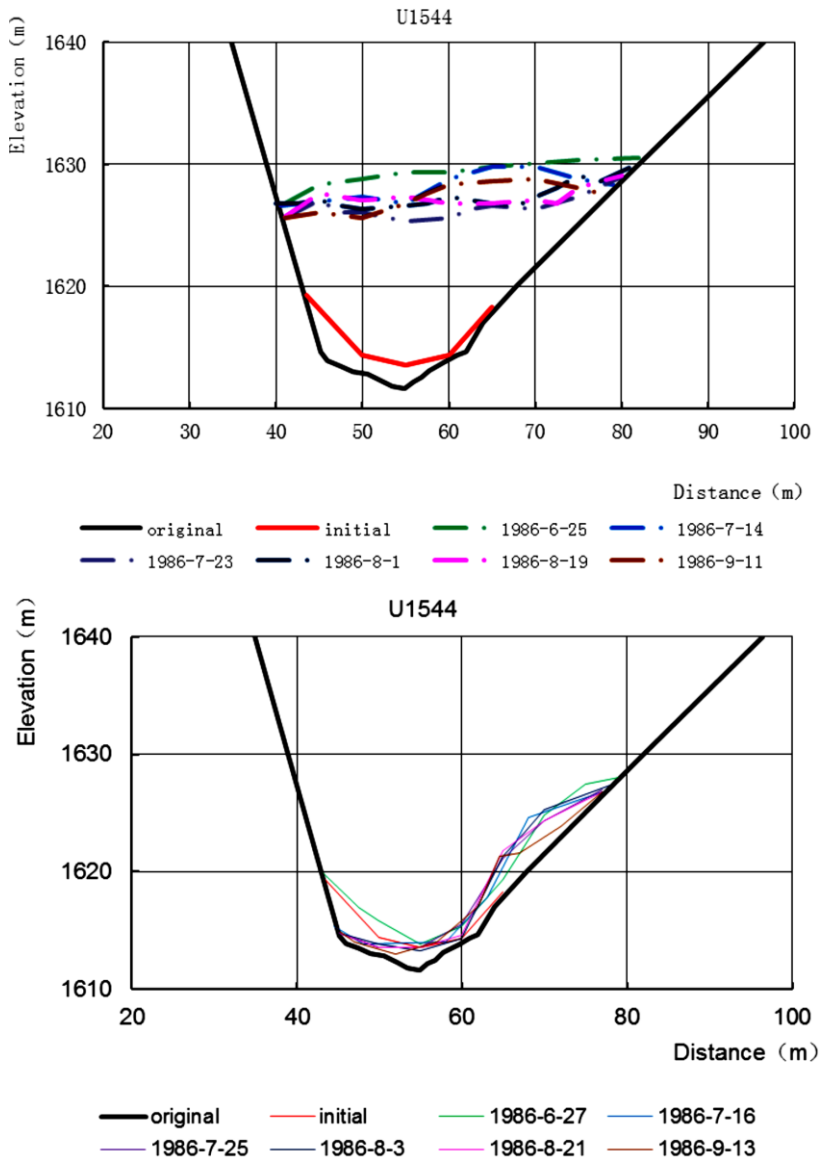

Figure C. 6 Before (left) and after (right) flushing cross section at 1544m from dam

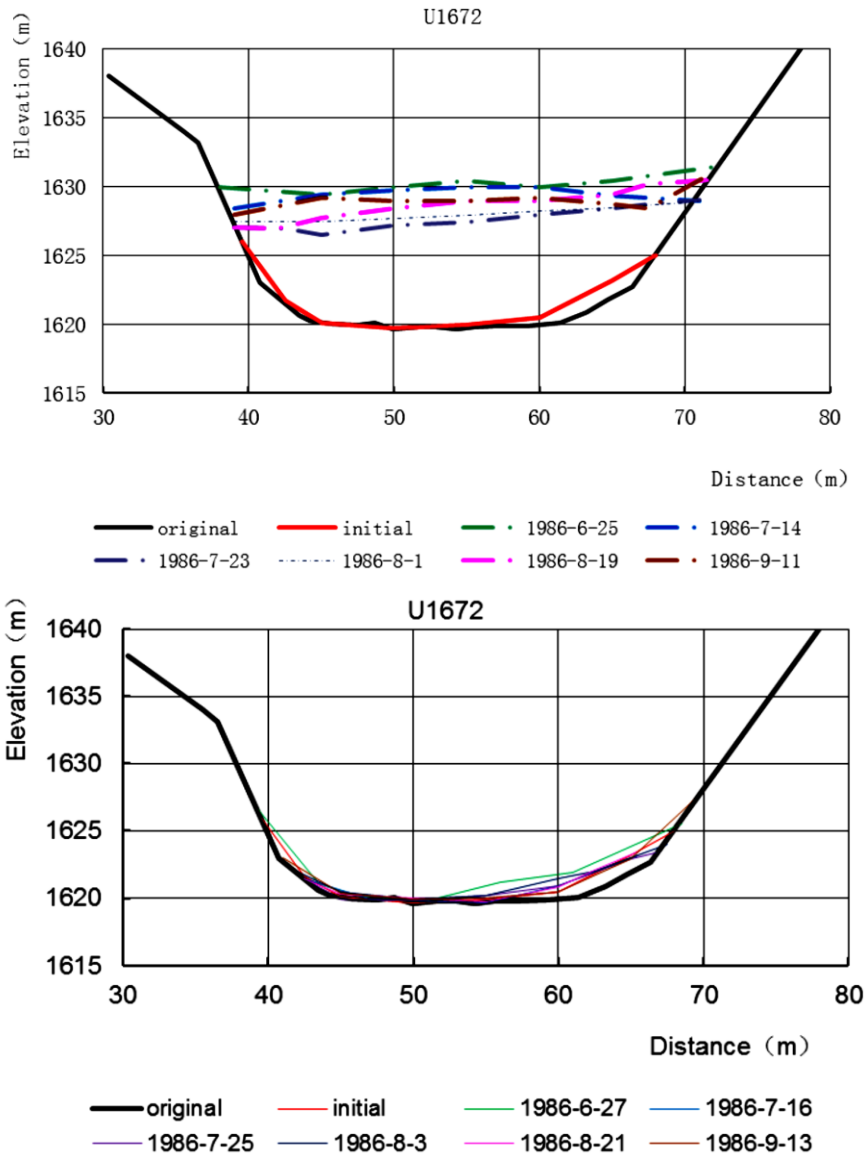

Figure C. 7 Before (left) and after (right) flushing cross section at 1672m from dam

Appendix D - Hydraulic Simulation

Details of Surface Velocities

Table D. 1 Detail surface velocities for each cross section

Cross Section	Easting	Northing	Easting for Interpol	Northing for Interpol	Physical Model Surface Velocity	Provided Velocity in drawing
					(m/s)	(m/s)
Upstream Section 3 (40-41)	541628.938	3069645.906	628.938	645.906	0.000	
	541628.938	3069645.861	628.938	645.861	1.064	
	541628.938	3069645.715	628.938	645.715	2.153	
	541628.934	3069645.554	628.934	645.554	3.228	3.24
	541628.932	3069645.412	628.932	645.412	3.006	
	541628.932	3069645.248	628.932	645.248	1.997	
	541628.928	3069645.095	628.928	645.095	1.457	
	541628.928	3069644.948	628.928	644.948	1.158	
	541628.926	3069644.804	628.926	644.804	0.930	
	541628.926	3069644.649	628.926	644.649	0.495	
	541628.926	3069644.563	628.926	644.563	0.000	
Upstream Section 2 (44)	541630.963	3069646.183	630.964	646.183	0.000	
	541630.988	3069646.008	630.988	646.008	0.623	
	541631.006	3069645.859	631.006	645.859	1.274	
	541631.032	3069645.709	631.033	645.709	2.053	
	541631.045	3069645.567	631.045	645.567	2.877	
	541631.071	3069645.420	631.072	645.420	3.260	3.28
	541631.084	3069645.260	631.084	645.260	2.605	
	541631.111	3069645.117	631.111	645.117	2.349	
	541631.124	3069644.960	631.124	644.960	1.973	
	541631.152	3069644.814	631.153	644.814	1.858	
	541631.166	3069644.678	631.166	644.678	0.000	
Upstream Section 1 (46-47)	541632.448	3069646.556	632.448	646.556	0.000	
	541632.475	3069646.421	632.476	646.421	2.363	
	541632.518	3069646.272	632.518	646.272	2.395	
	541632.558	3069646.127	632.559	646.127	2.546	
	541632.593	3069645.995	632.594	645.995	2.343	
	541632.636	3069645.848	632.636	645.848	2.490	
	541632.682	3069645.689	632.682	645.689	2.748	

	541632.723	3069645.545	632.724	645.545	2.775	
	541632.761	3069645.404	632.762	645.404	2.887	2.91
	541632.801	3069645.258	632.801	645.258	2.351	
	541632.829	3069645.145	632.830	645.145	1.974	
Downstream Section 1 (48-49)	541633.602	3069646.894	633.603	646.894	0.000	
	541633.656	3069646.720	633.656	646.720	0.097	
	541633.684	3069646.622	633.684	646.622	0.193	
	541633.726	3069646.486	633.726	646.486	0.475	
	541633.765	3069646.326	633.765	646.326	0.531	
	541633.780	3069646.269	633.780	646.269	0.555	
	541633.824	3069646.129	633.824	646.129	1.399	1.43
	541633.859	3069645.986	633.859	645.986	1.179	
	541633.901	3069645.832	633.902	645.832	1.175	
	541633.937	3069645.695	633.938	645.695	0.616	
	541633.971	3069645.547	633.971	645.547	0.245	
	541633.978	3069645.497	633.979	645.497	0.000	
Downstream Section 2 (49-51)	541634.430	3069647.209	634.431	647.209	0.000	
	541634.514	3069647.009	634.514	647.009	1.211	
	541634.573	3069646.868	634.574	646.868	1.363	
	541634.635	3069646.721	634.635	646.721	1.378	1.3
	541634.692	3069646.579	634.692	646.579	1.235	
	541634.748	3069646.447	634.749	646.447	0.888	
	541634.804	3069646.306	634.804	646.306	0.644	
	541634.858	3069646.168	634.859	646.168	0.292	
	541634.919	3069646.014	634.920	646.014	0.163	
	541634.971	3069645.882	634.972	645.882	0.228	
	541634.991	3069645.832	634.991	645.832	0.000	
SBT Section 1 (44-52)	541632.849	3069646.993	632.849	646.993	0.000	
	541632.922	3069646.942	632.923	646.942	1.936	
	541633.009	3069646.884	633.009	646.884	2.127	
	541633.088	3069646.826	633.089	646.826	2.064	
	541633.177	3069646.766	633.178	646.766	2.045	
	541633.261	3069646.706	633.262	646.706	2.037	
	541633.302	3069646.683	633.302	646.683	0.000	

SBT Section 2 (45-S1)	541633.091	3069647.326	633.091	647.326	0.000	
	541633.204	3069647.252	633.204	647.252	1.940	
	541633.281	3069647.188	633.281	647.188	2.219	
	541633.370	3069647.134	633.370	647.134	2.293	
	541633.441	3069647.078	633.441	647.078	1.503	
	541633.559	3069647.003	633.559	647.003	0.000	
SBT Section 3 (46-S2)	541633.362	3069647.692	633.362	647.692	0.000	
	541633.472	3069647.618	633.472	647.618	2.292	
	541633.508	3069647.586	633.508	647.586	1.962	
	541633.592	3069647.532	633.592	647.532	1.482	
	541633.678	3069647.459	633.678	647.459	1.320	
	541633.752	3069647.412	633.752	647.412	1.966	
	541633.819	3069647.362	633.819	647.362	0.000	

Detail Description of Data Set and Their Functions (Input files)

The algorithms used in the control file for the hydraulic simulation are explained in detail as follows. These have been extracted from SSIIM user manual.

F 2 UW: Automatic execution of hydraulic simulation is carried out by introducing this data set where *U* stands for reading *unstruc* file and *W* stands for water flow computation.

F 16 0.00339: The roughness of the river bed is set to 3.39mm.

F 64 11: This algorithm generates body-fitted grid lines in longitudinal and lateral directions giving priority to hexahedral cells close to bed. The hexahedral cells give better performance than tetrahedral cells.

F 65 10000000 10000000 10000000 10000000 10000000: As it is possible to expand the grid after it is read, it is necessary to provide the grid array sizes in the input file. Therefore, this data set allocates arrays for grid size. The five integers in the data set represent maximum number of grid cells in the grid, maximum number of surfaces in the grid, maximum number of grid corner points, maximum number of surfaces in connection between blocks, maximum number of connection points, used in grid editor respectively.

F 102 1: The algorithm is invoked to change the shape of grid cells close to the boundary and improve the bank smoothness.

F 112 1: This algorithm is added after the water level in the koordina file has been added. This data set lowers down the water level as specified in the koordina file. The grid is regenerated using the koordina file after reading the *unstruc* file.

G 1 280 90 6 1: The first, second and third integers indicate maximum number of grid lines in x, y and z directions respectively. The fourth integer is the number of sediment sizes.

G 3 0 20 40 60 80 100: Specifies the vertical distribution of grid cells. The number of vertical distributions in this data set should be equal to the number specified in G 1 data set.

W 1 80.6 0.04961 32.5: The three integers are Strickler's number, inflow discharge and d/s water level respectively.

W 2 3 1 135 271: This data set identifies which cross sections are used in the initial backwater surface computation. The first integer specifies the number of cross sections used. The other three integers represent the specific number of each cross section used to form the grid.

K 1 60000 60000: The two integers invoke algorithms for number of iterations for the flow procedure and number of minimum iterations between water surface updates. The first integer will be different in sediment simulation.

K 2 0 1: The two integers indicate if the wall laws are being used for water flow computation. If 0, wall laws are used, and if 1, zero-gradients are used. The first integer applies to side walls and second to the surface. Wall laws are always used for bed unless modified by W 4 data set.

K 3 0.1 0.1 0.1 0.1 0.1 0.1: Six floats are read. The first three are relaxation factors for three velocity equations. Fourth float is for pressure correction equation and last two are for k and e equations. Higher relaxation coefficients give more instabilities than lower relaxation, but the computational time is faster. Higher coefficients are to be used initially to

see whether the solution converges or not, if not the coefficients are lowered gradually. The default values are K 3 0.8 0.8 0.8 0.2 0.5 0.5

K 6 0 0 0 0 0 0: Six integers in this data set are for six water flow equations. The integers indicate the choice of discretization scheme for convective terms. 0 represent first order power law (POW) and 1 represent second-order upwind (SOU) scheme. The options apply to velocity and turbulence equations only.

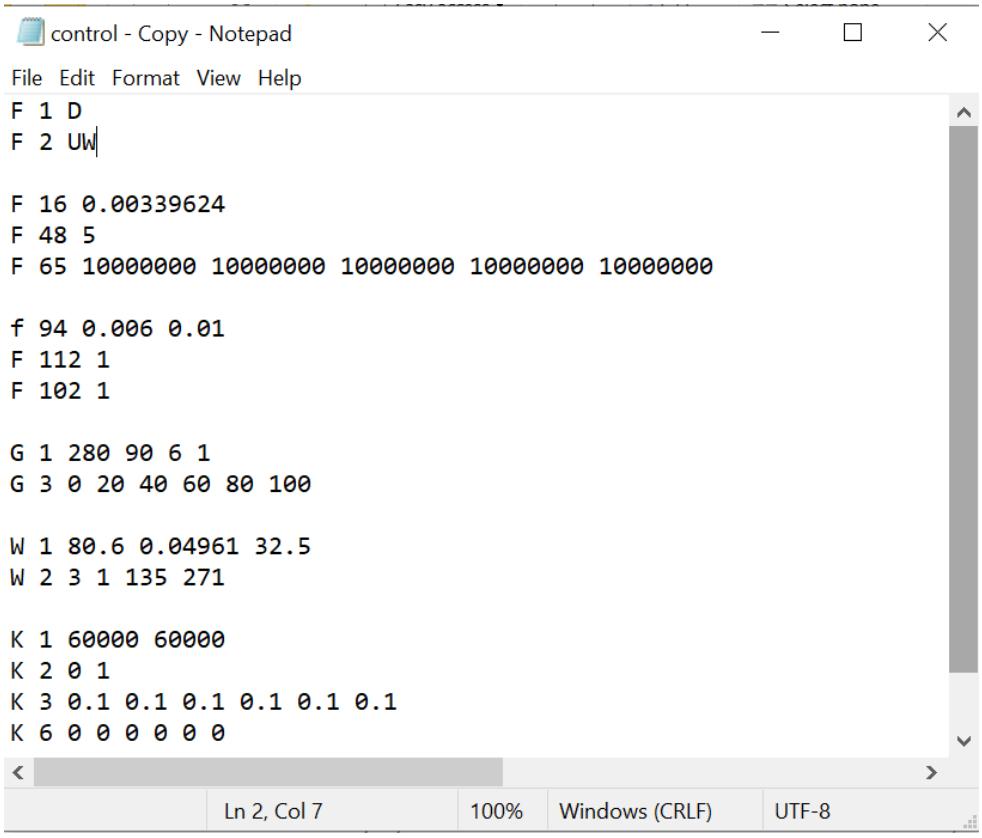

Figure D. 1 Typical control file for hydraulic simulation

Graphical Representation of Surface Velocity for Hydraulic Simulation

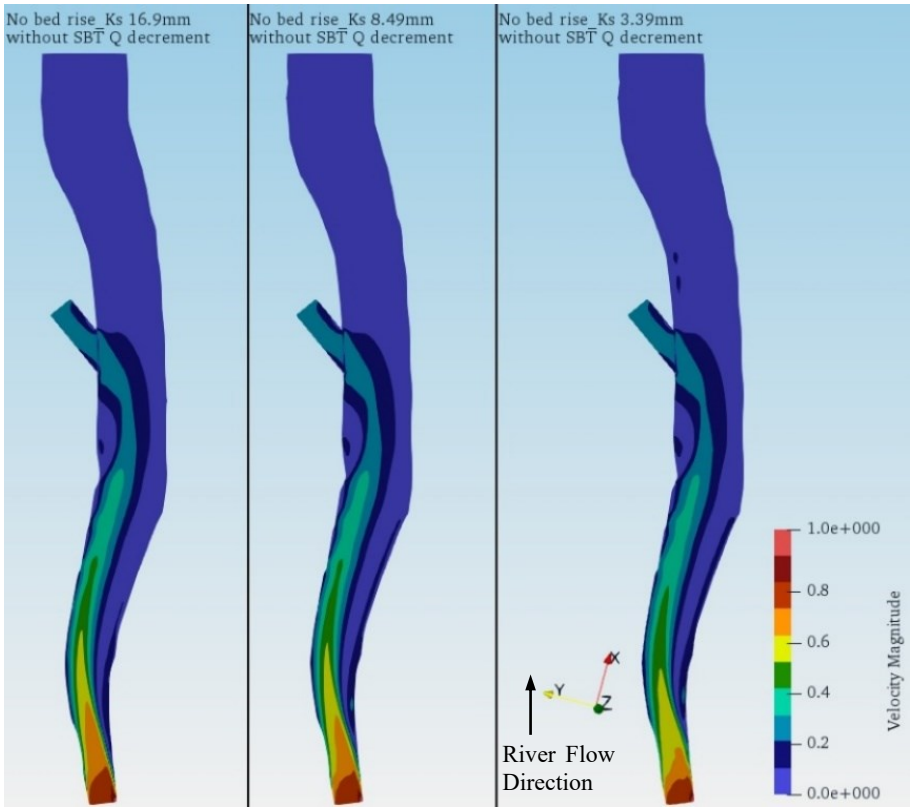

Figure D. 2 Surface velocity for no bed rise and without SBT discharge decrement

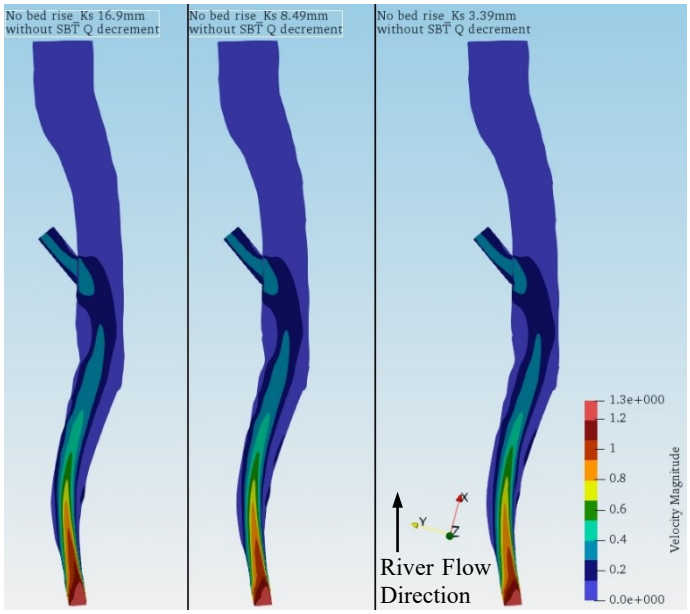

Figure D. 3 Surface velocity for 4cm bed rise without SBT discharge decrement

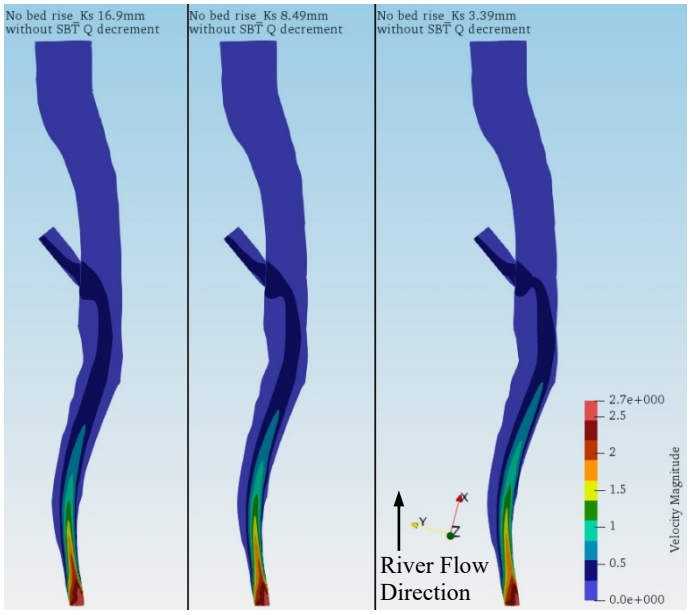

Figure D. 4 Surface velocity for 8cm bed rise without SBT discharge decrement

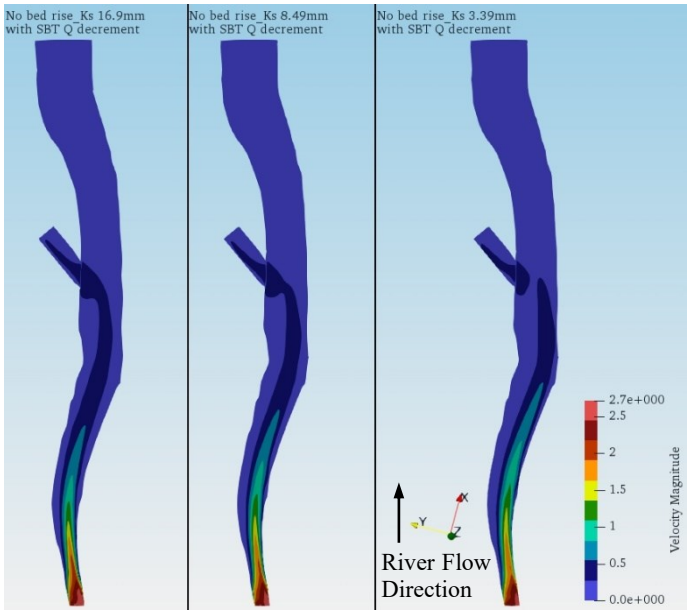

Figure D. 5 Surface velocity for 8cm bed rise with SBT discharge decrement

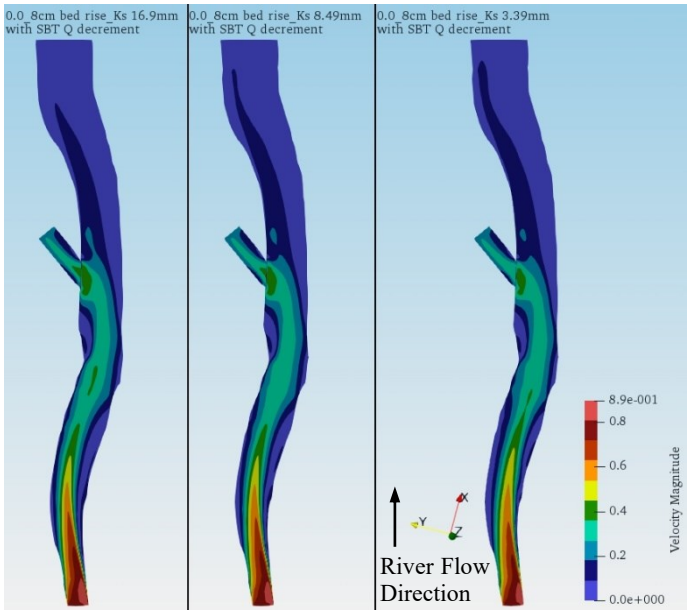

Figure D. 6 Surface velocity for combination of no bed rise and 8cm bed rise with SBT discharge decrement

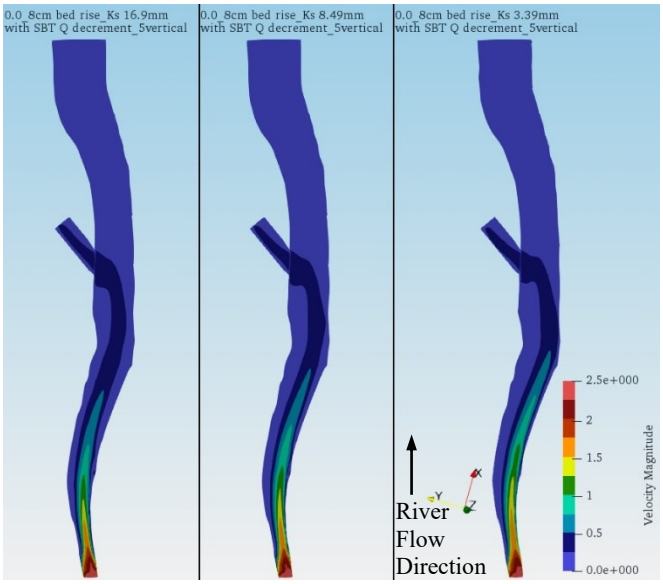

Figure D. 7 Surface velocity for 8cm bed rise with SBT discharge decrement and 5 vertical cells

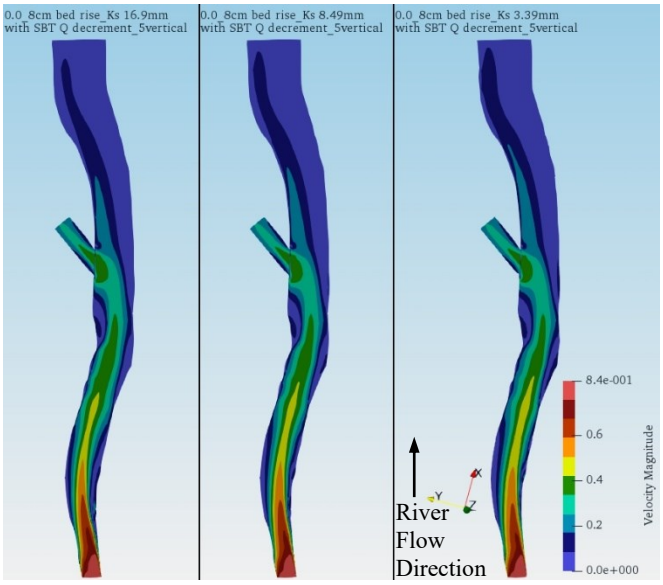

Figure D. 8 Surface velocity for combination of no bed rise and 8cm bed rise with SBT discharge decrement and 5 vertical cells

Appendix E - Sediment Simulation

Detail Description of Data Set and Their Functions (Input files)

Most of the input files have already been discussed in the Appendix D - Hydraulic Simulation. Those data sets that are further added for sediment simulations have been discussed here.

F 2 UIS: Sediment simulation is executed by this data set where U reads *unstruc* file, I initialize sediment concentration computation and S calculates sediment concentration.

F 11 1.33 -0.047: Density of sediments and Shield's coefficient of critical bed shear for movement of a sediment particle. The negative value will let the program to calculate the Shield's coefficient according to a parameterization of the original curve.

F 33 10 250: This data set activates transient term in the model where the time step (10) and number of inner iterations (250) per iteration per time step are defined.

F 36 2: Options for computation of the vertical elevation of the water surface. The integer 2 uses computed pressure field algorithm.

F 37 2: Transient sediment computation. This data set invokes time-dependent computation of sediment transport. The integer 2 denotes different algorithm for bed cells where sediment concentration formula is converted into an entrainment rate.

F 68 0: Parameter for choice of water flow computation. The integer 0 will cause the transient sediment computation to re-compute the water flow field after an update of the bed.

F 84 0: F 84 data set indicates the use of sediment transport formula. Integer 0 invokes suspended sediment formula by Van Rijn.

F 94 0.01 0.02: This sets the minimum grid corner height and maximum grid corner height for generation of one cell to 10mm and 20mm respectively. If the cell height is below first integer, then it is set to zero. Whereas, if the cell height is greater than first integer, but less or equal to second integer then only one cell in vertical direction is created. This data set only works for F 64 11 and 13 options.

F 102 1: The algorithm is invoked to change the shape of grid cells close to the boundary and improve the bank smoothness.

F 112 1: This algorithm is added after the water level in the *koordina* file has been added. The grid is regenerated after reading the *unstruc* file.

F 113 7: F 113 data set stabilizes the solution in very shallow regions near to the side walls. Integer 7 is used as flux limiter which means the extra term from Rhie and Chow interpolation should be less than 20% of the linear interpolation term.

F 168 8: Multi-block solver for pressure- correction equation. The integer 8 indicates the number of levels in grid nesting.

F 206 4: This data set specifies the maximum number of processors used for the parallel versions of SSIIM. The integer 4 specifies four processors will be used.

F 235 10: This algorithm is invoked to improve stability in triangular cells. 10 is a successful algorithm which gives extra relaxation in the triangular cells.

F 329: F 329 data set specifies print out options. A series of upto 19 integers are read. Each integer specifies a file that can be printed out each time the P 10 iteration is reached.

G 6 19128 0 0 0.001 0.01: This data set is used for calculating water surface elevation with an adaptive grid. Three integers and two floats are read.

The first three integers indicate a cell in the grid. The water surface in this cell is not moved. The second and third integers can be zero. The last two integers are RelaxSurface variable and ConvSurface variable.

G 24 25 u 6 0 w 6 0: This data set determines which variables are written in Paraview files. The first integer reads the number of variables given on the data set. For each variable, a character and two integers are read. The character indicates the name of the variable.

S 1 0.003 0.094: This data set gives the size and fall velocity of the sediments under consideration. At first, an integer is read which indicates the size group. After that sediment size in meter and fall velocity in m/s is given.

N 0 1 1.0: This data set comprises of size fractions of different bed sediment groups. The first integer indicates the group; the first group has index 0. The second integer indicates the sediment size from S data set. Then a is float read at last which indicates the fraction of size in the group.

B 0 0 0 0 0: B data sets invokes algorithm to distribute different bed sediment groups to different locations of the geometry. The first integer indicates group number. Second and third integers are cell numbers in the streamwise direction. The last two integers are cell numbers in the lateral direction. The information on sediment distribution at different locations are not available, so the integers are 0.

P 10 68: This data set specifies the number of global iterations between printing result files for time dependent computations. This is used along F

329 data set. The integer 69 specified, that the result files are written after each 68 iterations.

K 1 2444 60000: The two integers invoke algorithms for number of iterations for the flow procedure and number of minimum iterations between water surface updates. However, the first integer in sediment simulation is derived by dividing the total simulation time by time step in F 33 data set.

K 5 0 0 0 10 0 0: This algorithm is used to invoke multi grid algorithm in SSIIM 2. The integer 10 used in connection with F 168 data set will invoke the multi grid algorithm.

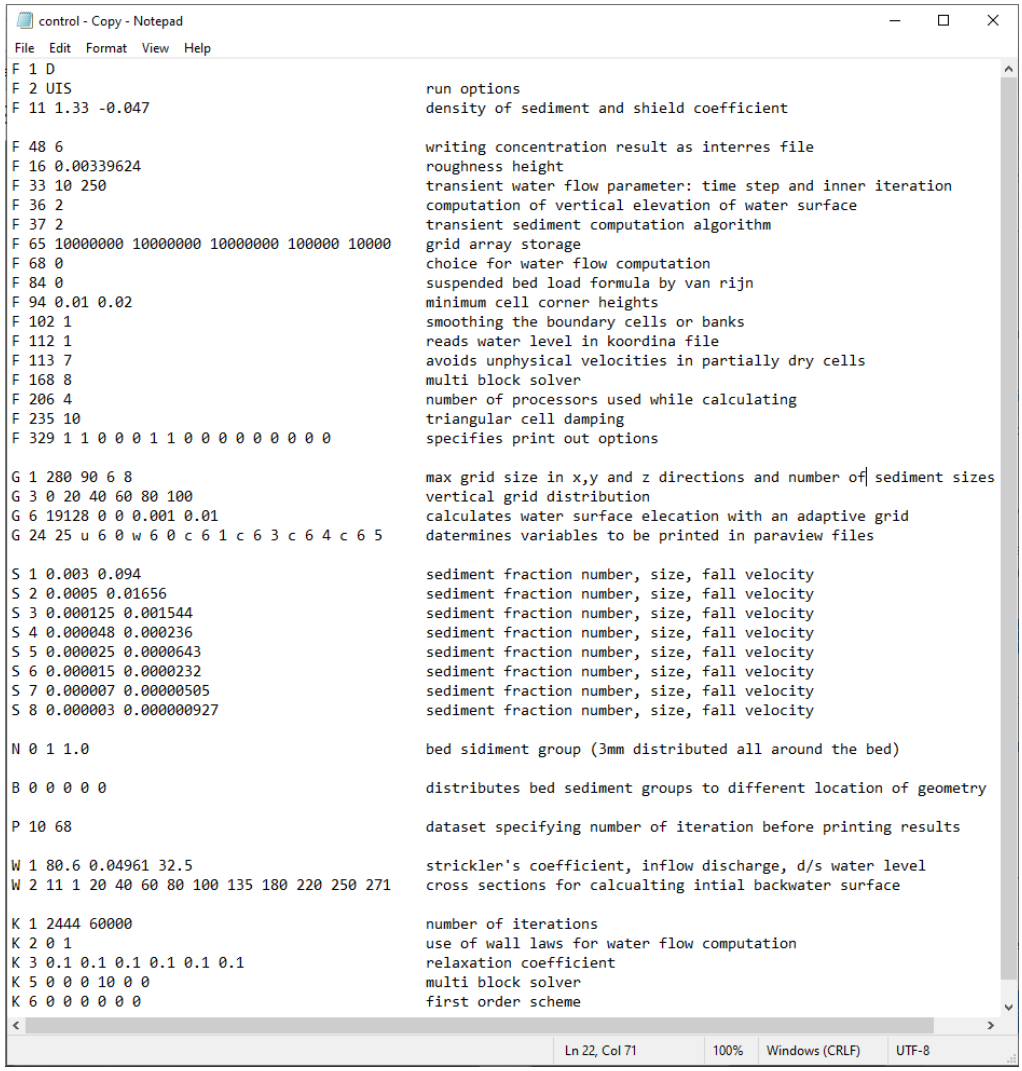

Figure E. 1 Typical control file for sediment simulation

Graphical Representation of Various Results for Sediment Simulation

Result based on velocity, bed shear and bed changes

The model has been rotated by 180 degrees to show the bed shear at bed.

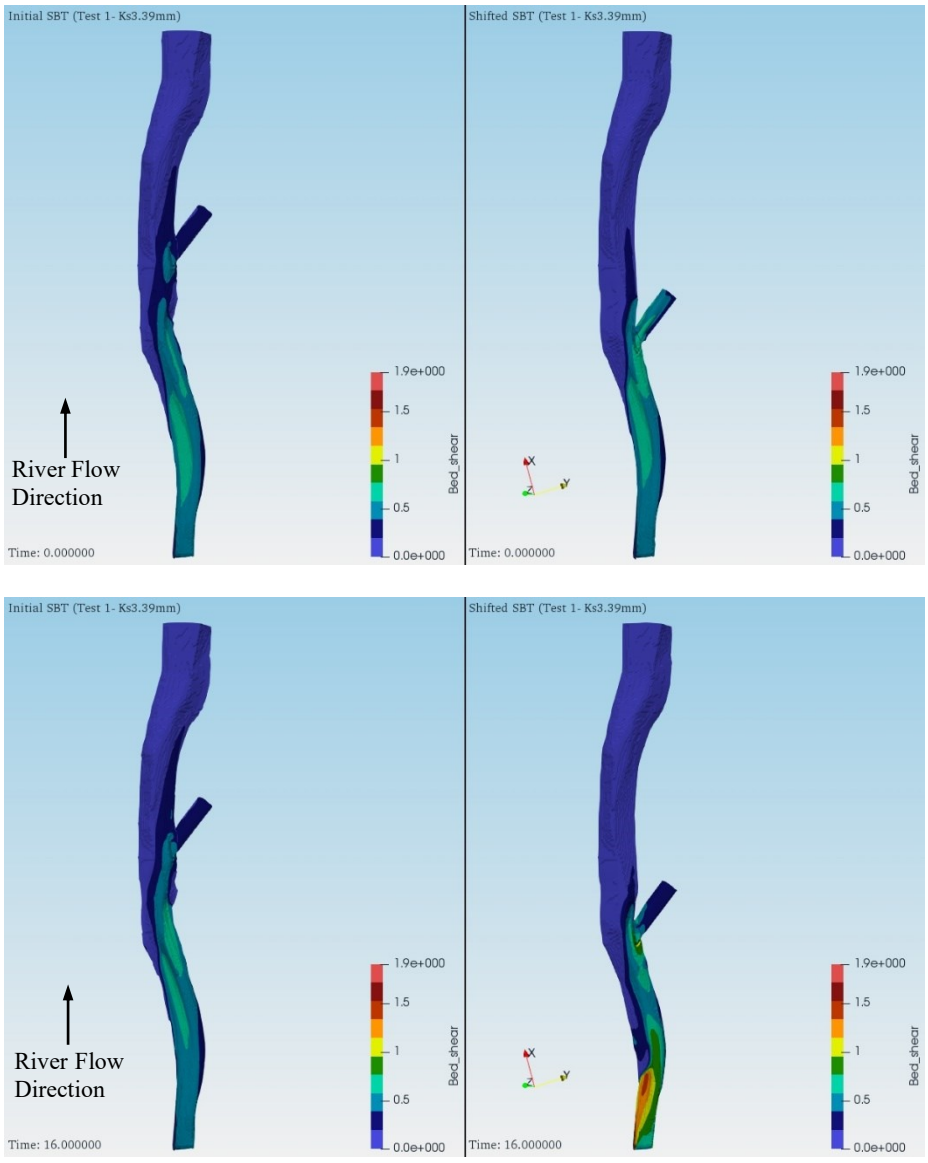

Figure E. 2 Bed shear for initial and shifted model at different timeframes

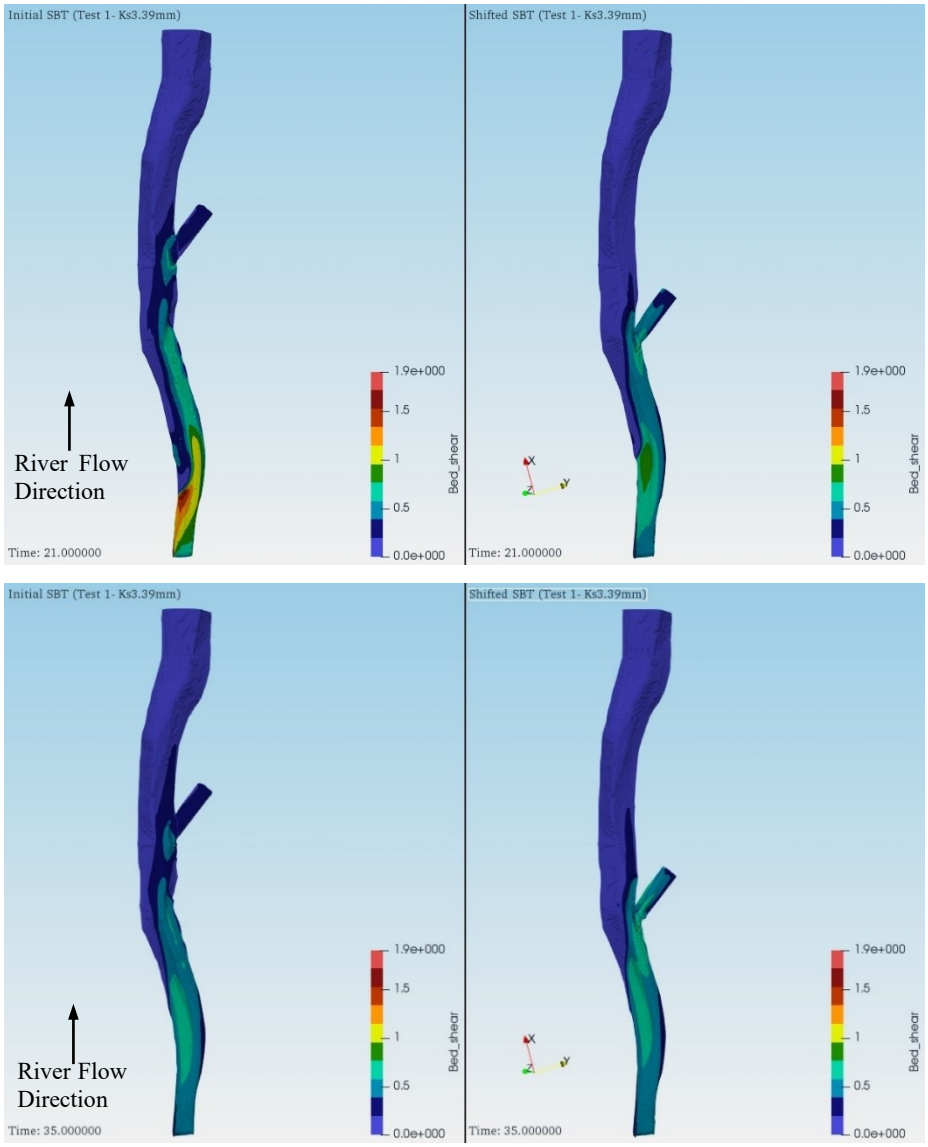

Figure E. 3 Bed shear for initial and shifted model for different timeframes

Results of sensitivity analysis

Description for Figure E. 4 to Figure E. 11

Figures represents the sediment outflow concentration/weight of each sediment size from SBT and main river outlets. The vertical axis in the figures represents the weight of sediment outflow from each outlet. The sediment outflow weight at each outlet has been calculated based on the outflow concentration at the end of simulation.

While, the horizontal axis represents the different sensitivity test as described in Table 7-4. The figures below have been compacted to compare the results of all the sensitivity test cases to the base case (Test 1) of initial as well as shifted model. Similarly, the results for the same test case between initial and shifted model can also be compared.

The blue bar graph represents the outflow sediment weight of different sensitivity test cases at SBT and main river outlets for initial model. Similarly, the orange bar graph represents the results for shifted model. Whereas, the horizontal black and orange line represents the base case (Test 1) for initial and shifted model respectively. Further, the light blue line represents the inflow sediment weight at each outlet. The inflow sediment weight is calculated based on the inflow concentration provided to the numerical model. Inflow to SBT outlet has only been shown in figures below.

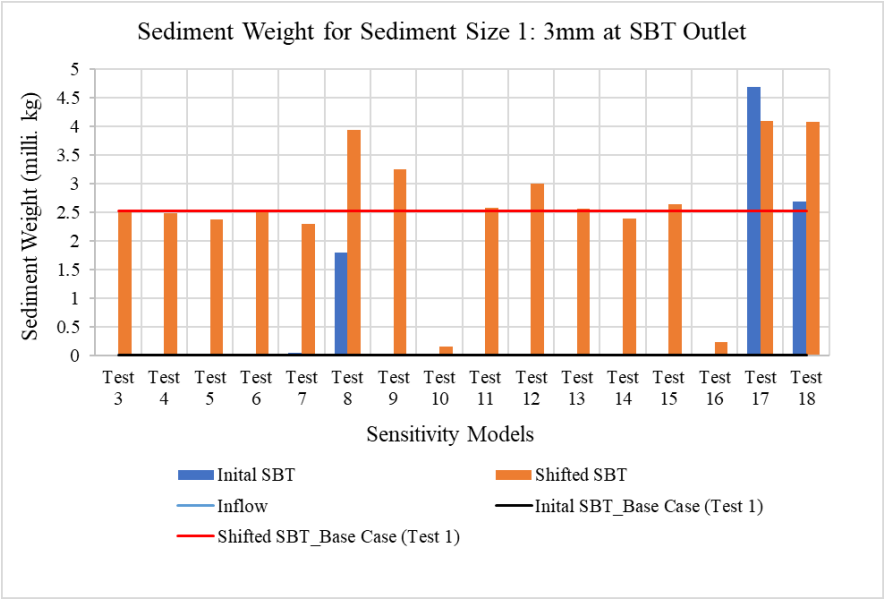

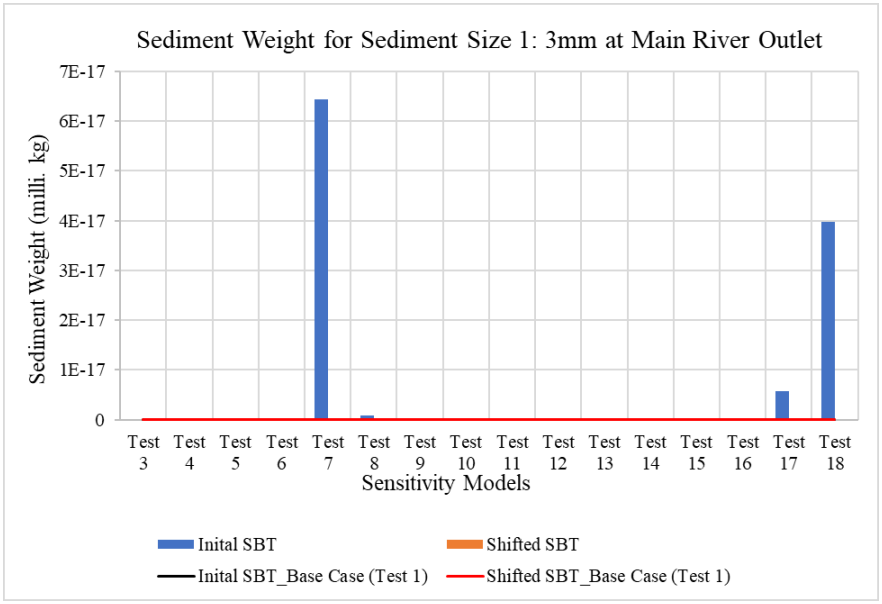

Figure E. 4 Comparison of sediment weight/concentration for Size 1: 3mm particles

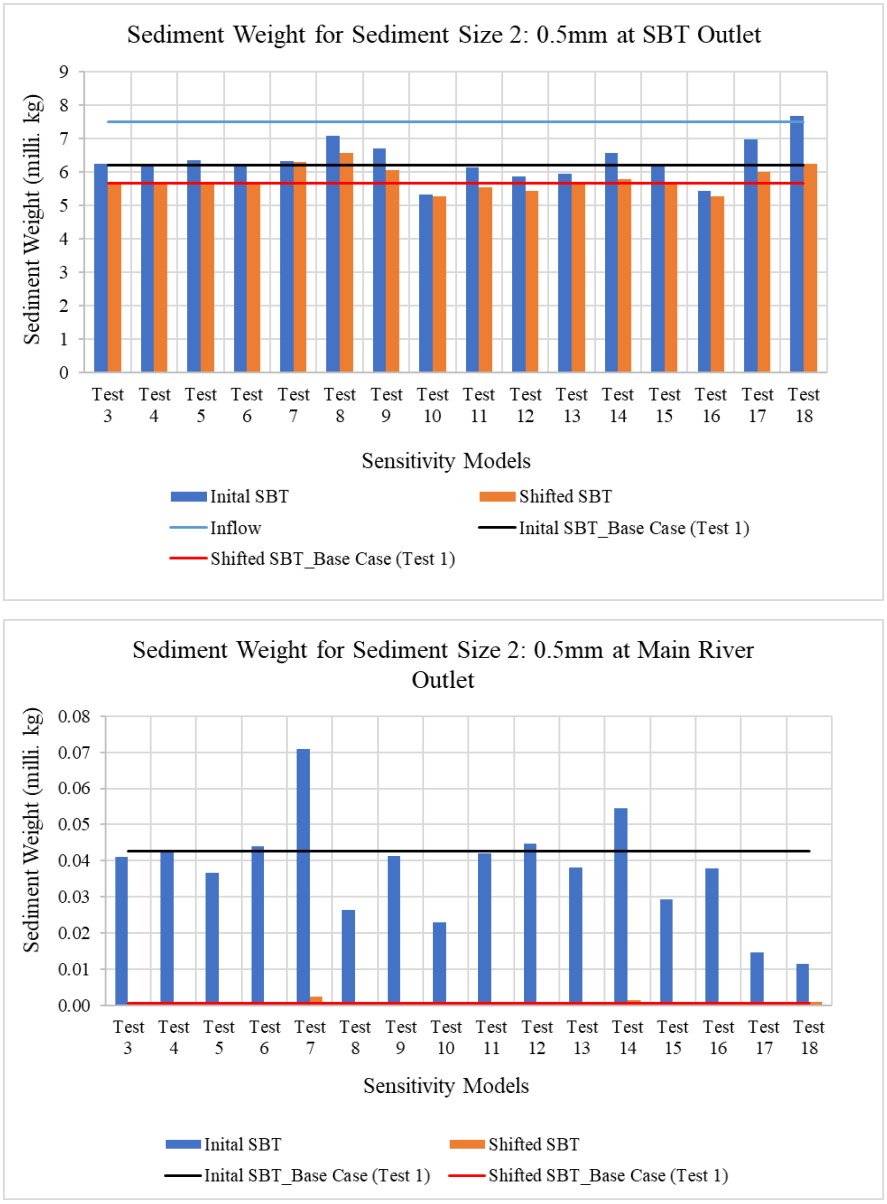

Figure E. 5 Comparison of sediment weight/concentration for Size 2: 0.5mm particles

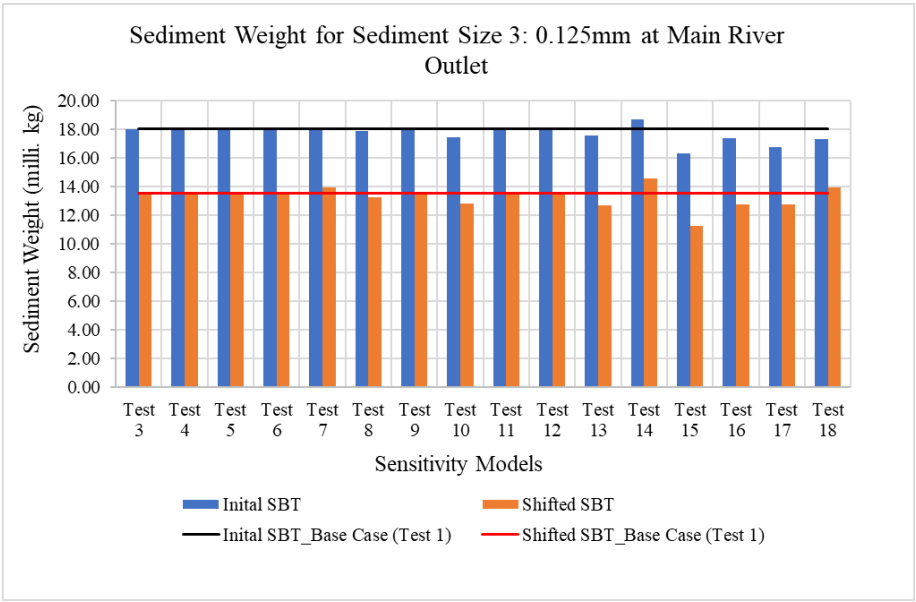

Figure E. 6 Comparison of sediment weight/concentration for Size 3: 0.125mm particles

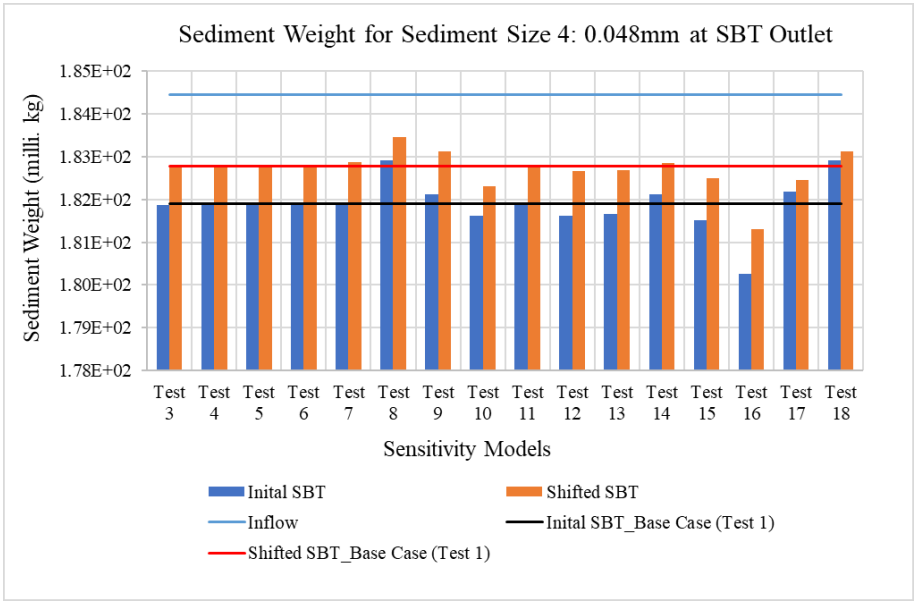

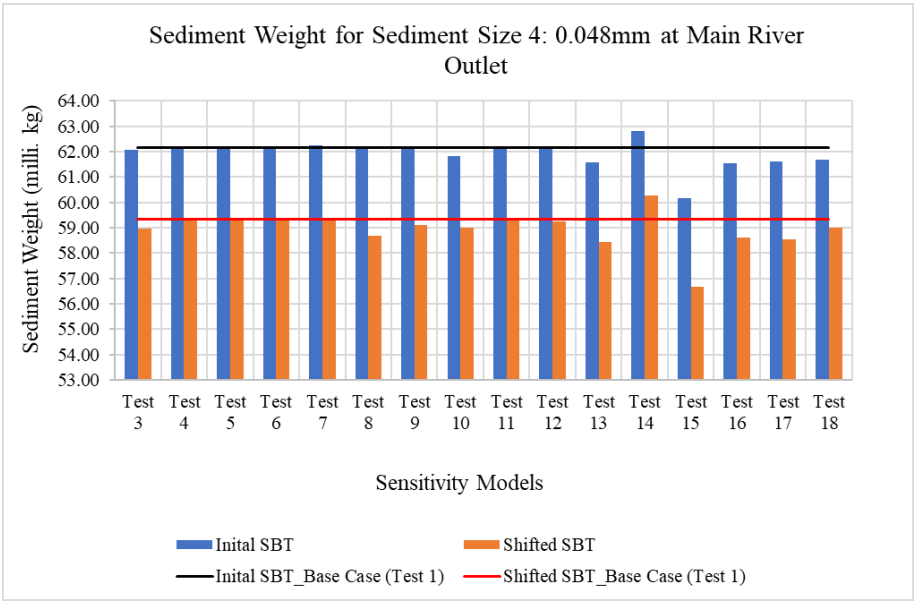

Figure E. 7 Comparison of sediment weight/concentration for Size 4: 0.048mm particles

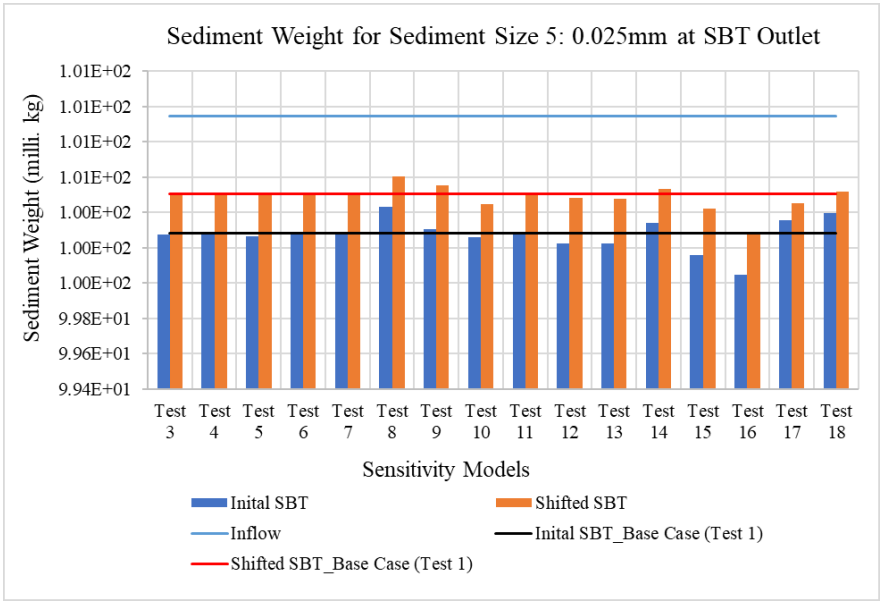

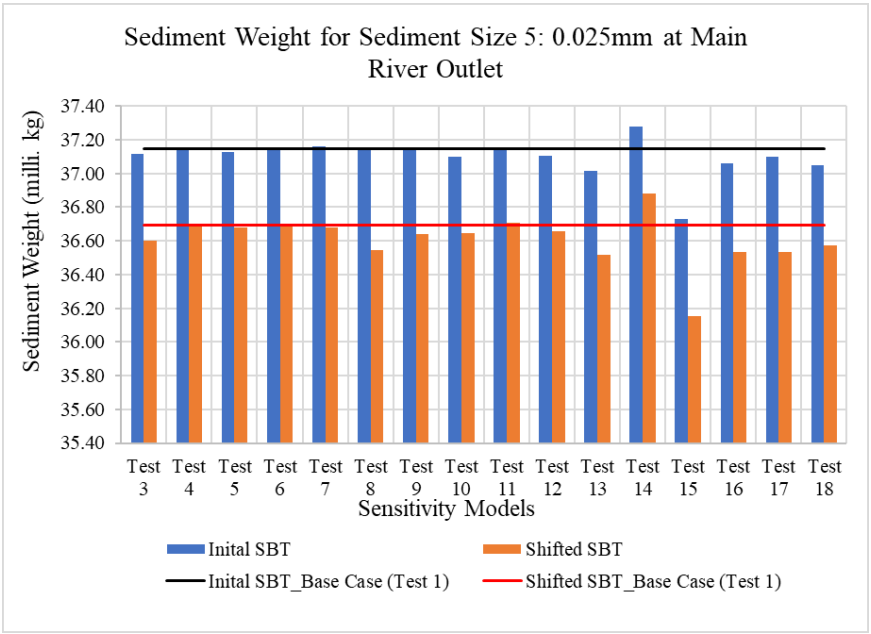

Figure E. 8 Comparison of sediment weight/concentration for Size 5: 0.025mm particles

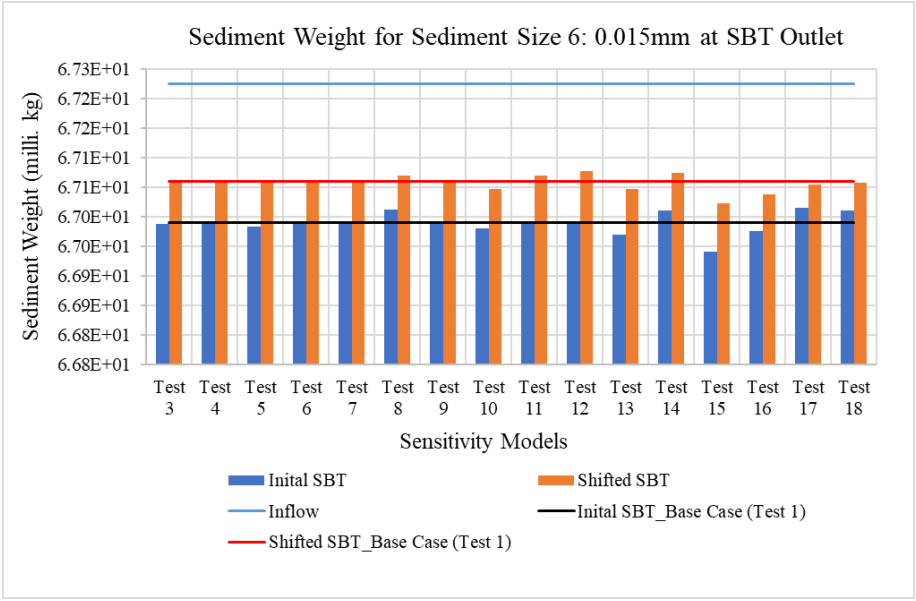

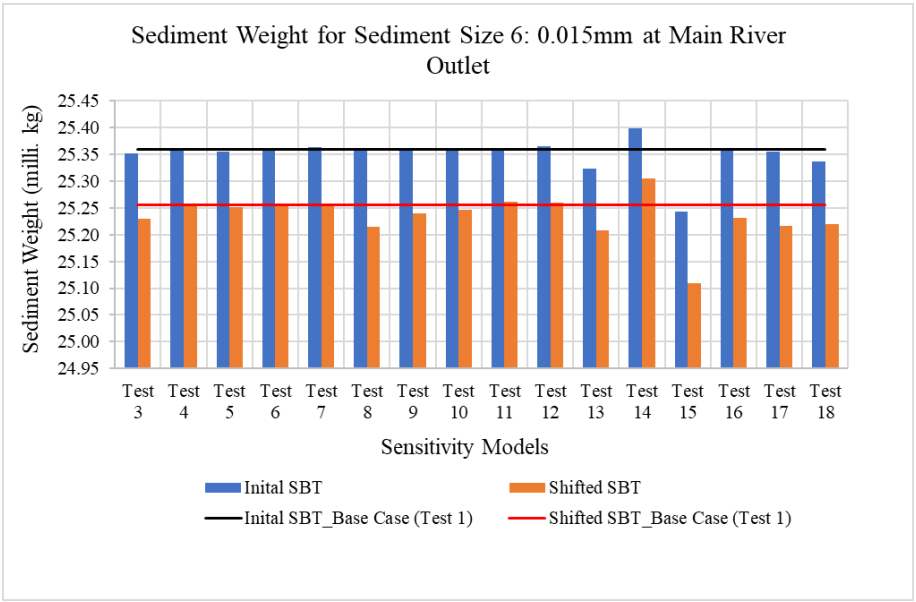

Figure E. 9 Comparison of sediment weight/concentration for Size 6: 0.015mm particles

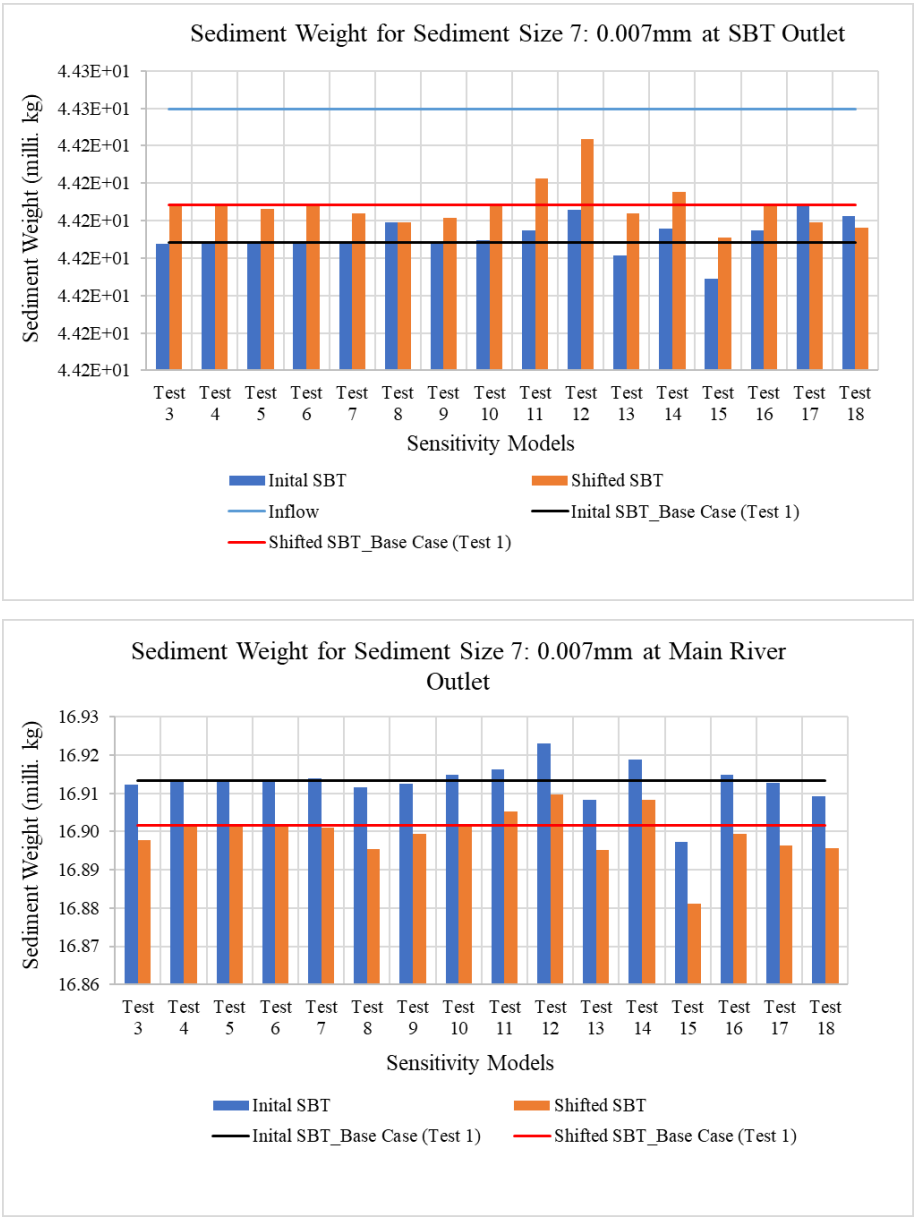

Figure E. 10 Comparison of sediment weight/concentration for Size 7: 0.007mm particles

Figure E. 11 Comparison of sediment weight/concentration for Size 8: 0.003mm particles

Appendix F - Discussion

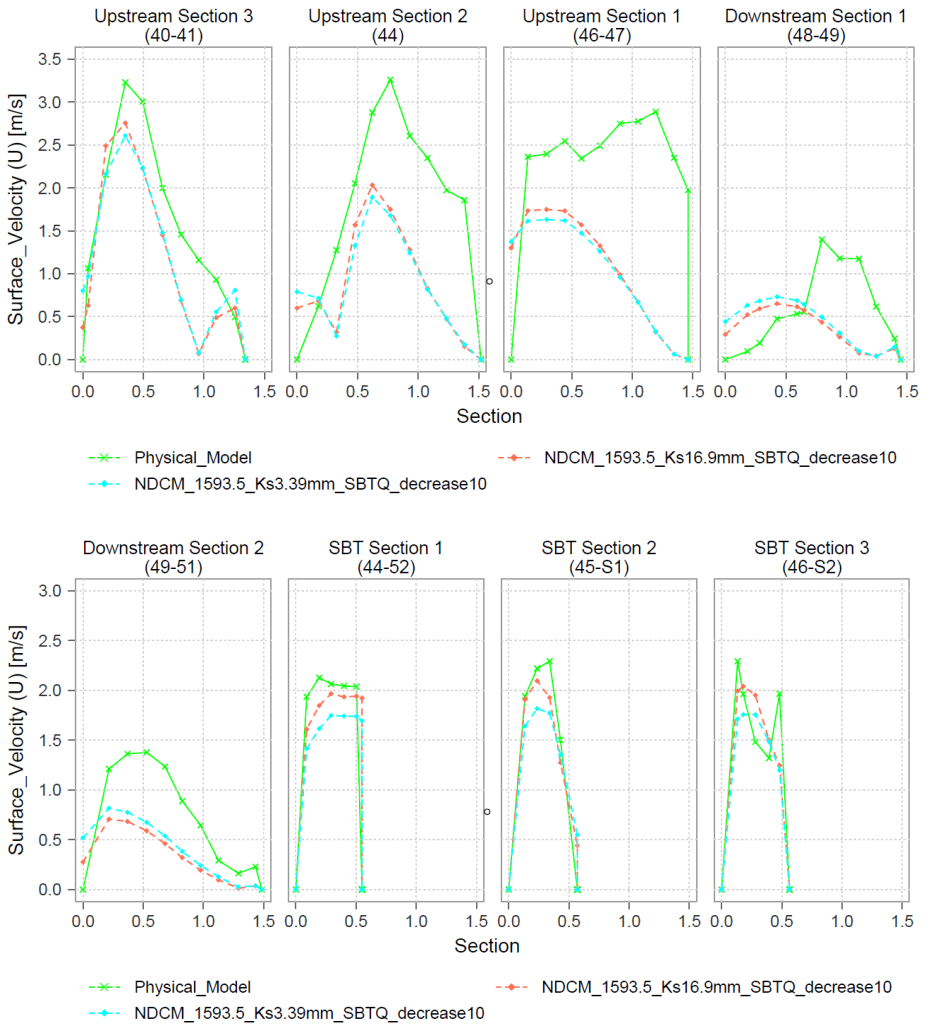

Figure F. 1 Comparison of surface velocity for without bed rise with k_s 16.9mm and 3.39mm; and SBT discharge decrement by 10%

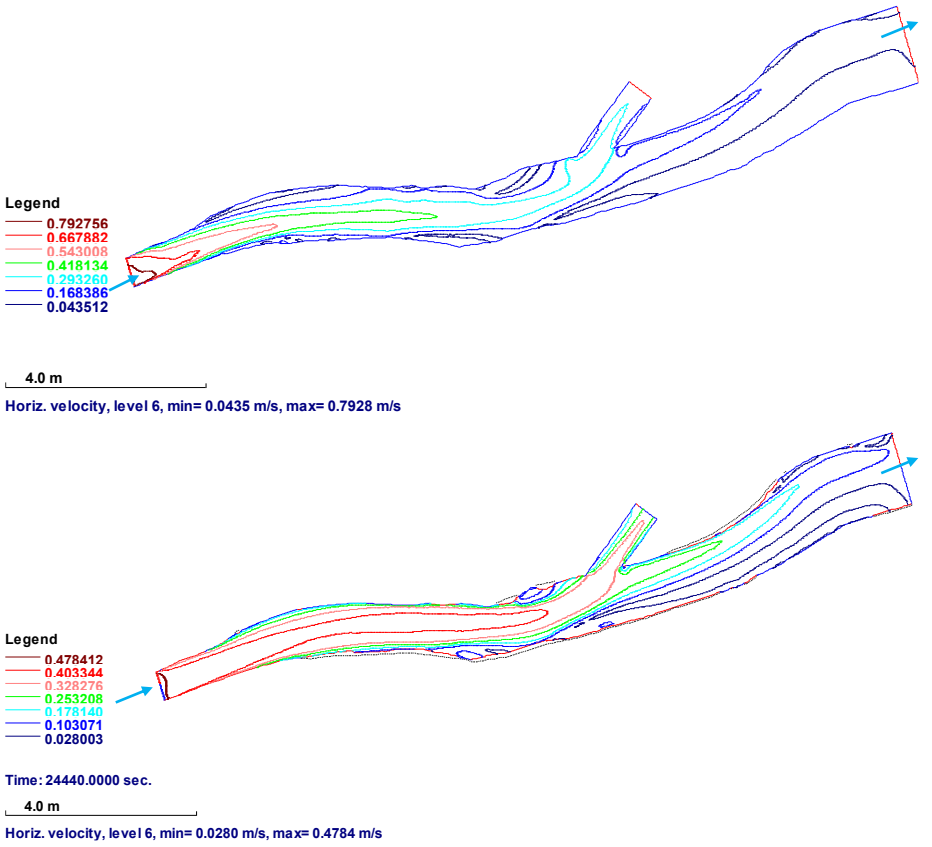

Figure F. 2 Comparison of horizontal velocities between hydraulic (upper) and sediment simulation (lower) for base case parameters

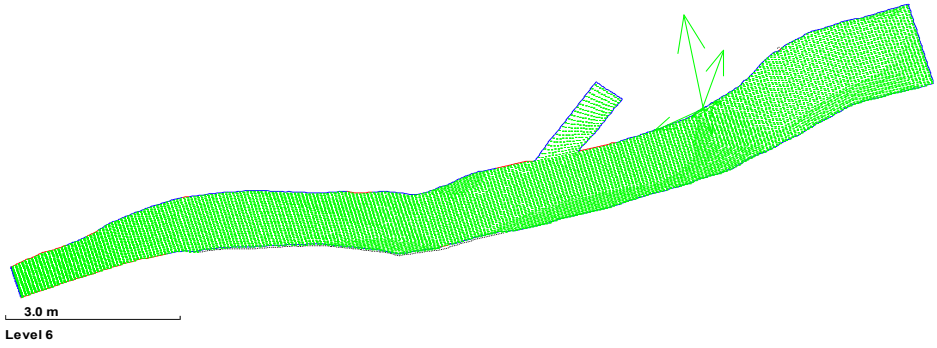

Figure F. 3 Divergence at boundary for Test 2 in initial model

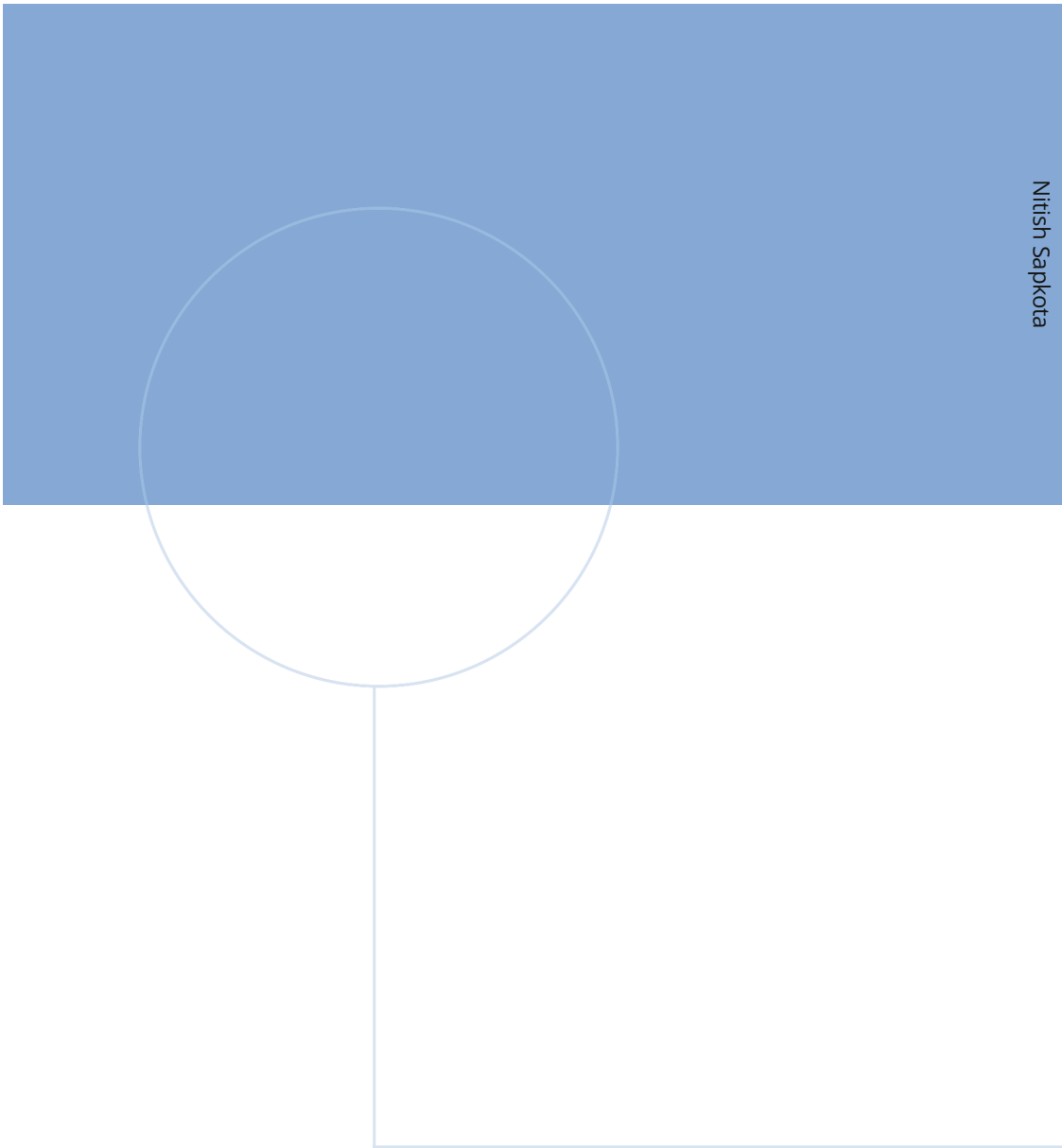

Nitish Sapkota

NTNU
Norwegian University of
Science and Technology